Periodic Controllers for Linear Time-invariant Systems

Meng Joo Er
B. Eng. (Hons.) N.U.S.
M. Eng. N.U.S.

March 1992

A thesis submitted for the degree of Doctor of Philosophy of the Australian National University

Department of Systems Engineering
Research School of Physical Sciences and Engineering
The Australian National University

Declaration

I hereby declare that the contents of this thesis are the results of original research and have not been submitted for a degree at any other university or educational institution.

A number of papers resulting from this work have been published or have been submitted to refereed journals for publication. These papers are:

- M.J. Er and B.D.O. Anderson, "Practical Issues in Multirate Output Controllers" *International Journal of Control*, vol. 53, No. 5, pp. 1005-1020, 1991.

- M.J. Er and B.D.O. Anderson, "Performance Study of Multirate Output Controllers Under Noise Disturbances", to appear in *International Journal of Control.*

- M.J. Er and B.D.O. Anderson, "Design of Reduced-order Multirate Output Observers for Linear State Feedback Laws", submitted for publication.

- M.J. Er and B.D.O. Anderson, "Design of Reduced-order Multirate Input Compensators for Output Injection Feedback Laws", submitted for publication.

- M.J. Er and B.D.O. Anderson, "Discrete-time Loop Transfer Recovery via Generalised Sampled-data Hold Functions Based Compensator", submitted for publication.

- M.J. Er, B.D.O. Anderson and W. Yan, "Gain Margin Improvement Using Generalised Sampled-data Hold Functions Based Multirate Output Compensator", submitted for publication.

During my doctoral studies, I also had the opportunity of working with Professor Darrell Williamson in the area of digital control of skew ratio sensitivity. This work is not reported in this thesis, but is contained in the following papers.

- M.J. Er and D. Williamson, "On the Effects of Skew Ratio on the Zeros of Sampled-data Systems", to be submitted for publication.
- M.J. Er and D. Williamson, "On Digital Control of Skew Ratio Sensitivity", to be submitted for publication.

My doctoral studies were conducted under the guidance of Professor Brian D.O. Anderson as my supervisor, and Professor John B. Moore and Dr. Robert R. Bitmead as my advisors. However, majority of the work, approximately 80 % is my own.

Meng Joo Er
Department of Systems Engineering,
Research School of Physical Sciences and Engineering,
The Australian National University,
Canberra, Australia.

Acknowledgements

It is an unforgettable and deeply cherished experience in my life to have pursued a Ph.D. degree for three years at the Department of Systems Engineering, Australian National University. I wish to take this opportunity to express my sincere gratitude to the following individuals and organizations. Without their support, this thesis would be impossible.

- My supervisor Professor Brian D.O. Anderson for his guidance, encouragement and kindness.
- The Australian National University for the Ph.D Scholarship.
- The Department of Systems Engineering for the stimulating academic environment and the advanced working facilities.
- My parents, brothers and sister for everything they have provided for me in terms of education, financial support and encouragement.
- My wife Soh Hwa for her love, understanding and support during the course of my studies.
- All my dear friends who have helped in one way or another during the course of my studies.

Abstract

The central theme of this research is periodic control of finite dimensional linear time-invariant (FDLTI) systems, in which several both theoretically interesting and practically significant issues are addressed and completely or essentially solved.

In this thesis, in-depth studies are conducted into six different topics. The first two topics seek to identify certain disadvantages of multirate output controllers. In one of these, we show via theory and simulations two situations giving rise to potential problems associated with the Multirate Output Controllers (MROC's). Specifically, we point out two situations where the gain matrix of the controller will acquire extremely large entries. As a consequence, although the ideal plant input will remain well-behaved, the actual plant input will not, since any inaccuracies in the output, due , for example, to noise or nonlinearity, will be amplified by the gain. To circumvent the problem, we provide some rules of thumb that will ensure that excessive gain values are avoided for both cases when using the MROC's.

Another topic in which we attempt to identify possible disadvantage of the MROC's concerns the operational aspects of MROC's under disturbances such as process and/or measurement noise. Here, we show that the MROC law performs poorer than two Linear Quadratic Gaussian (LQG) laws, termed LQG law I and LQG law II, in the presence of noise disturbances. Note that the LQG law here is in discrete-time and is associated with the equivalent discrete-time model of the underlying continuous-time plant; LQG law I uses a one-step prediction estimate of the state (so that the present control depends on measurements prior to the present time); LQG law II uses a true filtered estimate

of the state (so that the present control depends on measurements prior to and at the present time). The basis of comparison is to apply the two types of LQG law to a LTI continuous-time plant with white, gaussian measurement and process noise and compute the optimal linear quadratic performance index for the discretized plant. Next, the existing MROC law, seeking to implement the same state feedback law as the two LQG laws, is applied to the same plant. The equivalent noise matrices and performance index for the discretized plant with MROC law are then calculated. Simulation results show that the two types of LQG law perform better than the MROC law for a typical plant.

The next topic seeks to identify certain advantages, rather than disadvantages, of multirate output sampling. In this topic, some new ideas of designing reduced-order compensators using multirate sampling of the plant output are reported. Here, we show that in the case of estimating a single (but prespecified) linear functional of a system's state, a multirate output linear functional observers (employing multirate sampling of the plant output) of dimension much smaller than that of the single-rate output linear functional observer (employing single-rate sampling of the plant output) can be designed. Necessary and sufficient conditions for the existence of the single-rate output linear functional observer and multirate output linear functional observer are found. Design procedures for constructing these observers are also outlined. Furthermore, both types of observers are strictly causal and open-loop stable for sufficiently small sampling time. These observers then allow the implementation of observer-based compensators.

The fourth topic involves the design of reduced-order multirate input compensators for output injection feedback laws. Here, we seek to identify possible advantages of multirate input sampling, as opposed to multirate output sam-

pling, in designing reduced-order compensators. The concept of a dual-observer based compensator, whose implementation positions the closed-loop poles at the eigenvalues of the observer and those assignable by output injection feedback, is explored. We consider discrete-time systems and derive the equivalent dual-observer based compensator, herein called a single-rate input compensator. Further, we exploit the concept of multirate input sampling and show that a multirate input compensator (employing multirate sampling of the plant input) of dimension much smaller than that of the single-rate input compensator (employing single-rate sampling of the plant input) can be designed. Necessary and sufficient conditions for the existence of the single-rate input compensator and multirate input compensator are found. Design procedures for constructing these compensators are also outlined.

The second last topic in which we discover that periodic control is superior to LTI control concerns discrete-time loop transfer recovery. Loop transfer recovery (LTR) techniques are known to enhance the input or output robustness properties of LQG designs. Unfortunately, one restriction of the existing discrete-time LQG/LTR methods is that they can obtain arbitrarily good recovery only for minimum-phase plants. Although a number of researchers have attempted to devise new techniques to cope with nonminimum-phase plants and have achieved some degrees of success, their methods only work for a restricted class of nonminimum-phase systems. Here, a particular kind of digital controller which is synthesized as a series connection of a Kalman filter (current-estimation type) based compensator and a generalised sampled-data hold functions (GSHF) gain is proposed. It is shown to possess the capability of arbitrary zero placement for a nonminimum phase FDLTI continuous-time plant. Using this power of GSHF, any arbitrary continuous-time, strictly proper, FDLTI system can be

discretized to a minimum-phase one. As a consequence, discrete-time perfect loop recovery can always be asymptotically achieved irrespective of whether the underlying continuous-time plant is minimum-phase or not.

The last topic concerns gain margin improvement using a GSHF based dynamic compensator with multirate sampling of the plant output. A kind of digital controller with all its components time-invariant except a periodic gain and multirate sampling of the plant output is presented. It is shown to possess the capability of improving the closed-loop gain margin over a conventional periodic controller for single-input single-output (SISO), strictly proper, non-minimum phase, continuous-time, FDLTI system. An explicit formula for the maximum achievable gain margin and a design procedure for its construction are derived. Above all, the proposed controller is strictly causal, as opposed to just causal. As a consequence, it could be implemented in practice and is guaranteed to be robust against singular perturbations.

Contents

Notation

$\mathbb{C}$	field of complex numbers
H	open right half plane $= \{s \in \mathbb{C} : \mathrm{Re}\, s > 0\}$
$\bar{H}$	closed right half plane including the point at infinity $= \{s \in \mathbb{C} : \mathrm{Re}\, s \geq 0\}$
D	open unit disk $= \{ z \in \mathbb{C} : \lvert z \rvert < 1 \}$
$\bar{D}$	closed unit disk $= \{ z \in \mathbb{C} : \lvert z \rvert \leq 1 \}$
D^c	complement of open unit disk $= \{z \in \mathbb{C} : \lvert z \rvert \geq 1\}$
$\mathbb{R}$	field of real numbers
$\mathbb{R}^{n \times m}$	$n \times m$ matrices over the field of real numbers
X'	transpose of X
$\bar{x}$	complex conjugate of x
$\mathbb{Z}$	set of nonnegative integers
$\triangleq$	equal to, by definition
$x_d(k)$	$x(kT_0)$ where $k \in \mathbb{Z}$ and T_0 is the sampling time
$\lambda_i(A)$	eigenvalues of A
N_i^O	output-rate multiplicity
N_i^I	input-rate multiplicity
n_i^o	observability index
n_i^c	controllability index
T_i^O	multirate output sampling time
T_i^I	multirate input sampling time
T_0	frame period for multirate sampling $=$ sampling time for single-rate sampling

List of Abbreviations

AAF	Anti-aliasing Filter
FDLTI	Finite-dimensional Linear Time-invariant
GSHF	Generalised Sampled-data Hold Function
LQ	Linear Quadratic
LQG	Linear Quadratic Gaussian
LTR	Loop Transfer Recovery
MIMO	Multiple-input and Multiple-output
MISO	Multiple-input and Single-output
MROC	Multirate Output Controller
MRIC	Multirate Input Controller
OIV	Observability Index Vector
SIMO	Single-input and Single-output
SISO	Single-input and Single-output
ZOH	Zeroth-order Hold

Chapter 1

Introduction

1.1 Motivation of Thesis

In the last decade and particularly the last several years, a number of results on periodic controllers have been reported [4], [6]-[7], [14]-[16], [25],[31], [33], [38], [44], [49], [58] and [79]. Periodic controllers used in conjunction with finite-dimensional linear time-invariant (FDLTI) plants offer a new dimension of flexibility in the design process. In particular, they have been used to achieve equivalent state feedback without observers, pole assignment, zero assignment, gain margin improvement, strong and simultaneous stabilization and the removal of decentralised fixed modes in decentralised control. Evidently, periodic controllers can offer substantially more design freedom than conventional LTI controllers; also a periodic digital controller can be implemented in practice without any significant difficulty since it does not violate the constraint of finite memory in a computer. An overview of some existing periodic controllers which are relevant to this work will be given in the next chapter.

Multirate output controllers (MROC's), a special class of periodic controllers, are a new type of controller which detects the i^{th} plant output at N_i^O uniformly spaced times and changes the plant input once during one frame period T_0. The MROC's have the interesting features of allowing implementation of arbitrary linear state feedback and strong stabilization of unstable plant. Fur-

thermore, the computational efforts required in the design procedure are almost the same as those required for ordinary time-invariant controllers and they do not change the plant inputs as rapidly as the multirate-input controllers and other types of controllers which use frequent changes of gains for regulation.

However, to our knowledge, the operational aspects of MROC's such as performance under process and/or measurement noise disturbances are not yet reported in the literature. Despite the now well-known capability of allowing implementation of arbitrary linear state feedback and strong stabilisation, the suitability of MROC's for industrial applications is relatively unknown. It is thus both theoretically interesting and practically significant to attempt to identify the possible drawbacks, if any, of the MROC's so that they can be accepted by the control engineers and managers. This motivates the first two topics of our research.

The main motivation behind the next two topics is the issue of order reduction. It is well-known that simple (lower-order) linear controllers are normally to be preferred to complex (higher-order) linear controllers for FDLTI plants. Reasons for this include the higher reliability associated with lower complexity in the hardware, the lesser complexity of the software, and the higher computational efficiency associated with the reduced computational burden. Simple controllers are likely to be easier to understand at a conceptual level so that they are more likely to be accepted by design engineers and managers. Accordingly, there is a desire to have methods available to design a lower order controller for a higher order plant.

Often in control system design, it is only necessary to estimate a single (but pre-specified) linear function of the system's state for the purpose of implementing a feedback control law. In the continuous-time case, it has been shown that a linear functional observer of reduced complexity can be constructed which will produce this single quantity with the observer order depending on the sys-

tem's observability index. Roughly speaking, multirate output sampling produces extra independent values of the plant output during each frame period T_0. Intuitively, this is like maintaining the original T_0 but increasing the output dimension and the row rank of the output matrix, thereby reducing the observabiltiy index of the discretized plant. It follows that further reduction in the order of the observer should be possible with multirate output sampling. This inspires us to look into the feasibility of applying multirate output sampling to achieve reduced-order observers.

Other than linear state feedback as a well-known mechanism for pole-positioning, a less well-knwon mechanism is output injection feedback. Output injection feedback is a special kind of pole-positioning mechanism whereby linear combinations of the output measurements are fed directly into the plant's state. Using this mechanism, arbitrary closed-loop pole assignment can be achieved so long as the plant is completely observable. In the event that output injection feedback is not possible, a dual-observer based compensator can be used to realise the pole-positioning effect of output injection. The dual-observer based compensator is essentially obtained by first constructing a single linear functional observer for the dual of the original plant and then taking the dual of the constructed linear functional observer (plus feedback law). As will be shown in a later chapter, the dual of a discretized plant obtained via multirate sampling of the plant's input is like one obtained via applying multirate sampling to the plant's output. Given the possibility of order reduction by using multirate output sampling, it is reasonable to conjecture that one could achieve order reduction by exploring the design procedure for a dual-observer based compensator and the concept of mutlirate input sampling. This motivates the research in the fourth topic of the thesis.

As foreshadowed in the introduction, periodic controllers have been used to achieve a lot of interesting results which LTI controllers find it impossible

or hard to accomplish. It is of practical significance to know in what other aspects and to what extent periodic controllers are superior to LTI controllers. In particular, does periodic control offer more advantages than conventional control with respect to robustness?

One important robustness improvement issue is the recovery of robustness impaired by observers in LQG designs. LTR techniques are known to enhance the input or output robustness properties of LQG designs. Unfortunately, one restriction of the existing discrete-time LQG/LTR methods is that they can obtain arbitrarily good recovery only for minimum-phase plants. A number of researchers have attempted to devise new techniques to cope with nonminimum-phase plants and have achieved some degrees of success [36], [55], [65] and [81]. Nevertheless, their methods only work for a restricted class of nonminimum-phase systems. Given the superiority of periodic control over LTI control, it is natural to ask whether periodic control could offer any advantage in terms of achieving loop transfer recovery for nonminimum-phase plants. This motivates the research in discrete-time loop transfer recovery via generalised sampled-data hold functions (GSHF) based compensator.

Another aspect of robustness improvement concerns gain margin improvement. This question has drawn increasing attention in recent years. For instance, Khargonekar *et al.* [44] indicated the capability of periodic compensators improving arbitrarily the gain margin for *SISO discrete-time* FDLTI bicausal plants and Lee, Meerkov, and Runolfsson [49] proved a similar gain margin result for *SISO continuous-time* FDLTI plants with periodic *continuous-time* dynamic compensators with a particular form. More recently, Francis and Georgiou [25] showed that for a discrete-time FDLTI plant, LTI dynamic pre-compensation with decimation of the plant output (which is equivalent to use of a periodic dynamic compensator) can arbitrarily place nonzero zeros of the resulting system. Using this idea, they generalized the gain margin result in [44] to the

multivariable continuous-time case. In another direction, Kabamba [38] exhibited advantages of periodic output feedback based on the use of GSHF over LTI compensation for such purposes as simultaneous pole assignment and decoupling.

In [79], a periodic GSHF dynamic compensator is presented and shown to be able to achieve an arbitrarily prescribed gain margin for a *multivariable continuous-time* plant. Nevertheless, for a SISO, *strictly proper*, nonminimum phase, continuous-time, FDLTI plant, although the closed-loop gain margin obtained via the proposed compensator is significantly improved over that achieved by a conventional periodic controller, the compensator so designed is not necessarily strictly causal. A nonstrictly causal compensator has two major disadvantages: first, it is practically difficult and sometimes impossible to be implemented in practice; second, as has been shown in [77], stabilisation by a nonstrictly proper controller is never robust against singular perturbations whereas stabilisation by a strictly proper controller is always robust against singular perturbations. Naturally, there is a desire to have a strictly causal compensator while attaining at least the same maximum level of gain margin improvement as that achieved in [79]. This is the motivation for the last topic of the research.

1.2 Structure of Thesis

This thesis is organized as follows. The next chapter gives an overview of the five existing periodic controllers which are relevant to this work, namely multirate input controllers (MRIC's), multirate output controllers (MROC's), conventional periodic controllers, generalised sampled-data hold functions (GSHF) based dynamic compensator, and GSHF based nondynamic compensator.

In Chapter 3, the potential problems associated with the operation of the MROC's are highlighted. Specifically, we show via theory and simulations two situations giving rise to large entries in the gain matrix of the controller. As a

consequence, although the ideal plant input will remain well-behaved, the actual plant input will not since any inaccuracies in the output, due, for example, to noise or nonlinearity, will be amplified by the gain matrix. Further, we provide some rules of thumb that will ensure that excessive gain values are avoided when using the MROC's.

In Chapter 4, we present a comparative study of the performance of a MROC with a LQG controller in the presence of noise disturbances and anti-aliasing filters. The basis of comparison is to apply LQG law with one-step ahead prediction-type Kalman filter (thereafter called LQG law I) and LQG law with current estimation-type Kalman filter (thereafter called LQG law II) to a LTI continuous-time plant model with white, gaussian process and measurement noise and compute a linear quadratic performance index for the discretized plant. Equivalent noise matrices for using the MROC law are derived and the same quadratic performance index computed. In order to have a fair comparison, the cutoff frequency of the anti-aliasing filter used to remove high frequency noise components prior to sampling is also kept the same when applying both laws. Applications of both laws in typical situations show that the performance of the MROC law is worse than LQG law I and LQG law II.

Chapter 5 is concerned with the design of reduced-order multirate output observers for linear state feedback laws. In this chapter, we explore the concept of multirate output sampling and show that a linear functional observer employing multirate sampling of the plant output can be designed with a dimension much smaller than that of the linear functional observer employing single-rate sampling of the plant output. Necessary and sufficient conditions for the existence of the single-rate output linear functional observer and multirate output linear functional observer are found. Design procedures for constructing these observers are also outlined. Furthermore, both types of observers are strictly causal and open-loop stable for sufficiently small sampling time.

In Chapter 6, the design of reduced-order multirate input compensators for output injection feedback laws is attempted. Here, we consider discrete-time systems and derive the equivalent dual-observer based compensator, herein termed single-rate input compensator. Further, we explore the concept of multirate input sampling and show that a multirate input compensator (employing multirate sampling of the plant input) of dimension much smaller than that of the single-rate input compensator (employing single-rate input sampling of the plant input) can be designed. Necessary and sufficient conditions for the existence of both types of compensators are found. Design procedures for constructing these compensators are also outlined.

The capability of periodic controllers with respect to robustness improvement is demonstrated in Chapter 7. Here, we look at the issue of discrete-time loop transfer recovery. We explore the zero placement capability of GSHF developed in [38] and show that using this power of GSHF, the discretized plant can always be made minimum-phase. As a consequence, we are able to achieve discrete-time perfect recovery using a GSHF based compensator irrespective of whether the underlying continuous-time plant is minimum-phase or not.

In Chapter 8, the advantage of periodic controllers with respect to robustness improvement is further demonstrated. In this chaper, we address the issue of gain margin improvement using periodic controllers. We propose a new type of GSHF based compensator which employs multirate sampling of the plant output with output-rate multiplicity, $N_O = 2$. Using the proposed compensator, not only the same level of gain margin as in [79] can be achieved , but also, more importantly, the compensator is strictly causal. As a consequence, the compensator could be implemented in practice and is guaranteed to be robust against singular perturbations.

The conclusions together with directions for future development appear in Chapter 9 .

1.3 Point Summary of Contributions

- Identification of two situations giving rise to large entries in the gain marix of the MROC's.
- Derivation of rules of thumb for selection of the frame period to avoid large entries in the gain of a MROC.
- Examination of the perfomance of a MROC in comparison to a LQG controller under noise disturbances.
- Derivation of MROC control law in the presence of process and measurement noise disturbances and anti-aliasing filters.
- Use of the multirate output sampling concept in designing reduced-order multirate output linear functional observers for linear state feedback laws.
- Derivation of design procedure for reduced-order multirate output linear functional observers.
- Use of the multirate input sampling concept in designing reduced-order multirate input compensators for output injection feedback laws.
- Derivation of design procedure for reduced-order multirate input compensators.
- Use of periodic control for achieving discrete-time perfect loop transfer recovery for nonminimum-phase continuous-time plants with zeros at infinity of order one.
- Derivation of procedure for discretizing a strictly proper nonminimum-phase continuous-time system to a minimum-phase one.

- Use of the multirate output sampling concept and the GSHF idea in designing a practically realisable robust controller that improves the gain margin over conventional periodic controller.
- Derivation of design procedure for the construction of the proposed GSHF based multirate output compensator.
- Simplification of existing formula for the maximal gain margin achievable by GSHF based dynamic compensator

Chapter 2

Overview of Periodic Controllers

2.1 Introduction

As foreshadowed in the introduction, there are many types of periodic controllers. To facilitate the development of the subsequent chapters, an overview of the five which are more relevant to this work, namely multirate input controllers (MRIC's), multirate output controllers (MROC's), conventional periodic controllers, generalised sampled-data hold function (GSHF) based dynamic compensators and GSHF based nondynamic compensators are presented in this chapter. The main features together with their capabilities in solving certain control problems are summarised here. Further, their possible drawbacks are highlighted.

2.2 Multirate Input Controllers

MRIC's, developed by [7], are a special class of periodic controller which detects the plant outputs once and changes the i^{th} entry of the plant input N_i^I times over the time interval $[kT_0, \overline{k+1}T_0)$, $k = 0, 1, 2, \cdots$, where the integer N_i^I $(i = 1, 2, \cdots, m)$ is termed the input-rate multiplicity. A block diagram showing the closed-loop configuration with a MRIC is shown in Figure 2.2.1.

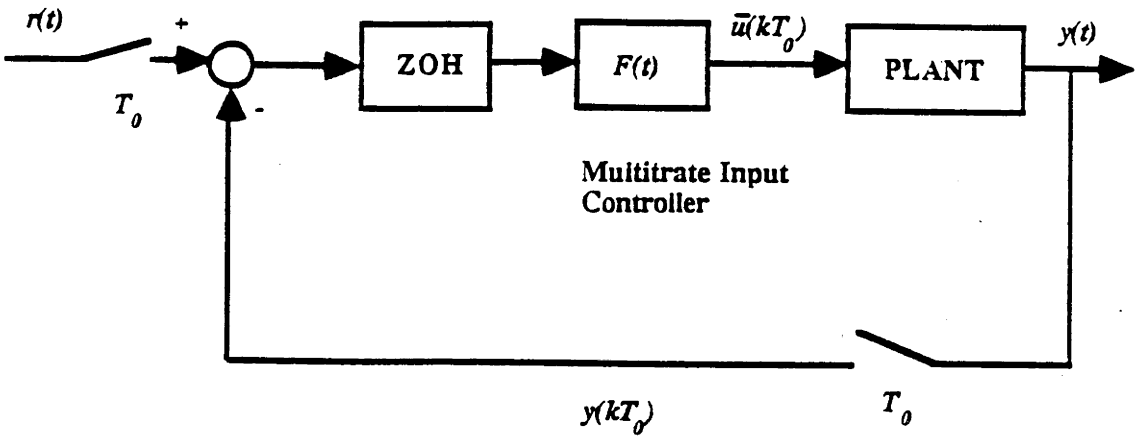

Figure 2.2.1: Closed-loop Configuration With a MRIC

Here, $F(t) = F(t + T_0)$ where T_0 is the frame period.

The main features of the MRIC's are:

- The input-rate multiplicity, N_i^I and the controllability index, n_i^c are related by $N_i^I \geq n_i^c$.
- They can achieve arbitrary symmetric pole assignment.
- For $N_i^I \geq n_i^c$, they use only gain feedback and are always stable.
- The computational effort in pole assignment is the same as for conventional LTI controllers

The only drawback with the MRIC's is that the plant inputs will often take large positive and negative values during the transient response to, for example, a step. As a consequence, the controller is often not suitable for industrial applications.

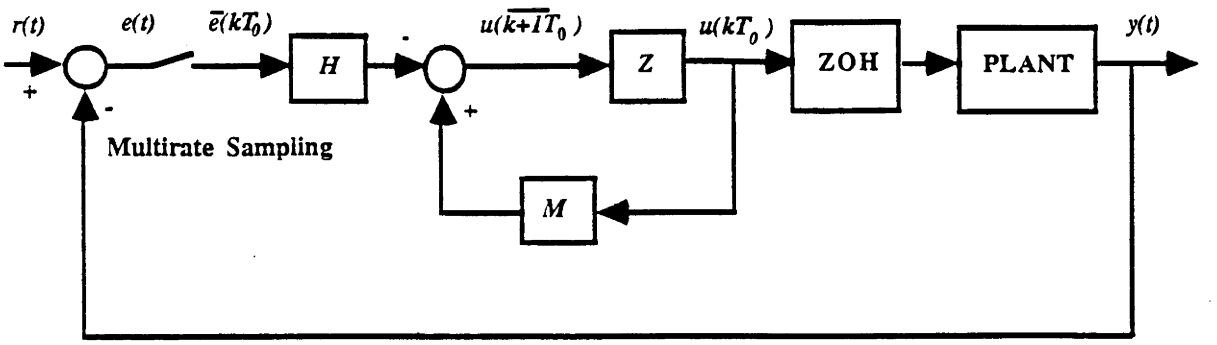

Figure 2.3.1: Closed-loop Configuration with a MROC

Note that the controllers of [16] are a special case of the MRIC's with $N_1^I = N_2^I = \cdots = N_m^I = N^I$ i.e. the controllers of [16] corresponds to a MRIC with uniform input-rate multiplicity, N^I.

2.3 Multirate Output Controllers

MROC's are another special class of periodic controllers which employs multirate sampling. Contrary to MRIC's, the sampling mechanism involves detecting the i^{th} plant output at N_i^O uniformly spaced times and changes the plant input once during one frame period, T_0, see [33] for details. A block diagram of the closed-loop configuration with a MROC is shown in Figure 2.3.1.

The main features of the MROC's are:

- The output-rate multiplicities, N_i^O and the observability index, n_i^o are related by $N_i^O \geq n_i^o$.

- They overcome the major drawback of MRIC's in that the plant inputs

do not change rapidly.

- For $N_i^O \geq n_i^o$, the control law uses only output measurements and is equivalent to a state feedback law. As a consequence, observers are not needed in the absence of state measurements.
- For $N_i^O > n_i^o$, they can always achieve strong stabilization of an unstable plant i.e. stabilization using an asymptotically stable controller.
- The computational efforts in pole assignment are the same as LTI controllers.

The control law of the MROC's takes the general form

$$u(\overline{k+1}T_0) = Mu(kT_0) + H\bar{e}(kT_0) \tag{2.3.1}$$

where $M \in \mathbb{R}^{m\times m}$, $H \in \mathbb{R}^{m\times \bar{N}^O}$, $\bar{N}^O = \sum_{i=1}^{p} N_i^O$, $e(t) = r(t) - y(t)$ and

$$\bar{e}(kT_0) = \begin{bmatrix} e_1(kT_0) \\ \vdots \\ e_1(kT_0 + \overline{N_1^O - 1}T_1^O) \\ \vdots \\ e_p(kT_0) \\ \vdots \\ e_p(kT_0 + \overline{N_p^O - 1}T_p^O) \end{bmatrix} \tag{2.3.2}$$

which is a collection of the sampled values of the plant output obtained over $[kT_0, (k+1)T_0)$ $k = 0, 1, 2, \cdots$.

The above equation means that the control inputs for the $\overline{k+1}^{th}$ frame period are determined based on the values of the control inputs for the k^{th} frame period, $u(kT_0)$ and the sampled values of the errors, $\bar{y}(kT_0)$ obtained during the k^{th} frame period. The time available for the computation of $u(\overline{k+1}T_0)$ is evidently $min_{1\leq i\leq p}T_i^O$

A review of the operation of MROC's will be given in the next chapter.

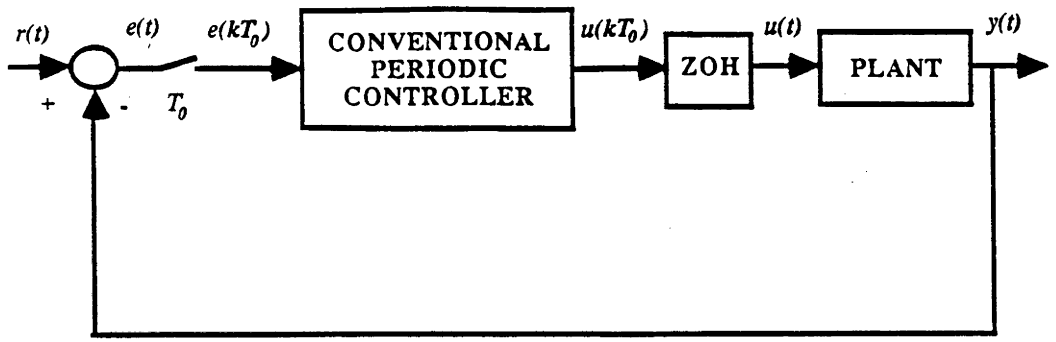

Figure 2.4.1: Conventional Periodic Controller

2.4 Conventional Periodic Controllers

A conventional periodic controller, developed in [25], is a dynamical system with periodically time varying elements and is composed of a sampler, a periodic discrete-time dynamic compensator and a zeroth-order hold. This type of controller is depicted in Figure 2.4.1. Notice the hybrid aspect in this configuration.

A state-space model of this type of controller is given by

$$\xi_d(k+1) = A_d(k)\xi_d(k) + B_d(k)e(kT_0) \tag{2.4.1}$$

$$u(kT_0) = C_d(k)\xi_d(k) + D_d(k)e(kT_0) \tag{2.4.2}$$

where $e(t) = r(t) - y(t)$ and $A_d(k)$, $B_d(k)$, $C_d(k)$ and $D_d(k)$ are m-periodic i.e.

$$A_d(k) = A_d(k+m) \qquad B_d(k) = B_d(k+m)$$

$$C_d(k) = C_d(k+m) \qquad D_d(k) = D_d(k+m)$$

The main features of the conventional periodic controllers are:

- Closed-loop zeros can be arbitrarily placed by the controllers.
- Gain margin obtained by the controllers can be significantly improved over that achieved by LTI controllers.

The design procedure consists of

- discretizing the plant.
- designing a LTI dynamic forward-compensator with decimation of the plant output (which is equivalent to the use of a particular form of linear periodic dynamic compensator) to position the zeros of the discretized plant.
- designing a LTI feedback compensator which positions the poles of the discretized plant.

From this procedure, it is not difficult to see that the order of such a controller may be very high due to the introduction of pre-compensation. Another disadvantage, as mentioned in [25], is that the sampling time may have to be very small to permit an increase in the gain margin.

2.5 Generalised Sampled-data Hold Function Based Dynamic Compensators

A generalised sampled-data hold function (GSHF) based dynamic compensator consists of a sampler, a LTI dynamic compensator and a periodic control gain known as a GSHF, see [79] for details. This type of controller is pictured in Figure 2.5.1.

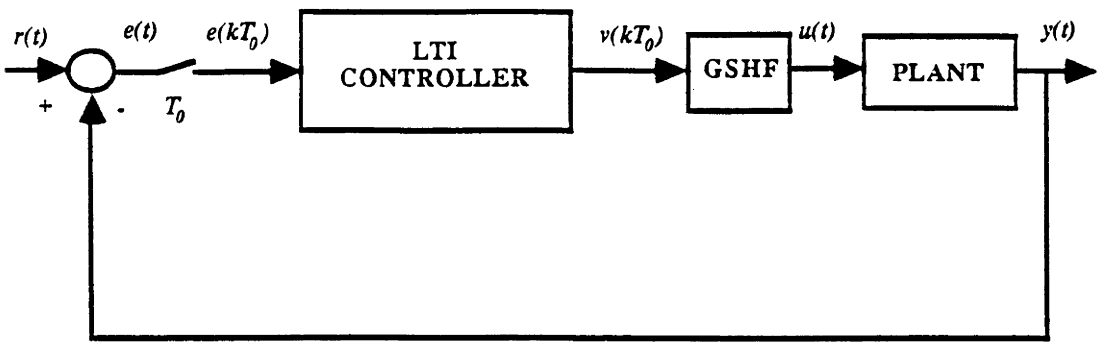

Figure 2.5.1: GSHF Based Dynamic Compensator

Like a conventional periodic controller, the special feature of a generalised sampled-data hold functions (GSHF) based compensator is the hybrid aspect. The main difference between this configuration and the previous configuration lies in the periodicity; the periodicity of a conventional periodic controller occurs in the dynamic component while the periodicity of a GSHF compensator occurs only in the GSHF gain with the dynamic components time-invariant. The implication of this is that in practice, a GSHF dynamic compensator could be more easily implemented than a conventional periodic digital controller.

A state-space model of a GSHF dynamic compensator is given by

$$z_d(k+1) = A_c z_d(k) + B_c e(kT_0) \tag{2.5.1}$$

$$v(kT_0) = C_c z_d(k) + D_c e(kT_0) \tag{2.5.2}$$

$$u(t) = F(t)v(kT_0) \tag{2.5.3}$$

$$F(t) = F(t+T_0) \tag{2.5.4}$$

$$t \in [kT_0, (k+1)T_0)$$

$$k = 0, 1, 2, \cdots$$

where $e(t) = r(t) - y(t)$ and $T_0 > 0$ is the frame period, A_c, B_c, C_c and D_c are constant matrices of appropriate dimensions and $F(t)$ is a periodic integrable and bounded function matrix of an appropriate dimension.

The capability of the GSHF based dynamic compensator is summarised below:

- For a SISO, strictly proper, continuous-time, FDLTI plant, the closed-loop gain margin obtained via the compensator can be significantly improved over that achieved via a conventional periodic controller.
- For SISO bicausal and MIMO continuous-time FDLTI plants, infinite gain margin is achieved.

The only drawback of the above controller is that for a SISO strictly proper conitnuous-time FDLTI plant, the compensator so designed is not strictly causal. The disadvantages of a nonstrictly causal compensator are two fold: first, it is well-known that it is practically difficult and sometimes impossible to implement a nonstrictly causal compensator; second, as has been pointed out by [77], stabilisation by a nonstrictly proper compensator is never robust against singular perturbations.

2.6 GSHF Based Nondynamic Compensator

The GSHF based nondynamic compensator corresponds to the special case of the GSHF based dynamic compensator i.e. $A_c = B_c = C_c = 0$, $D_c = I$ in (2.5.1)-(2.5.2), see [38] for details.

Several interesting results are achieved by the GSHF based nondynamic compensator. They are

- *Simultaneous Pole Assignment*: A sufficient condition for simultaneous pole assignability of a finite number of systems by GSHF control is derived.
- *Optimal Noise Rejection*: A GSHF can be chosen to minimize the sensitivity of the state vector to noise at the sampling times.
- *Simultaneuous Optimal Noise Rejection*: Optimal noise rejection problem can be solved in a finite number of systems simultaneously by a single GSHF controller.
- *Model Matching*: A class of closed-loop transfer functions achievable by GSHF control was characterised.
- *Decoupling*: When decoupling by GSHF is possible and what diagonal closed-loop transfer functions can be achieved were characterised.
- *Stability Robustness Analysis*: For stable GSHF control loops, perturbations of the open-loop which do not destabilise the closed-loop were characterised.

Note that if the GSHF gain $F(t)$ is implemented on a digital computer by its piecewise constant equivalent, we effectively obtain MRIC's. (See [79] for details on obtaining a piecewise constant equivalent of $F(t)$). Therefore, results achievable by MRIC's as well as the associated drawbacks are applicable to this type of controller.

2.7 Summary and Remarks

In this chapter, we have briefly presented an overview of five periodic controllers which are relevant to our work. In summary, the conventional periodic controller is very different from the multirate controllers in terms of its configuration. We also see that MRIC's are really a special case of the GSHF based nondynamic

controller in that the GSHF gain is implemented on a digital computer in a piecewise constant manner. In turn, a GSHF based nondynamic compensator is really a special case of its dynamic counterpart.

As we have seen, several interesting results have been accomplished by these five controllers. Given the advantages and disadvantages associated with these controllers, it is natural to ask the following questions:

1. Can one find ways to circumvent their drawbacks ?

2. Can one identify any potential problem associated with the MROC's although they are the only controllers which do not appear to have any drawback ?

3. Can one possibly employ these controllers or their mechanisms in solving other control problems ?

4. Can one devise other periodic controllers, possibly a mixture of the above, to achieve even more interesting and fruitful control objectives ?

In the subsequent chapters of this thesis, we shall attempt to answer these questions.

Chapter 3

Practical Issues in Multirate Output Controllers

3.1 Introduction

In this chapter, we seek to identify certain disadvantages of MROC's. We show that frame periods and ouput sampling periods must fulfill certain inequality constraints to avoid the gains in the controller becoming very large. Large gains will have the effect of amplifying noise substantially, but not of introducing large controls (in the absence of noise or other non-ideal behaviour). For ease of explanation, the term "frame period" T_0 is used to refer to the "cycle" of the controllers and the term "sampling period" is used to indicate the interval in which the plant outputs are detected or inputs are applied; often such sampling periods are multiples or submultiples of T_0.

Section 3.2 reviews the operation of MROC's. Section 3.3 highlights the potential problems via theory and examples and Section 3.4 introduces how these can be avoided through appropriate choice of frame and sampling periods. Section 3.5 contains concluding remarks.

3.2 Review of Operation of MROC's

As foreshadowed in the introduction, MROC's are a special class of periodic controllers which detects the i^{th} plant output at N_i^O uniformly spaced times and changes the plant input once during one frame period. In order to understand the operation of a MROC, let us first review the concept of multirate output sampling developed in [33]. The MROC's sampling mechanism involves detecting the i^{th} plant output y_i at every T_i^O seconds where T_i^O is a submultiple of the so-called frame period T_0 as shown in Figure 3.2.1. At time kT_0, all outputs are sampled and all inputs are changed simultaneously. The sampled values of the plant output obtained over $[kT_0, (k+1)T_0)$ are stored in a vector $\bar{y}(kT_0)$ as shown below:

$$\bar{y}(kT_0) = \begin{bmatrix} y_1(kT_0) \\ \vdots \\ y_1(kT_0 + \overline{N_1^O - 1}T_1^O) \\ \vdots \\ y_p(kT_0) \\ \vdots \\ y_p(kT_0 + \overline{N_p^O - 1}T_p^O) \end{bmatrix} \tag{3.2.1}$$

In Figure 3.2.1, $N_1^O = 3$ and $N_2^O = 2$. The input dimension m as well as the output dimension p is 2.

The vector $\bar{y}(kT_0)$ is used in the control law, which changes the value of u(.) every T_0 seconds. The nature of this control law will now be explained.

Suppose the continuous-time FDLTI plant is described by

$$\dot{x}(t) = Ax(t) + Bu(t) \tag{3.2.2}$$

$$y(t) = Cx(t) \tag{3.2.3}$$

where the state $x \in \mathbb{R}^n$, the plant input $u \in \mathbb{R}^m$ and the plant output $y \in \mathbb{R}^p$ and

$$u(t) = u(kT_0) \quad (kT_0 \leq t < \overline{k+1}T_0) \tag{3.2.4}$$

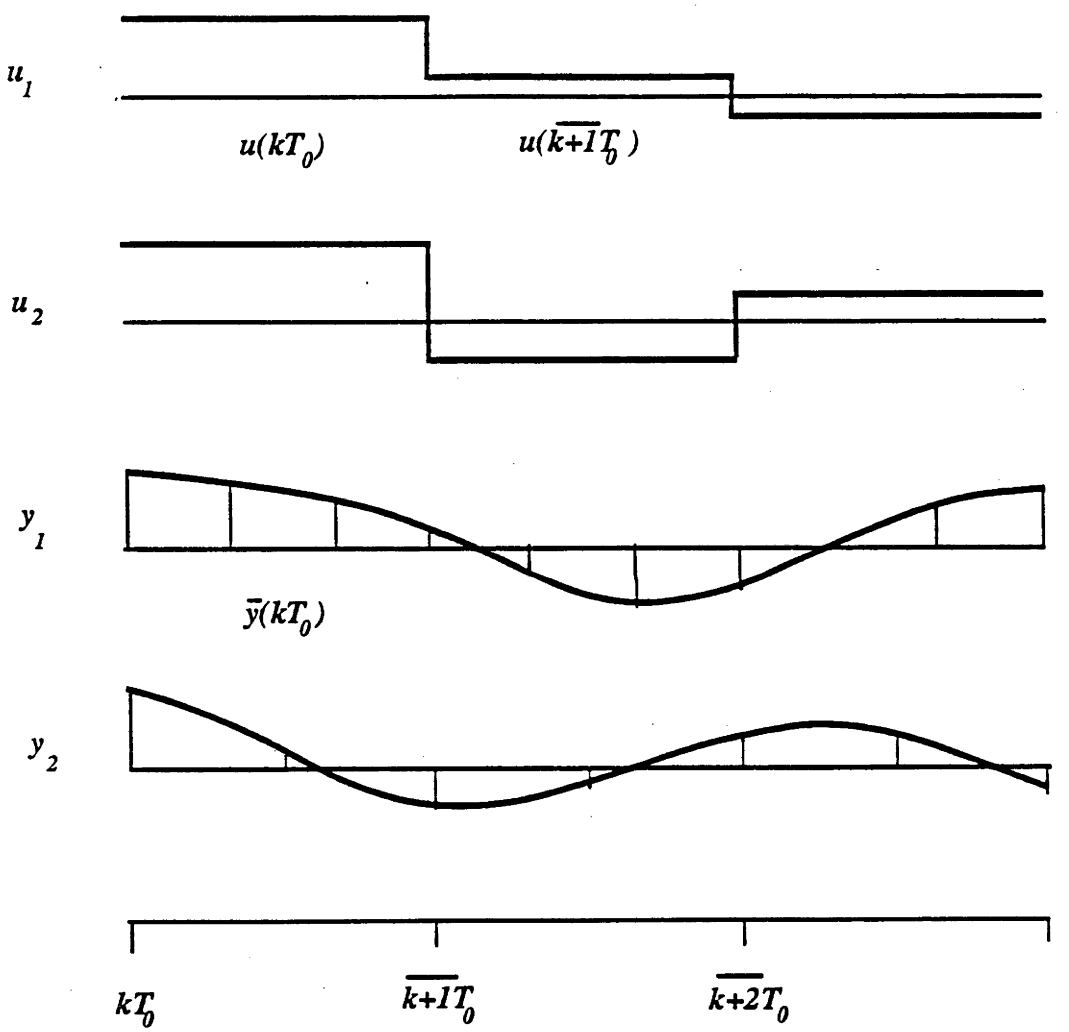

Figure 3.2.1: Multirate-output Sampling Mechanism

We can express the basic formula of the MROC sampling mechanism in a vector-matrix form given by

$$\hat{C}x(\overline{k+1}T_0) = \bar{y}(kT_0) - \hat{G}u(kT_0) \tag{3.2.5}$$

Here, $\hat{C} \in \mathbb{R}^{\bar{N}^O \times n}$ and $\hat{G} \in \mathbb{R}^{\bar{N}^O \times m}$ are respectively given by

$$\hat{C} = \begin{bmatrix} c_1 \exp(-AN_1^O T_1^O) \\ \vdots \\ c_1 \exp(-AT_1^O) \\ \vdots \\ c_p \exp(-AN_p^O T_p^O) \\ \vdots \\ c_p \exp(-AT_p^O) \end{bmatrix} \tag{3.2.6}$$

$$\hat{G} = \begin{bmatrix} c_1 \int_0^{-N_1^O T_1^O} \exp(At)B\,dt \\ \vdots \\ c_1 \int_0^{-T_1^O} \exp(At)B\,dt \\ \vdots \\ c_p \int_0^{-N_p^O T_p^O} \exp(At)B\,dt \\ \vdots \\ c_p \int_0^{-T_p^O} \exp(At)B\,dt \end{bmatrix} \tag{3.2.7}$$

where c_i is the i^{th} row of C. Equation (3.2.5) gives the relation of the vector $\bar{y}(kT_0)$ for the inputs at the beginning of each frame period and the final state of the frame period.

The integer $\bar{N}^O$ is given by

$$\bar{N}^O = \sum_{i=1}^{p} N_i^O \tag{3.2.9}$$

(The reader is referred to [33] for detailed derivation.)

To facilitate the following discussion, the term "observability index vector" is defined.

Definition 3.2.1 *Consider an observable pair* (A, C) *where* $A \in \mathbb{R}^{n\times n}$ *and* $C \in \mathbb{R}^{p\times n}$. *Expressing* C *as*

$$C = [c_1^T, \cdots, c_p^T]^T$$

then a set of p *integers* $(n_1, \cdots, n_p)$ *is said to be an observability index vector (abbreviated as OIV) of the pair* (A,C) *if*

$$\sum_{i=1}^{p} n_i = n \tag{3.2.10}$$

and

$$rank[\ c_1', A'c_1', \cdots, A'^{(n_1-1)}c_1', \cdots, c_p', A'c_p', \cdots, A'^{(n_p-1)}c_p'\ ] = n \tag{3.2.11}$$

Consider the matrix $\hat{C}$ of the basic formula (3.2.5). In [33], it is proven that the matrix $\hat{C}$ given by (3.2.6) has full column rank $(= n)$ for almost every frame period T_0 if the output-rate multiplicities $(N_1^O, \cdots, N_p^O)$ satisfy

$$N_i^O \ \geq \ n_i^o \quad (i = 1, \cdots, p) \tag{3.2.14}$$

where $(n_1, \cdots, n_p)$ is an OIV of the pair (A,C).

A related result, also proved in [33], is the following. Suppose that (A,C) is an observable pair and that

$$\text{rank} \begin{pmatrix} A & B \\ C & 0 \end{pmatrix} \ = \ n + m \tag{3.2.15}$$

(which means that $p \geq m$, the plant is nondegenerate and the plant has no zero at the origin). Then the matrix $[\hat{C}\ \ \hat{G}]$ given by (3.2.6) and (3.2.7) has full column rank$(= n + m)$ for almost every frame period T_0 if the output-rate multiplicities $(N_1^O, \cdots, N_p^O)$ satisfy

$$N_i^O \ \geq \ m_i \quad (i = 1, \cdots, p) \tag{3.2.18}$$

where $(m_1, \cdots, m_p)$ is an OIV of the augmented system pair

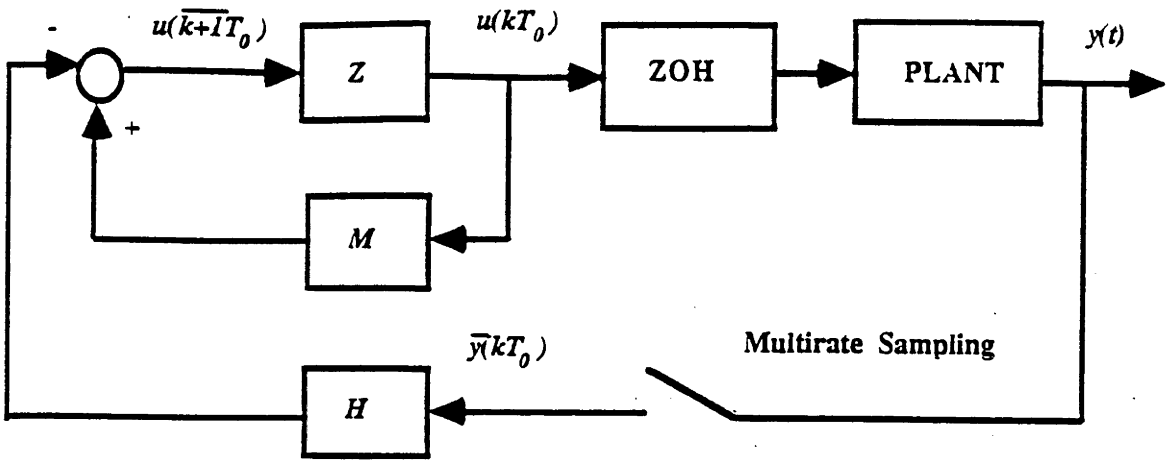

Figure 3.2.2: Closed-loop Configuration with a MROC

$$\left(\begin{bmatrix} A & B \\ C & 0 \end{bmatrix} \begin{bmatrix} C & 0 \end{bmatrix} \right)$$

The closed-loop configuration with a MROC is shown in Figure 3.2.2. The control law of the MROC takes the general form

$$u(\overline{k+1}T_0) = Mu(kT_0) - H\bar{y}(kT_0) \tag{3.2.19}$$

where $M \in \mathbb{R}^{m \times m}$ and $H \in \mathbb{R}^{m \times \bar{N}^O}$

The above equation means that the control inputs for the $\overline{k+1}^{th}$ frame period are determined based on the values of the control inputs for the k^{th} frame period, $u(kT_0)$ and the sampled values of the outputs, $\bar{y}(kT_0)$ obtained during the k^{th} frame period. The time available for the computation of $u(\overline{k+1}T_0)$ is evidently $min_{1 \le i \le p} T_i^O$.

Now, suppose that (A, C) is an observable pair and the output-rate multiplicities $(N_1^O, \cdots, N_p^O)$ satisfy (3.2.14) where $(n_1, \cdots, n_p)$ is an OIV of the pair (A, C). Then, if the matrix H can be chosen to satisfy

$$H\hat{C} = F \tag{3.2.21}$$

and if we set

$$M = H\hat{G} \tag{3.2.22}$$

we can make the control law equivalent to any state feedback control law

$$u(kT_0) = -Fx(kT_0) \quad (k \geq 1) \tag{3.2.23}$$

This can be argued from (3.2.5) and (3.2.19).

Two separate cases can now be considered.

CASE I: Suppose that the output-rate multiplicities $(N_1^O, \cdots, N_p^O)$ are set to the minimum values i.e.

$$N_i^O = n_i^o \quad (i = 1, \cdots, p) \tag{3.2.26}$$

Then the matrix $\hat{C}$ becomes a square matrix and H is uniquely determined by

$$H = F\hat{C}^{-1} \tag{3.2.27}$$

In this case, M is completely determined and this means that the stability of the open-loop controller (which is governed by the eigenvalues of M) depends solely (and indirectly) on the choice of the state feedback matrix F.

CASE II: Suppose that the output-rate multiplicities $(N_1^O, \cdots, N_p^O)$ are chosen larger than the minimum values as

$$N_i^O > n_i^o \tag{3.2.28}$$

Then we can find, in general, infinitely many matrices H which satisfy (3.2.21) and it becomes plausible that we can select H so that the matrix M given by (3.2.22) becomes stable, i.e. has all eigenvalues with magnitude less than 1.

As an approach to achieving this, the authors of [33] proceed as follows. Suppose that (A, C) is an observable pair and that

$$\text{rank}\begin{pmatrix} A & B \\ C & 0 \end{pmatrix} = n + m \tag{3.2.30}$$

Further suppose that the output-rate multiplicities $(N_1^O, \cdots, N_p^O)$ satisfy

$$N_i^O \geq m_i \quad (i = 1, \cdots, p) \tag{3.2.31}$$

where $(m_1, \cdots, m_p)$ is an OIV of the augmented system.

Then for almost every frame period T_0, there exists a matrix $H \in \mathbb{R}^{m \times \bar{N}^O}$ such that (3.2.21) and (3.2.22) are both satisfied and where $F \in \mathbb{R}^{m \times n}$ is the desired state feedback and $M \in \mathbb{R}^{m \times m}$ is an arbitrary specified matrix corresponding to the desired state transition matrix of the controller itself. This is because $[\hat{C} \;\; \hat{G}]$ has full column rank under the stated assumption, and accordingly, H can be found to satisfy

$$H[\hat{C} \;\; \hat{G}] = [F \;\; M] \tag{3.2.32}$$

(We simply choose $H = [F \;\; M]E$ where E is a left inverse of $[\hat{C} \;\; \hat{G}]$)

The above implies that we can equivalently realize any state feedback F by a MROC possessing any prescribed degree of stability since we can choose the matrix M arbitrarily. The choice $M = 0$ is of course permissible.

The procedure for strong stabilization of the original plant boils down to choosing a stable feedback matrix F which makes $(A_s - B_s F)$ stable where

$$A_s = \exp(AT_0) \tag{3.2.33}$$

$$B_s = \int_0^{T_0} \exp(At) B \, dt \tag{3.2.34}$$

and then choosing a stable matrix M. Finally, it involves determining H by

$$H = [F \;\; M][\hat{C} \;\; \hat{G}]^{-L} \tag{3.2.35}$$

where $[\hat{C} \;\; \hat{G}]^{-L}$ is a left inverse of $[\hat{C} \;\; \hat{G}]$.

3.3 Potential Problems of MROC's

In this section, we identify two situations giving rise to potential problems associated with the MROC's. Specifically, we point out two situations for case I ($N_i^O = n_i^o$) and for case II ($N_i^O > n_i^o$) where the matrix $\hat{C}$ or $[\hat{C}\ \hat{G}]$ can approach a rank deficient matrix. The consequence of this is that for almost all desired feedback gains F, the gain matrix H of the controller will acquire extremely large entries. Although the ideal plant input $u(kT_0)$ will remain well-behaved, taking the value $-Fx(kT_0)$, the actual plant input will not, since any inaccuracies in the output, due , for example, to noise or nonlinearity, will be amplified by H.

To fix ideas, assume that A has distinct eigenvalues; then we can always find an invertible matrix T such that

$$A_d = T^{-1}AT \tag{3.3.1}$$

$$B_d = T^{-1}B \tag{3.3.2}$$

$$C_d = CT \tag{3.3.3}$$

with A_d in Jordan form.

For convenience, let us also assume that A has real eigenvalues; this keeps the algebra simpler. Further, we arrange A_d such that it is given as follows:

$$A_d = \begin{bmatrix} A_1 & 0 \\ 0 & \alpha \end{bmatrix} \tag{3.3.4}$$

where $A_d \in \mathbb{R}^{n\times n}$, $A_1 = \text{diag}(\lambda_i)$, $(i = 1, \cdots, (n-1))$ and $|\alpha| > |\lambda_i|, \alpha \in \mathbb{R}\backslash\{0\}$ and the λ_i's are distinct.

Let us also define

$$B_d = \begin{bmatrix} B_1 \\ B_2 \end{bmatrix} \tag{3.3.5}$$

where $B_d \in \mathbb{R}^{n\times m}$, $B_1 \in \mathbb{R}^{(n-1)\times m}$, $B_2 \in \mathbb{R}^{1\times m}$ and

$$\begin{aligned} C_d &= \begin{bmatrix} c_1 \\ c_2 \\ \vdots \\ c_p \end{bmatrix} \\ &= \begin{bmatrix} c_{11} & c_{12} \\ c_{21} & c_{22} \\ \vdots & \vdots \\ c_{p1} & c_{p2} \end{bmatrix} \end{aligned} \tag{3.3.6}$$

where $C_d \in \mathbb{R}^{p\times n}$, $c_k \in \mathbb{R}^{1\times n}$, $c_{k1} \in \mathbb{R}^{1\times(n-1)}$ and $c_{k2} \in \mathbb{R}^1$.

Thus we have

$$\hat{C} = \begin{bmatrix} c_1 \exp(-A_d N_1^O T_1^O) \\ \vdots \\ c_1 \exp(-A_d T_1^O) \\ \vdots \\ c_p \exp(-A_d N_p^O T_p^O) \\ \vdots \\ c_p \exp(-A_d T_p^O) \end{bmatrix}$$

$$= \begin{bmatrix} c_{11} \exp(-A_1 N_1^O T_1^O) & c_{12} \exp(-\alpha N_1^O T_1^O) \\ \vdots & \vdots \\ c_{11} \exp(-A_1 T_1^O) & c_{12} \exp(-\alpha T_1^O) \\ \vdots & \\ c_{p1} \exp(-A_1 N_p^O T_p^O) & c_{p2} \exp(-\alpha N_p^O T_p^O) \\ \vdots & \vdots \\ c_{p1} \exp(-A_1 T_p^O) & c_{p2} \exp(-\alpha T_p^O) \end{bmatrix}$$

$$= \begin{bmatrix} c_{11} \exp(-A_1 T_0) & c_{12} \exp(-\alpha T_0) \\ \vdots & \vdots \\ c_{11} \exp(-\frac{A_1 T_0}{N_1^O}) & c_{12} \exp(-\frac{\alpha T_0}{N_1^O}) \\ \vdots & \vdots \\ c_{p1} \exp(-A_1 T_0) & c_{p2} \exp(-\alpha T_0) \\ \vdots & \vdots \\ c_{p1} \exp(-\frac{A_1 T_0}{N_p^O}) & c_{p2} \exp(-\frac{\alpha T_0}{N_p^O}) \end{bmatrix} \tag{3.3.7}$$

(Recall that $T_i^O = \frac{T_0}{N_i^O}$)

$$\hat{G} = \begin{bmatrix} c_1 \int_0^{-N_1^O T_1^O} \exp(A_d t) B_d \, dt \\ \vdots \\ c_1 \int_0^{-T_1^O} \exp(A_d t) B_d \, dt \\ \vdots \\ c_p \int_0^{-N_p^O T_p^O} \exp(A_d t) B_d \, dt \\ \vdots \\ c_p \int_0^{-T_p^O} \exp(A_d t) B_d \, dt \end{bmatrix}$$

$$= \begin{bmatrix} c_1 A_d^{-1}[\exp(-A_d N_1^O T_1^O) - I] B_d \\ \vdots \\ c_1 A_d^{-1}[\exp(-A_d T_1^O) - I] B_d \\ \vdots \\ c_p A_d^{-1}[\exp(-A_d N_p^O T_p^O) - I] B_d \\ \vdots \\ c_p A_d^{-1}[\exp(-A_d T_p^O) - I] B_d \end{bmatrix}$$

$$= \begin{bmatrix} \begin{bmatrix} c_{11} & c_{12} \end{bmatrix} \begin{bmatrix} A_1^{-1} & 0 \\ 0 & \frac{1}{\alpha} \end{bmatrix} \begin{bmatrix} \exp(-A_1 T_0) - I & 0 \\ 0 & \exp(-\alpha T_0) - 1 \end{bmatrix} \begin{bmatrix} B_1 \\ B_2 \end{bmatrix} \\ \vdots \\ \begin{bmatrix} c_{11} & c_{12} \end{bmatrix} \begin{bmatrix} A_1^{-1} & 0 \\ 0 & \frac{1}{\alpha} \end{bmatrix} \begin{bmatrix} \exp(-\frac{A_1 T_0}{N_1^O}) - I & 0 \\ 0 & \exp(-\frac{\alpha T_0}{N_1^O}) - 1 \end{bmatrix} \begin{bmatrix} B_1 \\ B_2 \end{bmatrix} \\ \vdots \\ \begin{bmatrix} c_{p1} & c_{p2} \end{bmatrix} \begin{bmatrix} A_1^{-1} & 0 \\ 0 & \frac{1}{\alpha} \end{bmatrix} \begin{bmatrix} \exp(-A_1 T_0) - I & 0 \\ 0 & \exp(-\alpha T_0) - 1 \end{bmatrix} \begin{bmatrix} B_1 \\ B_2 \end{bmatrix} \\ \vdots \\ \begin{bmatrix} c_{p1} & c_{p2} \end{bmatrix} \begin{bmatrix} A_1^{-1} & 0 \\ 0 & \frac{1}{\alpha} \end{bmatrix} \begin{bmatrix} \exp(-\frac{A_1 T_0}{N_p^O}) - I & 0 \\ 0 & \exp(-\frac{\alpha T_0}{N_p^O}) - 1 \end{bmatrix} \begin{bmatrix} B_1 \\ B_2 \end{bmatrix} \end{bmatrix}$$

$$= \begin{bmatrix} c_{11}A_1^{-1}(\exp(-A_1T_0) - I)B_1 + \frac{c_{12}}{\alpha}(\exp(-\alpha T_0) - 1)B_2 \\ \vdots \\ c_{11}A_1^{-1}(\exp(-\frac{A_1T_0}{N_1^O}) - I)B_1 + \frac{c_{12}}{\alpha}(\exp(-\frac{\alpha T_0}{N_1^O}) - 1)B_2 \\ \vdots \\ c_{p1}A_1^{-1}(\exp(-A_1T_0) - I)B_1 + \frac{c_{p2}}{\alpha}(\exp(-\alpha T_0) - 1)B_2 \\ \vdots \\ c_{p1}A_1^{-1}(\exp(-\frac{A_1T_0}{N_p^O}) - I)B_1 + \frac{c_{p2}}{\alpha}(\exp(-\frac{\alpha T_0}{N_p^O}) - 1)B_2 \end{bmatrix} \tag{3.3.8}$$

3.3.1 CASE I: $N_i^O = n_i^o$

In the previous section, we mentioned that when $N_i^O = n_i^o$, the state transition matrix M of the controller cannot be freely chosen. In this case, $\hat{C}$ is square and the design procedure is as follows:

1. Choose the closed-loop poles to be assigned and calculate the state feedback matrix F which realizes those poles;

2. Determine H uniquely by

$$H = F\hat{C}^{-1}; \tag{3.3.9}$$

3. Determine the state transition matrix M of the controller by

$$\begin{aligned} M &= H\hat{G} \\ &= F\hat{C}^{-1}\hat{G}. \end{aligned} \tag{3.3.10}$$

Now, we shall exhibit conditions under which $\hat{C}$ approaches a singular matrix. Observe first that when $T_0 \to 0$,

$$\hat{C} \to \begin{bmatrix} c_{11} & c_{12} \\ \vdots & \vdots \\ c_{11} & c_{12} \\ \vdots & \vdots \\ c_{p1} & c_{p2} \\ \vdots & \vdots \\ c_{p1} & c_{p2} \end{bmatrix}$$

Evidently, $\hat{C} \in \mathbb{R}^{\bar{N}^O \times \bar{N}^O}$ and we have $\sum_{i=1}^{p}(N_i^O - 1)$ rows identical. Now $N_i^O > 1$ for at least one i , else we do not have different input and output sampling rates; hence the limiting matrix is again singular.

Next, suppose that $\alpha > 0$ i.e. the plant is open-loop unstable. (Note that the conclusion above made no assumption concerning stability or instability). As $T_0 \to \infty$, the last column of $\hat{C}$ in (3.3.7) tends to zero and the limiting matrix is again singular.

We can also observe that as $\alpha \to \infty$, then

$$\hat{C} \to \begin{bmatrix} c_{11}\exp(-A_1T_0) & 0 \\ \vdots & \vdots \\ c_{11}\exp(-\frac{A_1T_0}{N_1^O}) & 0 \\ \vdots & \vdots \\ c_{p1}\exp(-A_1T_0) & 0 \\ \vdots & \vdots \\ c_{p1}\exp(-\frac{A_1T_0}{N_p^O}) & 0 \end{bmatrix}$$

and once again, we see that the limiting matrix is singular.

Let us indicate a subtle point regarding this result. Consider a SISO system, such that

$$c(sI - A)^{-1}b = \frac{n(s)}{d_1(s)(s+\alpha)}$$

with all coefficients of $n(s)$, $d_1(s)$ fixed and α variable. Then an easy calculation shows that $\|c_{11}\|$ depends inversely on α and $\|c_{12}\|$ is independent of α, if b_{11}, b_{12} are chosen independently of α. The whole transfer function goes to zero as $\alpha \to \infty$.

If, on the other hand,

$$c(sI - A)^{-1}b = \frac{[n_1(s) + \alpha n_2(s)]}{d_1(s)(s+\alpha)}$$

with $n_2(s)$ chosen so that the transfer function does not go to zero as $\alpha \to \infty$, then $\|c_{12}\| \to \infty$, again assuming b_{11}, b_{12} are chosen independently of α. In

either case when $\alpha \to \infty$, viz $n_2(s) = 0$ or $n_2(s)$ nonzero, the conclusion that $\hat{C}$ approaches a singular matrix as $\alpha \to \infty$ remains valid, despite the dependence of c_{11}, c_{12} on α. The conclusion obviously also applies to the multivariable case.

3.3.2 CASE II: $N_i^O > n_i^o$

For $N_i^O > n_i^o$, the state transition matrix M can be freely chosen. The design procedure is different from the previous case when $N_i^O = n_i^o$. Here, the procedure is as follows:

1. Choose the state transition matrix of the controller M so that it is stable;
2. Choose the closed-loop poles to be assigned and calculate the state feedback matrix F which realizes these poles;
3. Determine H by the following matrix equation

$$H = [F \quad M][\hat{C} \quad \hat{G}]^{-L}. \tag{3.3.11}$$

Now, we will study situations where $[\hat{C} \quad \hat{G}]$ approaches a matrix with deficient column rank. First, when $T_0 \to 0$,

$$[\hat{C} \quad \hat{G}] \to \begin{bmatrix} c_{11} & c_{12} & 0 \\ \vdots & \vdots & \vdots \\ c_{11} & c_{12} & 0 \\ \vdots & \vdots & \vdots \\ c_{p1} & c_{p2} & 0 \\ \vdots & \vdots & \vdots \\ c_{p1} & c_{p2} & 0 \end{bmatrix}$$

Obviously, the limiting matrix fails to have full column rank.

Next, suppose that $\alpha > 0$ (so that the plant is open-loop unstable). As $T_0 \to \infty$, the second last column of $\hat{C}$ goes to zero while other columns of

$[\hat{C}\ \hat{G}]$ may tend to infinity or zero or remains finite and nonzero. Thus one can anticipate that a left inverse of the matrix could become unbounded as $T_0 \to \infty$ and this is borne out by a later example.

Also as $\alpha \to \infty$,

$$[\hat{C}\ \hat{G}] \to \begin{bmatrix} c_{11}\exp(-A_1T_0) & 0 & c_{11}A_1^{-1}(\exp(-A_1T_0)-I)B_1+B_2 \\ \vdots & \vdots & \vdots \\ c_{11}\exp(-\frac{A_1T_0}{N_1^O}) & 0 & c_{11}A_1^{-1}(\exp(-\frac{A_1T_0}{N_1^O})-I)B_1+B_2 \\ \vdots & \vdots & \vdots \\ c_{p1}\exp(-A_1T_0) & 0 & c_{p1}A_1^{-1}(\exp(-A_1T_0)-I)B_1+B_2 \\ \vdots & \vdots & \vdots \\ c_{p1}\exp(-\frac{A_1T_0}{N_p^O}) & 0 & c_{p1}A_1^{-1}(\exp(-\frac{A_1T_0}{N_p^O})-I)B_1+B_2 \end{bmatrix} \tag{3.3.12}$$

The loss of column rank for the limiting matrix is evident.

3.4 Examples

To illustrate the above observations, we provide results for some stable and unstable plants in which T_0 tends to zero and infinity and α tends to infinity for each of the two cases.

Figure 3.4.1 is for the stable plant

$$A = \begin{bmatrix} -1 & 0 \\ 0 & -4 \end{bmatrix} \quad B = \begin{bmatrix} -1.5 \\ 1 \end{bmatrix} \quad C = \begin{bmatrix} 1 & 4.5 \end{bmatrix}$$

with transfer function given by $\frac{3(s-0.5)}{(s+1)(s+4)}$. Since the plant has an observability index of 2, let the output-rate multiplicity be $N_1^O = 2$. The graph shows that when T_0 tends to zero, entries of the gain vector H blow up. The entries remain finite when T_0 becomes large.

Figure 3.4.2 is for the unstable plant

$$A = \begin{bmatrix} 1 & 0 \\ 0 & 4 \end{bmatrix} \quad B = \begin{bmatrix} -0.5 \\ 1 \end{bmatrix} \quad C = \begin{bmatrix} 1 & 3.5 \end{bmatrix}$$

with transfer function given by $\frac{3(s-0.5)}{(s-1)(s-4)}$. Again, since the plant has an observability index of 2, let the output-rate multiplicity be $N_1^O = 2$ for case I. The

graph shows that when T_0 is too small or too big, entries of the gain vector H blow up.

The previous two graphs show the effect of T_0 on stable and unstable plants with fixed α. Figure 3.4.3 shows the effect of varying α with fixed T_0 for

$$A = \begin{bmatrix} 1 & 0 \\ 0 & \alpha \end{bmatrix} \quad B = \begin{bmatrix} -0.5 \\ 1 \end{bmatrix} \quad C = \begin{bmatrix} 1 & \alpha - 0.5 \end{bmatrix}$$

with transfer function given by $\frac{(\alpha-1)(s-0.5)}{(s-1)(s-\alpha)}$. Again, since the plant has an observability index of 2, we choose the output-rate multiplicity as $N_1^O = 2$ for case I. When α is too large, entries of H blow up. The graph also shows that when α is close to 1, entries of H blow up. This is due to the fact that the plant loses controllability when $\alpha = 1$ and so pole shifting becomes impossible.

For case II, Figures 3.4.4, 3.4.5 and 3.4.6 illustrate the effect of varying T_0 and α for stable and unstable plants.

Figure 3.4.4 is for

$$A = \begin{bmatrix} -1 & 0 \\ 0 & -4 \end{bmatrix} \quad B = \begin{bmatrix} -1.5 \\ 1 \end{bmatrix} \quad C = \begin{bmatrix} 1 & 4.5 \end{bmatrix}$$

with transfer function given by $\frac{3(s-0.5)}{(s+1)(s+4)}$. Since the plant has an observability index of 2, let the output-rate multiplicity be $N_1^O = 3$. The graph shows that when T_0 tends to zero. entries of the gain vector H blow up.

Figure 3.4.5 is for

$$A = \begin{bmatrix} 1 & 0 \\ 0 & 4 \end{bmatrix} \quad B = \begin{bmatrix} -0.5 \\ 1 \end{bmatrix} \quad C = \begin{bmatrix} 1 & 3.5 \end{bmatrix}$$

with transfer function given by $\frac{3(s-0.5)}{(s-1)(s-4)}$. Since the plant has an observability index of 2, we take the output-rate multiplicity as $N_1^O = 3$. The graph shows that when T_0 tends to zero or a very large value, entries of the gain vector H again blow up.

Figure 3.4.6 is for

$$A = \begin{bmatrix} 1 & 0 \\ 0 & \alpha \end{bmatrix} \quad B = \begin{bmatrix} -0.5 \\ 1 \end{bmatrix} \quad C = \begin{bmatrix} 1 & \alpha - 0.5 \end{bmatrix}$$

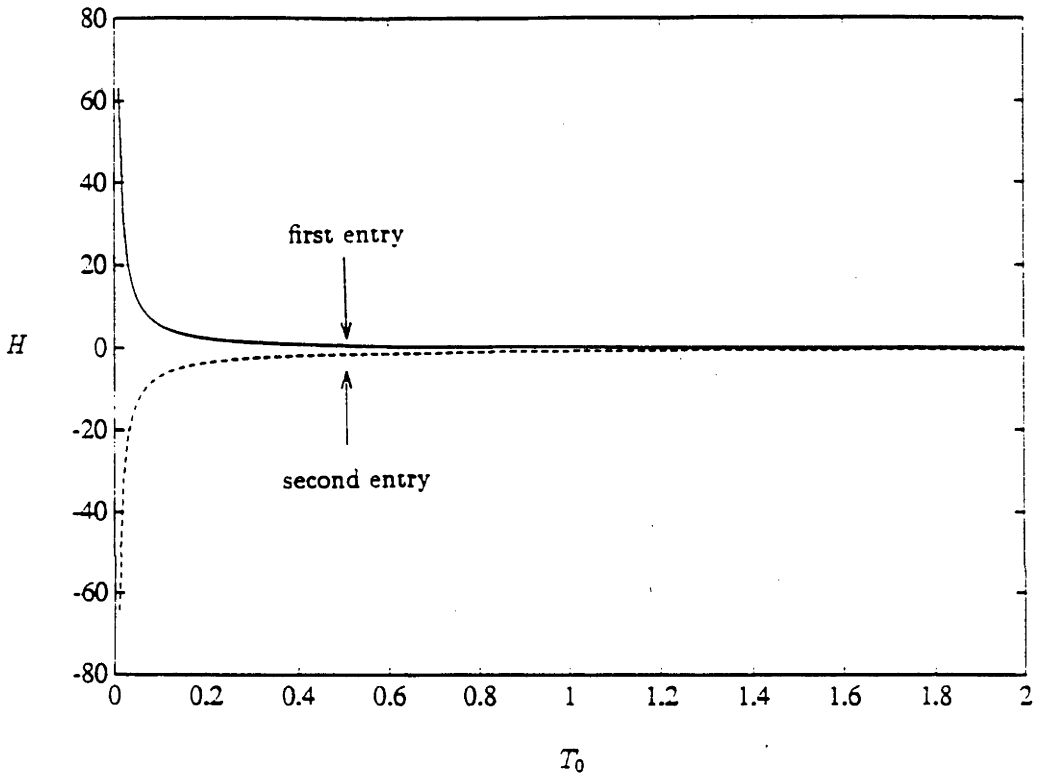

Figure 3.4.1: Entries of Gain Vector H vs Frame Period T_0 for

$$A = \begin{bmatrix} -1 & 0 \\ 0 & -4 \end{bmatrix} \quad B = \begin{bmatrix} -1.5 \\ 1 \end{bmatrix} \quad C = \begin{bmatrix} 1 & 4.5 \end{bmatrix}$$

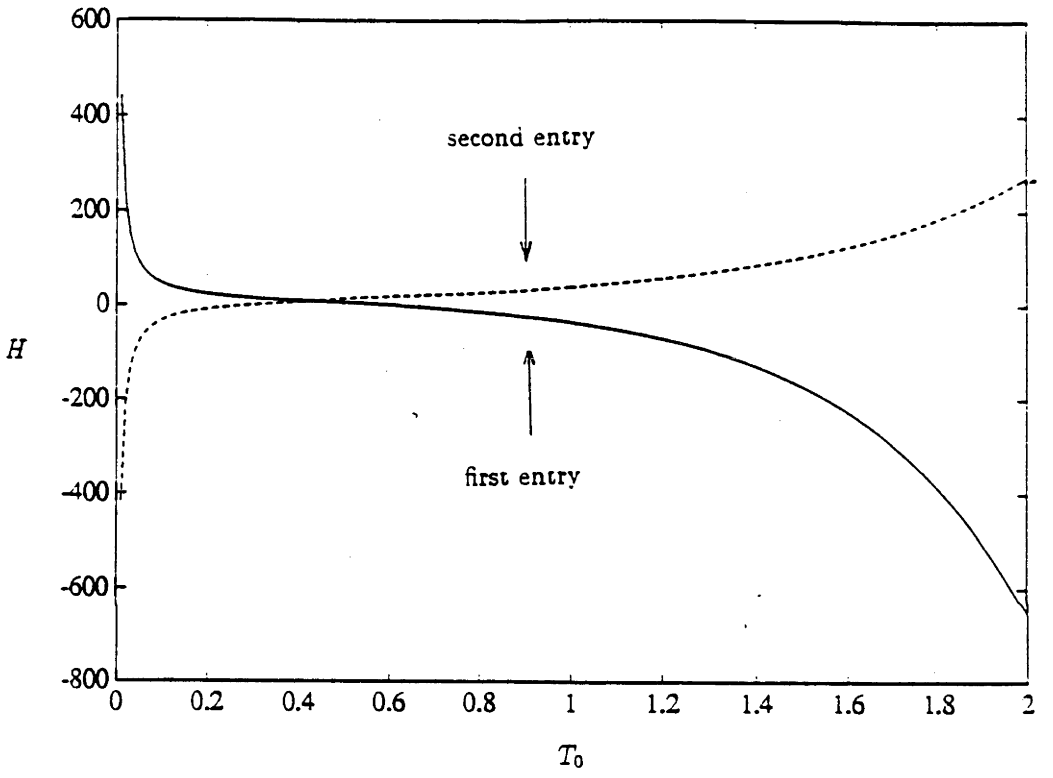

Figure 3.4.2: Entries of Gain Vector H vs Frame Period T_0 for

$$A = \begin{bmatrix} 1 & 0 \\ 0 & 4 \end{bmatrix} \quad B = \begin{bmatrix} -0.5 \\ 1 \end{bmatrix} \quad C = \begin{bmatrix} 1 & 3.5 \end{bmatrix}$$

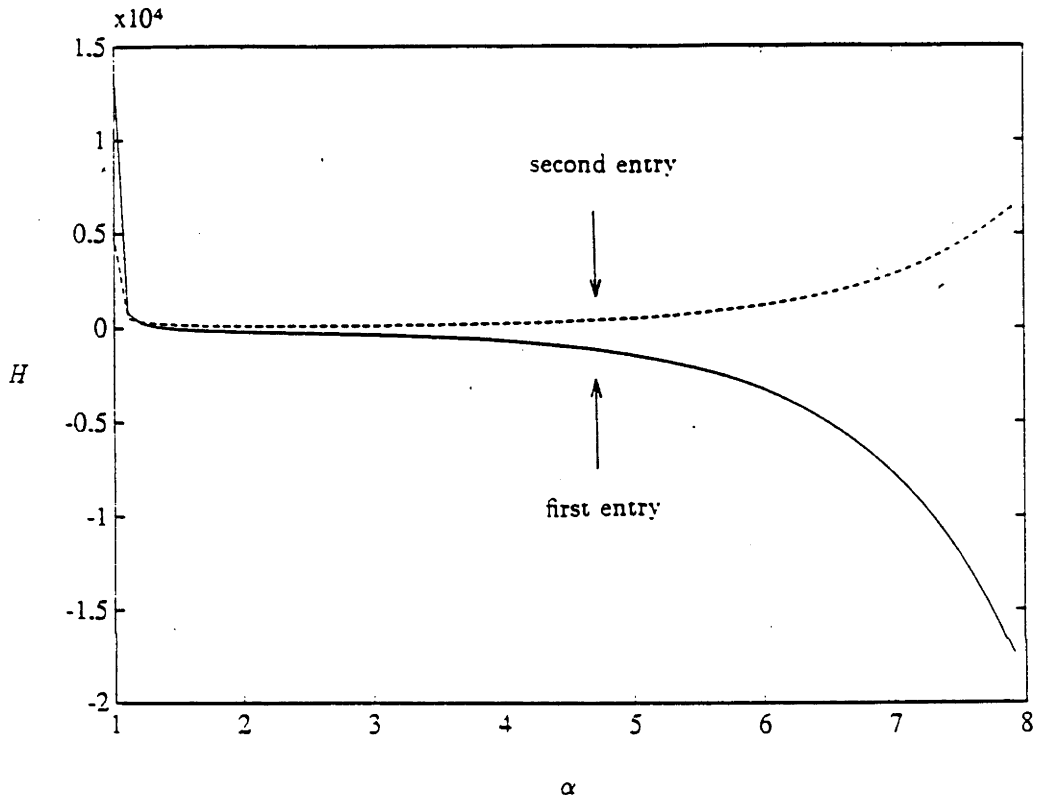

Figure 3.4.3: Entries of Gain Vector H vs Largest Mode α for

$$A = \begin{bmatrix} 1 & 0 \\ 0 & \alpha \end{bmatrix} \quad B = \begin{bmatrix} -0.5 \\ 1 \end{bmatrix} \quad C = \begin{bmatrix} 1 & \alpha - 0.5 \end{bmatrix}$$

with transfer function given by $\frac{(\alpha-1)(s-0.5)}{(s-1)(s-\alpha)}$. Take $N_1^O = 3$ with observability index of 2. The graph shows that when α tends to a very large value, entries of the gain vector H blow up.

3.5 Approaches To Avoid Problems

In this section, we indicate some rules of thumb that will ensure that excessive gain values are avoided for case I and case II.

3.5.1 CASE I: $N_i^O = n_i^o$

Effect of $T_0 \rightarrow 0$

Suppose (without loss of generality) that $\alpha > |\lambda_i|$, $i = 1, 2, \cdots, (n-1)$. When

$$T_0 \; < \; \frac{1}{20\alpha} \tag{3.5.1}$$

then $\exp(\alpha T_0) \simeq 1$ and the rest of the exponential terms $\exp(\frac{\alpha T_0}{N_i^O})$ and $\exp(-\frac{A_1 \mu T_0}{N_i^O})$, $\mu = 1, \cdots, (N_i^O - 1)$ appearing in $\hat{C}$ in (3.3.7) will also be approximately 1 i.e. $\hat{C}$ will be close to singular. Therefore, for proper operation of MROC's

$$\begin{aligned} T_0 \; &\geq \; \frac{1}{20\alpha} \\ \Rightarrow \quad \omega_0 \; &\leq \; 40\pi\alpha \; (rad/s) \end{aligned} \tag{3.5.2}$$

Note that this gives an upper-bound on the sampling frequency while the sampling theorem gives a lower-bound in that ω_0 must be at least two times the closed-loop bandwidth (In practice, a larger multiple value must be assumed).

Effect of $T_0 \rightarrow \infty$ for $\alpha > 0$

Examination of the last column of (3.3.7) shows that it will have very small entries when $T_0 > \frac{4N_{imax}}{\alpha}$. Here, $N_{imax} = max_{1 \leq i \leq p} N_i^O$. Accordingly, to avoid

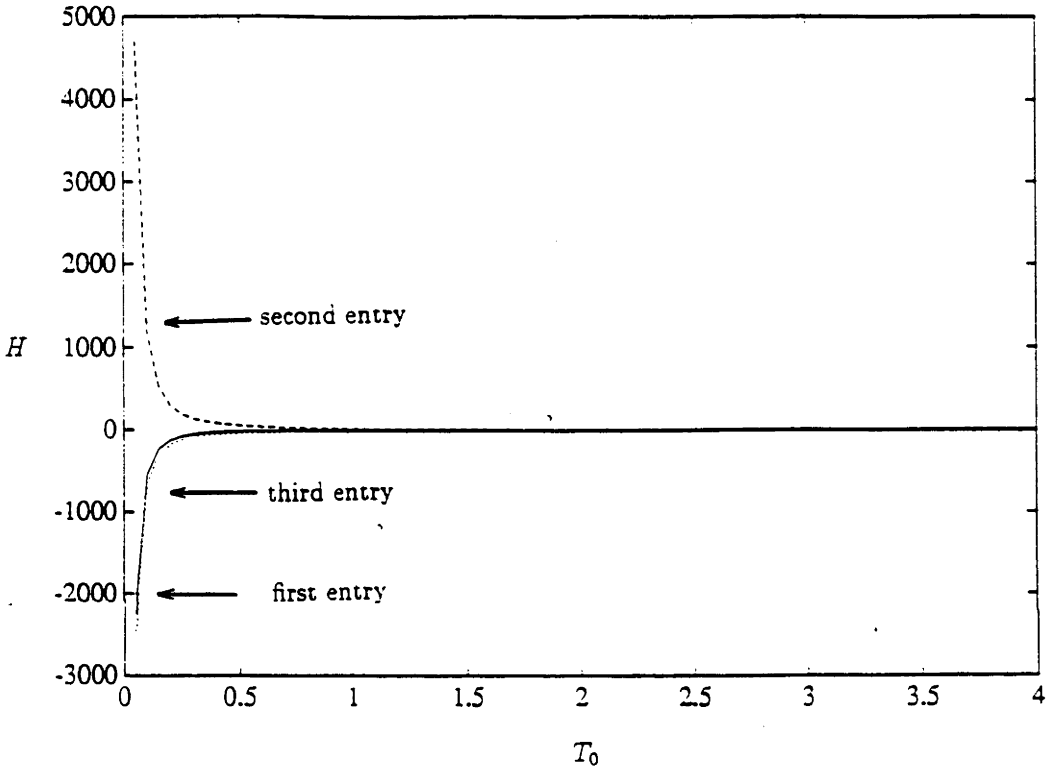

Figure 3.4.4: Entries of Gain Vector H vs Frame Period T_0 for

$$A = \begin{bmatrix} -1 & 0 \\ 0 & -4 \end{bmatrix} \quad B = \begin{bmatrix} -1.5 \\ 1 \end{bmatrix} \quad C = \begin{bmatrix} 1 & 4.5 \end{bmatrix}$$

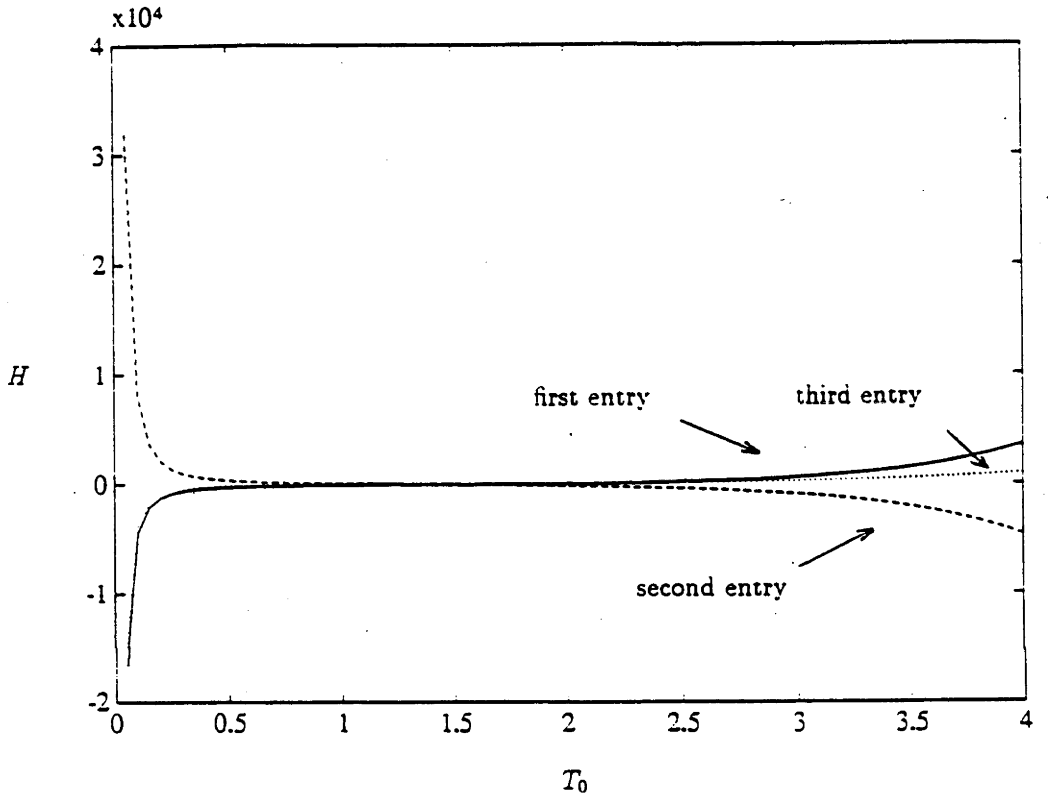

Figure 3.4.5: Entries of Gain Vector H vs Frame Period T_0 for

$$A = \begin{bmatrix} 1 & 0 \\ 0 & 4 \end{bmatrix} \quad B = \begin{bmatrix} -0.5 \\ 1 \end{bmatrix} \quad C = \begin{bmatrix} 1 & 3.5 \end{bmatrix}$$

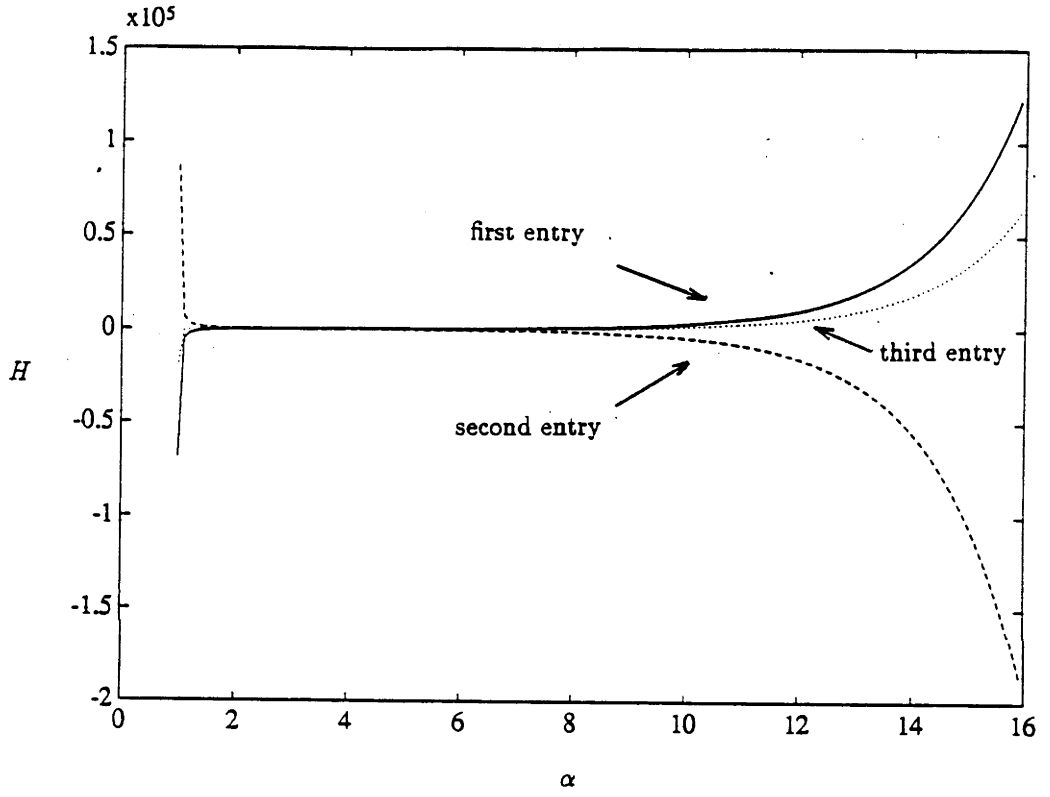

Figure 3.4.6: Entries of Gain Vector H vs Largest Mode α for

$$A = \begin{bmatrix} 1 & 0 \\ 0 & \alpha \end{bmatrix} \quad B = \begin{bmatrix} -0.5 \\ 1 \end{bmatrix} \quad C = \begin{bmatrix} 1 & \alpha - 0.5 \end{bmatrix}$$

problems, we want

$$\begin{aligned} T_0 &< \frac{4N_{imax}}{\alpha} \\ \Rightarrow \quad \omega_0 &> \frac{\pi\alpha}{2N_{imax}} \end{aligned} \tag{3.5.3}$$

This means that there are two constraints setting an lower-bound for ω_0, viz. the sampling theorem constraint requires that ω_0 exceed twice the closed-loop bandwidth as well as (3.5.3). Notice that (3.5.3) can also be regarded as a statement concerning a fast sampling frequency, viz. the sampling frequency $\omega_i = N_i^O \omega_0$ associated with the output for which N_i^O is maximum; calling this frequency ω_{imax}, (3.5.3) is equivalent to

$$\omega_{imax} > \frac{\pi\alpha}{2} \tag{3.5.4}$$

which is again a sort of sampling theorem.

Effect of $\alpha \to \infty$

When $\alpha > \frac{4N_{imax}}{T_0}$, $\exp(-\alpha T_0) \simeq 0$ and the last column of $\hat{C}$ in (3.3.7) will also be approximately zero. Thus for unstable plants with a fixed T_0, to ensure proper operation of the plant

$$\alpha < \frac{4N_{imax}}{T_0} \tag{3.5.5}$$

This is the same constraint as (3.5.3).

3.5.2 CASE II: $N_i^O > n_i^o$

Examination of the cases $T_0 \to 0$, $T_0 \to \infty$ for stable and unstable plants respectively and $\alpha \to \infty$ for unstable plants reveals that exactly the same constraint on T_0 *et al* apply for case II as apply for case I.

To summarize, (3.5.2) sets a lower-bound on T_0 in terms of the mode furthest from the origin whether or not the plant is stable while (3.5.3) sets an upper-bound on the product αT_0 when α is an unstable mode; this latter bound involves the maximum of the N_i^O's.

3.6 Summary

In this chapter, the potential problems of the MROC's are identified and approaches to avoid the problems are provided. For proper operation of the MROC, the authors of [33] have pointed out that N_i^O should be chosen sufficiently large. Here, we show that in addition to this, the frame period of the MROC, T_0 has to be chosen sufficiently large but for unstable plants not too large. Violation of the guidelines will mean that controller gains will be unacceptably large, leading to such problems as noise amplification in the controller. Section 3.4 contains quantitative guidelines.

Chapter 4

Performance Study of Multirate Output Controllers Under Noise Disturbances

4.1 Introduction

In this chapter, we study the performance of MROC's under disturbances such as process and/or measurement noise. In the previous chapter, we show that the frame periods and output sampling periods must fulfill certain inequality constraints to avoid the gains in the controller in becoming very large; here, we seek to identify yet another drawback of MROC's under noise disturbances. We show that the MROC law performs poorer than two LQG laws, termed LQG law I and LQG law II, in the presence of noise disturbances. Note that the LQG law here is in discrete-time and is associated with the equivalent discrete-time model of the underlying continuous-time plant; LQG law I uses a one-step prediction estimate of the state (so that the present control depends on measurements prior to the present time); LQG law II uses a true filtered estimate of the state (so that the present control depends on measurements prior to and at the present time). The basis of comparison is to apply the two types of LQG law to a LTI continuous-time plant with white, gaussian measurement and process noise and compute the optimal linear quadratic performance index for the discretized

plant. Next, the MROC law used in [33], seeking to implement the same state feedback law as the two LQG laws, is applied to the same plant. The equivalent noise matrices and performance index for the discretized plant with MROC law are then calculated. Simulation results show that the two types of LQG law perform better than the MROC law for a typical plant.

This chapter is organised as follows. Section 4.2 describes the LQG and MROC problem. Specifically, we formulate the underlying continuous-time model based upon which the equivalent discrete-time models for using LQG law and MROC law are derived. In Section 4.3, the performance indices for using the MROC law and LQG law I are computed. The performance index associated with the MROC law is formulated in a form similar to that associated with the LQG law. Section 4.4 presents a typical industrial plant to demonstrate that the MROC law has poorer performance than LQG law I and LQG law II. Section 4.5 contains concluding remarks.

4.2 The LQG and MROC Problem

One prime concern here will be to compare the two types of LQG law and the MROC law. At time $(k+1)T_0$, the two LQG laws feed back a linear feedback gain times an estimate of $x(\overline{k+1})T_0$. In the case of LQG law I, this estimate is obtained from measurements at times $\cdots, (k-2)T_0, (k-1)T_0$ and kT_0. For LQG law II, the estimate is obtained from measurements at times $\cdots, (k-2)T_0, (k-1)T_0, kT_0$ and $\overline{k+1}T_0$. By contrast, the MROC law uses a different set of measurements; for each i, the i^{th} plant output values at times $kT_0, kT_0+T_i^O, kT_0+2T_i^O, \cdots, (k+1)T_0-T_i^O$ are used where $T_i^O = T_0/N_i^O$, with T_0 the frame period and N_i^O the i^{th} output-rate multiplicity. Further, as it turns out, the MROC can be regarded as using these measurements to generate a (non-optimal) estimate of $x(\overline{k+1})T_0$ which is then multiplied by the same feedback gain as used in the two LQG laws. In comparison to LQG law I, the MROC

law uses more recent measurements, but uses a lesser number of measurements. In comparison to LQG law II, it uses mostly more recent measurements. It is therefore not a priori obvious on the basis of the measurement strategies whether an MROC law will be inferior or superior to the LQG laws. The MROC law also uses its measurements non-optimally in comparison with the LQG laws. Of course, the LQG law II always performs better than the LQG law I, since a current estimation-type Kalman filter always performs better than a one-step ahead prediction-type Kalman filter.

4.2.1 Continuous-time Plant Model

To fix ideas, we consider the following plant model which is a continuous-time FDLTI system given by

$$\dot{x}(t) = Ax(t) + Bu(t) + \omega_u(t) \tag{4.2.1}$$

$$y(t) = Cx(t) + \omega_y(t) \tag{4.2.2}$$

where the state vector $x \in \mathbb{R}^n$, the control $u \in \mathbb{R}^m$, the process noise $\omega_u \in \mathbb{R}^n$, the measurement vector $y \in \mathbb{R}^p$ and the measurement noise $\omega_y \in \mathbb{R}^p$. The initial condition $x(0)$ is a zero mean random vector with variance $E\{x(0)x'(0)\} = P_0$. The process disturbances $\omega_u(t)$ and $\omega_y(t)$ are assumed to be zero mean independent white noise processes with intensities $\Omega_u \geq 0$ and $\Omega_y \geq 0$.

As the output of the plant is contaminated by process noise (via the state) and measurement noise, the output needs to be filtered prior to sampling. This prefiltering is necessary to remove high frequency components which can confuse the interpretation of the sampled signal due to aliasing. The type of prefilter used for this purpose is called an analog anti-aliasing filter (AAF). There are many types of AAF's and a good discussion of them can be found in [10], [28], and [57]. For simplicity, we consider passing each entry of the plant output through an AAF of the low-pass filter type, i.e. one with transfer function

given by

$$H_{aa}(s) = \frac{\alpha}{s+\alpha} \tag{4.2.3}$$

where α is the bandwidth of the filter. Here the nominal α is chosen to be $\omega_s/2$ as a rule of thumb where $\omega_s = 2\pi/T_0$ with T_0 being the frame period. Note that the AAF is required even if there is only process noise and no measurement noise.

It is not difficult to see that the cascade of the plant with an AAF can be defined by the following augmented system:

$$\dot{\tilde{x}}(t) = \tilde{A}\tilde{x}(t) + \tilde{B}u(t) + \tilde{B}_1\tilde{\omega}_u(t) \tag{4.2.4}$$

$$\tilde{y}(t) = \tilde{C}\tilde{x}(t) \tag{4.2.5}$$

where

$$\tilde{A} = \begin{bmatrix} A & 0 \\ \alpha C & -\alpha I \end{bmatrix} \tag{4.2.6}$$

$$\tilde{B} = \begin{bmatrix} B \\ 0 \end{bmatrix} \tag{4.2.7}$$

$$\tilde{B}_1 = \begin{bmatrix} I & 0 \\ 0 & \alpha I \end{bmatrix} \tag{4.2.8}$$

$$\tilde{C} = [0 \quad I] \tag{4.2.9}$$

$$\tilde{x}(t) = \begin{bmatrix} x(t) \\ y_f(t) \end{bmatrix} \tag{4.2.10}$$

$$\tilde{\omega}_u(t) = \begin{bmatrix} \omega_u(t) \\ \omega_y(t) \end{bmatrix} \tag{4.2.11}$$

and $\tilde{\omega}_u(t)$ has covariance

$$E[\tilde{\omega}_u(t)\tilde{\omega}_u'(s)] = \tilde{\Omega}_u\delta(t-s) = \begin{bmatrix} \Omega_u & 0 \\ 0 & \Omega_y \end{bmatrix}\delta(t-s) \tag{4.2.12}$$

The conventional discrete-time system will be obtained by sampling $\tilde{y}(t)$ every T_0 seconds and applying an input $u(.)$, which is a pulse amplitude modulated signal defined below, to (4.2.4)-(4.2.5).

$$u(t) = \sum_k u_d(k)p(t-kT_0) \qquad k = 1, 2, \cdots \tag{4.2.13}$$

where $p(t) = 1$ for $0 \leq t < T_0$ but is otherwise zero. The MROC system is obtained by using the same style of input, but by sampling the output a number of times in an interval of length T_0.

4.2.2 Equivalent Discrete-time Model of Augmented System

Conventional sampling of the model (4.2.4)-(4.2.5) yields the discrete time model

$$\tilde{x}_d(k+1) = F\tilde{x}_d(k) + Gu_d(k) + \omega_{ud}(k) \tag{4.2.14}$$

$$\tilde{y}_d(k) = \tilde{C}\tilde{x}_d(k) \tag{4.2.15}$$

where

$$F = \exp(\tilde{A}T_0) \tag{4.2.16}$$

$$G = \int_0^{T_0} \exp(\tilde{A}\sigma)\tilde{B}d\sigma \tag{4.2.17}$$

$$\omega_{ud}(k) = \int_0^{T_0} \exp[\tilde{A}(T_0 - \sigma)]\tilde{B}_1\tilde{\omega}_u(\sigma + kT_0)d\sigma \tag{4.2.18}$$

The process $\omega_{ud}(k)$ is zero mean and white with

$$E\{\omega_{ud}(k)\omega'_{ud}(l)\} = \int_0^{T_0} \exp(\tilde{A}\tau)\tilde{B}_1\tilde{\Omega}_u\tilde{B}_1' \exp(\tilde{A}'\tau)\delta_{kl}d\tau \geq 0 \tag{4.2.19}$$

$$= \hat{Q}\delta_{kl}$$

4.2.3 Equivalent MROC Model of Augmented System

Before describing the model when noise is present, we recall the construction applicable in the noiseless case. This construction is applied to the system (4.2.4)-(4.2.5) and it is crucial (and therefore assumed) that this system is observable. Let us therefore note the following simple result.

Lemma 4.2.1 *Consinder the systems (4.2.1)-(4.2.2) and (4.2.14)-(4.2.15) with the pairs (A, C) and $(\tilde{A}, \tilde{C})$ related as in (4.2.6)-(4.2.11). Then (A, C) is observable if and only if $(\tilde{A}, \tilde{C})$ is observable.*

Proof: Define

$$O(C,A) \triangleq [C' \;\; A'C' \;\; \cdots \;\; A'^{(n-1)}C']$$
$$O_a(\tilde{C},\tilde{A}) \triangleq [\tilde{C}' \;\; \tilde{A}'\tilde{C}' \;\; \cdots \;\; \tilde{A}'^{(n-1)}\tilde{C}']$$

then substituting $\tilde{C}$ and $\tilde{A}$ into $O_a(\tilde{C}, \tilde{A})$ gives

$$O_a(\tilde{C},\tilde{A}) = \begin{bmatrix} 0 & \alpha C' & \alpha A'C' - \alpha^2 C' & \cdots \\ I & -\alpha I & \alpha^2 I & \cdots \\ & & \alpha A'^{(n+p-2)}C' - \alpha^2 A'^{(n+p-3)}C' + \cdots + (-1)^{(n+p-2)}\alpha^{(n+p-1)}C' \\ & & (-1)^{(n+p-1)}\alpha^{(n+p-1)}I \end{bmatrix}$$

Next, elementary column operations give

$$O_a(\tilde{C},\tilde{A}) = \begin{bmatrix} 0 & \alpha C' & \alpha A'C' & \cdots & \alpha A'^{(n+p-2)}C' \\ I & 0 & 0 & \cdots & 0 \end{bmatrix}$$

It is then easy to see that

$$\text{rank}\{O_a(\tilde{C},\tilde{A})\} = n+p \iff \text{rank}\{O(C,A)\} = n$$

i.e. (C, A) is observable $\iff$ $(\tilde{C}, \tilde{A})$ is observable. □

Sampling rates for the different entries of the output $\tilde{y}(t)$ of (4.2.5) need to be defined. Let us suppose that the i^{th} entry of $\tilde{y}(t)$ is sampled N_i^O times in each interval T_0 i.e. its sampling interval is $T_i^O = T_0/N_i^O$. Every T_0 seconds, the input changes and all outputs are synchronously sampled; additional output samples are taken before another T_0 seconds elapses. Further, $\sum N_i^O \geq n$.

It follows that, in the noiseless case,

$$\tilde{y}_i(kT_0 + jT_i^O) = \tilde{c}_i \exp(j\tilde{A}T_i^O)\tilde{x}_d(k) + \tilde{c}_i \int_0^{jT_i^O} \exp(\tilde{A}\sigma)\tilde{B}d\sigma u_d(k) \quad (4.2.20)$$

where $\tilde{x}_d(k) \triangleq \tilde{x}(\overline{k+1}T_0)$ and $\tilde{c}_i$ is the i^{th} row of $\tilde{C}$, $i = 1, 2, \cdots, p$ and $j = 1, 2, \cdots, (N_i^O - 1)$.

Since in the noiseless case

$$\tilde{x}_d(k+1) = F\tilde{x}_d(k) + Gu_d(k) \tag{4.2.21}$$

with F invertible, one can express all the output samples collected in $[kT_0, \overline{k+1}T_0)$, $k = 0, 1, 2, \cdots$ as a linear combination not of $\tilde{x}_d(k)$ and $u_d(k)$, but of $\tilde{x}_d(k+1)$ and $u_d(k)$ as in (4.2.20), so that,

$$\bar{y}_d(k) = \hat{C}\tilde{x}_d(k+1) + \hat{G}u_d(k) \tag{4.2.22}$$

where

$$\bar{y}_d(k) = \begin{bmatrix} \tilde{y}_1(kT_0) \\ \vdots \\ \tilde{y}_1(kT_0 + \overline{N_1^O - 1}T_1^O) \\ \vdots \\ \tilde{y}_p(kT_0) \\ \vdots \\ \tilde{y}_p(kT_0 + \overline{N_p^O - 1}T_p^O) \end{bmatrix} \tag{4.2.23}$$

$$\hat{C} = \begin{bmatrix} \tilde{c}_1 \exp(-\tilde{A}N_1^O T_1^O) \\ \vdots \\ \tilde{c}_1 \exp(-\tilde{A}T_1^O) \\ \vdots \\ \tilde{c}_p \exp(-\tilde{A}N_p^O T_p^O) \\ \vdots \\ \tilde{c}_p \exp(-\tilde{A}T_p^O) \end{bmatrix} \tag{4.2.24}$$

$$\hat{G} = \begin{bmatrix} \tilde{c}_1 \int_0^{-N_1^O T_1^O} \exp(\tilde{A}t)\tilde{B}dt \\ \vdots \\ \tilde{c}_1 \int_0^{-T_1^O} \exp(\tilde{A}t)\tilde{B}dt \\ \vdots \\ \tilde{c}_p \int_0^{-N_p^O T_p^O} \exp(\tilde{A}t)\tilde{B}dt \\ \vdots \\ \tilde{c}_p \int_0^{-T_p^O} \exp(\tilde{A}t)\tilde{B}dt \end{bmatrix} \tag{4.2.25}$$

The reason for obtaining (4.2.22) is that it serves as the basis for defining a feedback law; this point is reviewed subsequently. Note that the observability assumption implies that $\hat{C}$ has full column rank i.e. has a left inverse, see [33].

Now, we aim to indicate the changes to (4.2.21) and (4.2.22) when noise is included. The change to (4.2.21) has already been recorded in (4.2.14). To obtain the change to (4.2.22), consider first the variation to (4.2.20). It easily follows from (4.2.4)-(4.2.5) that

$$\begin{aligned}\tilde{y}_i(kT_0 + jT_i^O) &= \hat{c}_i \exp(j\hat{A}T_i^O)\tilde{x}_d(k) + \tilde{c}_i \int_0^{jT_i^O} \exp(\tilde{A}\sigma)\tilde{B}d\sigma u_d(k) \\ &\quad + \hat{c}_i \int_{kT_0}^{kT_0+jT_i^O} \exp[\tilde{A}(kT_0 + jT_i^O - \sigma)]\tilde{B}_1\tilde{\omega}_u(\sigma)d\sigma \quad (4.2.26)\end{aligned}$$

The third summand reflects the noise. However, an additional noise term enters when we seek to replace $\tilde{x}_d(k)$ in (4.2.26) using (4.2.14):

$$\tilde{x}_d(k) = F^{-1}\tilde{x}_d(k+1) - F^{-1}Gu_d(k) - F^{-1}\int_0^{T_0} \exp[\tilde{A}(T_0 - \sigma)]\tilde{B}_1\tilde{\omega}_u(\sigma + kT_0)d\sigma \quad (4.2.27)$$

The overall result is

$$\bar{y}_d(k) = \hat{C}\tilde{x}_d(k+1) + \hat{G}u_d(k) + \omega_{\bar{y}}(k) \quad (4.2.28)$$

where

$$\omega_{\bar{y}}(k) = \begin{bmatrix} \tilde{c}_1 \int_0^{-N_1^O T_1^O} \exp(\tilde{A}t)\tilde{B}_1\tilde{\omega}_u(kT_0 + T_1^O - t)\,dt \\ \vdots \\ \tilde{c}_1 \int_0^{-T_1^O} \exp(\tilde{A}t)\tilde{B}_1\tilde{\omega}_u(kT_0 + (N_1^O - 1)T_1^O - t)\,dt \\ \vdots \\ \tilde{c}_p \int_0^{-N_p^O T_p^O} \exp(\tilde{A}t)\tilde{B}_1\tilde{\omega}_u(kT_0 + T_p^O - t)\,dt \\ \vdots \\ \tilde{c}_p \int_0^{-T_p^O} \exp(\tilde{A}t)\tilde{B}_1\tilde{\omega}_u(kT_0 + (N_p^O - 1)T_p^O - t)\,dt \end{bmatrix} \quad (4.2.29)$$

4.2.4 Comparison of Feedback Law Implementation

Suppose that our desire is to implement, to the best extent possible, a discrete-time feedback law

$$u_d(k) = -L\tilde{x}_d(k) \tag{4.2.30}$$

(which may be derived by minimizing a linear-quadratic law). With the conventional discrete time system, (4.2.30) is replaced by either

$$u_d(k) = -L\hat{\tilde{x}}_d(k/k) \tag{4.2.31}$$

or

$$u_d(k) = -L\hat{\tilde{x}}_d(k/\overline{k-1}) \tag{4.2.32}$$

where $\hat{\tilde{x}}_d(k/k)$ and $\hat{\tilde{x}}_d(k/\overline{k-1})$ are the true filtered estimates, and one-step ahead predicted estimate of $\tilde{x}_d(k)$, generated using a Kalman filter.

To understand the arrangement for the MROC case with noise, we recall first the noiseless case in [33]. A controller of the form

$$u_d(k+1) = Mu_d(k) - H\bar{y}_d(k) \tag{4.2.33}$$

is adopted. Note that it is causal (in fact strictly causal). In the light of (4.2.22), this means that

$$u_d(k+1) = Mu_d(k) - H\hat{C}\tilde{x}_d(k+1) - H\hat{G}u_d(k) \tag{4.2.34}$$

Accordingly, the choice of H so that

$$H\hat{C} = L \tag{4.2.35}$$

(i.e. $H = L\hat{C}^{-L}$, with $\hat{C}^{-L}$ a left inverse for $\hat{C}$) and then M so that

$$M = H\hat{G} \tag{4.2.36}$$

yields (4.2.30) (with time index adjusted by 1).

In the noisy case, since obviously we need to work with measurable quantities, we adopt the same controller (4.2.33), with (4.2.35) and (4.2.36) still determining H and M. Now, however, (4.2.34) does not hold. Rather, from (4.2.28), what is actually implemented, is

$$\begin{aligned} u_d(k+1) &= Mu_d(k) - H\hat{C}\tilde{x}_d(k+1) - H\hat{G}u_d(k) - H\omega_{\bar{y}}(k) \\ &= -L\tilde{x}_d(k+1) - H\omega_{\bar{y}}(k) \end{aligned} \tag{4.2.37}$$

Evidently, noise is perturbing the correct feedback signal, so that, as with the conventional approach of (4.2.30), the feedback is inexact. The actual error in the feedback signal is however different in (4.2.33) to that in (4.2.30).

Note that because $H = L\hat{C}^{-L}$, we can rewrite (4.2.37) as

$$u_d(k+1) = -L[\tilde{x}_d(k+1) + \hat{C}^{-L}\omega_{\bar{y}}(k)] \tag{4.2.38}$$

This has the interpretation that we are using an estimate of $\tilde{x}_d(k+1)$ with error $\hat{C}^{-L}\omega_{\bar{y}}(k)$, as opposed to $\tilde{x}_d(k+1)$ itself, in the linear feedback law.

In summary, the following observation can be made about the two different systems. For the conventional system, the state estimate used in $u_d(k)$ depends on samples of $\tilde{y}(t)$ at times T_0 apart i.e. on either $\cdots, \tilde{y}[(k-j)T_0], \tilde{y}[(k-j+1)T_0], \cdots, \tilde{y}[(k-1)T_0]$ or on $\cdots, \tilde{y}[(k-j)T_0], \tilde{y}[(k-j+1)T_0], \cdots, \tilde{y}[(k-1)T_0], \tilde{y}(kT_0)$. For the MROC system, in effect we are also using a state estimate, computed using a different set of measurements. If $N_1^O = N_2^O = \cdots = N^O$, these are $\tilde{y}[(k-1)T_0], \tilde{y}[(k-1+\frac{1}{N^O})T_0], \cdots, \tilde{y}[(k-1+\frac{N^O-1}{N^O})T_0]$. This latter estimate is not necessarily optimal. Hence, there is no obvious comparison of the quality of the estimates, since it is not the case that one set of measurements includes the other.

4.3 Performance Comparison

In order to compare the performance of the non-MROC and MROC schemes, we shall use as an underlying criterion an LQG index. Thus we shall suppose that there is prescribed a performance index.

$$J = \lim_{N\to\infty} \frac{1}{N} E\{\sum_{k=0}^{N-1} [\tilde{x}_d'(k)Q\tilde{x}_d(k) + u_d'(k)Ru_d(k)]\} \tag{4.3.1}$$

This index may arise by discretizing a quadratic performance index associated with the underlying continuous time system (4.2.4)-(4.2.5) (in which case, there might arise an additional cross product term $2\tilde{x}_d'(k)Mu_d(k)$ which can be treated with very minor variations.)

The following result is reasonably well-known, and is relevant to both the non-MROC and MROC cases, since it depends purely on the state update equation (4.2.14), which is common to both. Nevertheless, for completeness, a proof is indicated in Appendix A.

Lemma 4.3.1 *Consider the discrete-time model (4.2.14)-(4.2.15),(4.2.16)-(4.2.19) and the index*

$$J_N = \frac{1}{N} E\{\sum_{k=0}^{N-1} [\tilde{x}_d'(k)Q\tilde{x}_d(k) + u_d'(k)Ru_d(k)]\} \tag{4.3.2}$$

Suppose that the sequences $P(k)$ and $L(k)$ are defined for $k = N-1, N-2, \cdots, 0$ by

$$P(k) = Q + F'P(k+1)F - P^*(k+1) \tag{4.3.3}$$

$$P^*(k+1) = F'P(k+1)G[R + G'P(k+1)G]^{-1}G'P(k+1)F \tag{4.3.4}$$

$$P(N) = 0 \tag{4.3.5}$$

$$L(k) = [R + G'P(k+1)G]^{-1}G'P(k+1)F \tag{4.3.6}$$

Assume further (as is reasonable) that $\tilde{x}_d(0)$ and, no matter how it is obtained, $u_d(k)$ (which is the value assumed by $u(t)$ in (4.2.4)-(4.2.5) at time

$t = kT_0$ and persisting over $[kT_0, \overline{k+1}T_0)$ is independent of $\omega_{ud}(k)$ (which depends on the noise input $\omega_u(t)$ to (4.2.4) over $[jT_0, \overline{j+1}T_0)$ for all $j \geq k$). Then,

$$\begin{aligned} J_N &= \frac{1}{N}E\{\tilde{x}_d'(0)P(0)\tilde{x}_d(0) \\ &\quad + \sum_{k=0}^{N-1}[u_d(k)+L(k)\tilde{x}_d(k)]'[R+G'P(k+1)G][u_d(k)+L(k)\tilde{x}_d(k)]\} \\ &\quad + \sum_{k=0}^{N-1} tr[\hat{Q}P(k+1)] \end{aligned} \tag{4.3.7}$$

Proof: See Appendix A. □

Now, for the purpose of comparing the different schemes, it is more straightforward to consider time-invariant problems. Accordingly, we shall adopt henceforth

Assumption 4.3.1: The pair $[F, G]$ is stabilizable and the pair $[F, Q^{1/2}]$ is detectable.

As is well-known, this ensures that when $N \to \infty$ in (4.3.3)-(4.3.6), the matrices $P(k)$ and $L(k)$ become independent of k and $F-GL$ has all eigenvalues inside the unit circle.

Now, let Σ_f and Σ_p denote the optimal error covariance associated with Kalman filter estimates $\hat{\tilde{x}}_d(k/k)$ and $\hat{\tilde{x}}_d(k/\overline{k-1})$ of $\tilde{x}_d(k)$. When such estimates are used in place of $\tilde{x}_d(k)$ in the optimal feedback law, $u_d(k)$ fulfills the independence requirement cited in the Lemma statement.

From (4.3.7), it follows that the optimal performance index associated with LQG law II is

$$\begin{aligned} J_f &= E\{[\tilde{x}_d(k)-\hat{\tilde{x}}_d(k/k)]'L'[R+G'PG]L[\tilde{x}_d(k)-\hat{\tilde{x}}_d(k/k)]\} + \mathrm{tr}[\hat{Q}P] \\ &= \mathrm{tr}[\Sigma_f L'(R+G'PG)L] + \mathrm{tr}[\hat{Q}P] \\ &= \mathrm{tr}[\Sigma_f P^*] + \mathrm{tr}[\hat{Q}P] \end{aligned} \tag{4.3.8}$$

where

$$\begin{aligned} P^* &= F'PG[R+G'PG]^{-1}G'PF \\ &= L'[R+G'PG]L \end{aligned} \tag{4.3.9}$$

Similarly, the optimal performance index associated with LQG law I is given by

$$J_p = \mathrm{tr}[\Sigma_p P^*] + \mathrm{tr}[\hat{Q}P] \tag{4.3.10}$$

Next, consider the cost of using MROC control. Observe first that $\omega_{\bar{y}}(k)$ depends on $\tilde{\omega}_u(t)$ for values of t in the interval $[kT_0, \overline{k+1}T_0)$; since by (4.2.37), $u_d(k)$ depends on $\omega_{\bar{y}}(k-1)$, this ensures that $u_d(k)$ possesses the independence property of the Lemma statement. Suppose that

$$E[\omega_{\bar{y}}(k)\omega'_{\bar{y}}(k)] = \hat{R} \tag{4.3.11}$$

Then, by (4.2.37) and (4.3.7), we have

$$\begin{aligned} J_{MROC} &= E\{\omega'_{\bar{y}}(k-1)(\hat{C}^{-L})'L'[R+G'PG]L\hat{C}^{-L}\omega_{\bar{y}}(k-1)\} + \mathrm{tr}[\hat{Q}P] \\ &= \mathrm{tr}[\hat{C}^{-L}\hat{R}(\hat{C}^{-L})'P^*] + \mathrm{tr}[\hat{Q}P] \end{aligned} \tag{4.3.12}$$

Consequently, despite the very different pattern in MROC control, *the performance is ultimately still dependent on the quality of the estimate of the state.* This is measured, for the three controllers considered, by Σ_f, Σ_p and $\hat{C}^{-L}\hat{R}(\hat{C}^{-L})'$ respectively. It therefore remains to obtain a feel for how these quantities are likely to compare in typical situations.

4.4 An Example

To illustrate the ideas presented, we provide performance comparison amongst the three controllers for control of the altitude of a single-axis satellite altitude given in [28]. The equation of motion of the system can be represented by the following state-space equation:

$$A = \begin{bmatrix} 0 & 1 \\ 0 & 0 \end{bmatrix} \quad B = \begin{bmatrix} 0 \\ 1 \end{bmatrix} \quad C = [1 \quad 0]$$

which is basically a double-integrator plant.

The output of the system is the angle of the satellite axis with respect to an "inertial" reference. Appropriate process noise intensity Ω_u, measurement noise intensity Ω_y and the weighting matrices Q_c and R_c include the following values:

$$\Omega_u = \begin{bmatrix} 0.1 & 0 \\ 0 & 0.1 \end{bmatrix} \quad \Omega_y = 0.1 \quad Q_c = \begin{bmatrix} 1 & 0 \\ 0 & 0 \end{bmatrix} \quad R_c = 0.2$$

respectively. The frame period, T_0 of 0.5 is selected according to the guidelines of T_0 for proper operation of MROC's given in the previous chapter and the recommended T_0 given in [10], [28] and [57].

It is easy to see that the augmented system is given by

$$\tilde{A} = \begin{bmatrix} 0 & 1 & 0 \\ 0 & 0 & 0 \\ \alpha & 0 & -\alpha \end{bmatrix} \quad \tilde{B} = \begin{bmatrix} 0 \\ 1 \\ 0 \end{bmatrix} \quad \tilde{C} = [0 \quad 1 \quad 0]$$

where the nominal $\alpha = \pi/T_0$. Since the augmented system has an observability index of 3, we let the output-rate multiplicity be $N_1^O = 3$. Further, since $\mathrm{tr}[\hat{Q}P]$ is common to the performance indices associated with the three controllers, it suffices to compare $\mathrm{tr}[\Sigma_f P^*]$, $\mathrm{tr}[\Sigma_p P^*]$ and $\mathrm{tr}[\hat{C}^{-L}\hat{R}(\hat{C}^{-L})'P^*]$ privided the value of $\mathrm{tr}[\hat{Q}P]$ does <u>not</u> swamp the values of $\mathrm{tr}[\Sigma_f P^*]$, *et al.*

Figure 4.4.1 shows the variation of $\mathrm{tr}[\Sigma_f P^*]$ and $\mathrm{tr}[\Sigma_p P^*]$ as a function of α/ω_s when LQG law I and LQG law II are applied to the plant respectively. Observe that the trace values reach a minimum value at $\alpha/\omega_s \simeq 0.2$. The reason why the trace values are increasing when α/ω_s becomes smaller than 0.2 is that measurement becomes poorer when α/ω_s gets smaller since the AAF bandwidth becomes sufficiently narrow that significant distortion is introduced. The implication of this is that the entries of the error covariance matrices Σ_f and Σ_p become much bigger as α/ω_s becomes smaller. On the other hand, the reason why the trace values are increasing when α/ω_s gets bigger than 0.2 is more noise passes through the AAF as α/ω_s increases. This also leads to

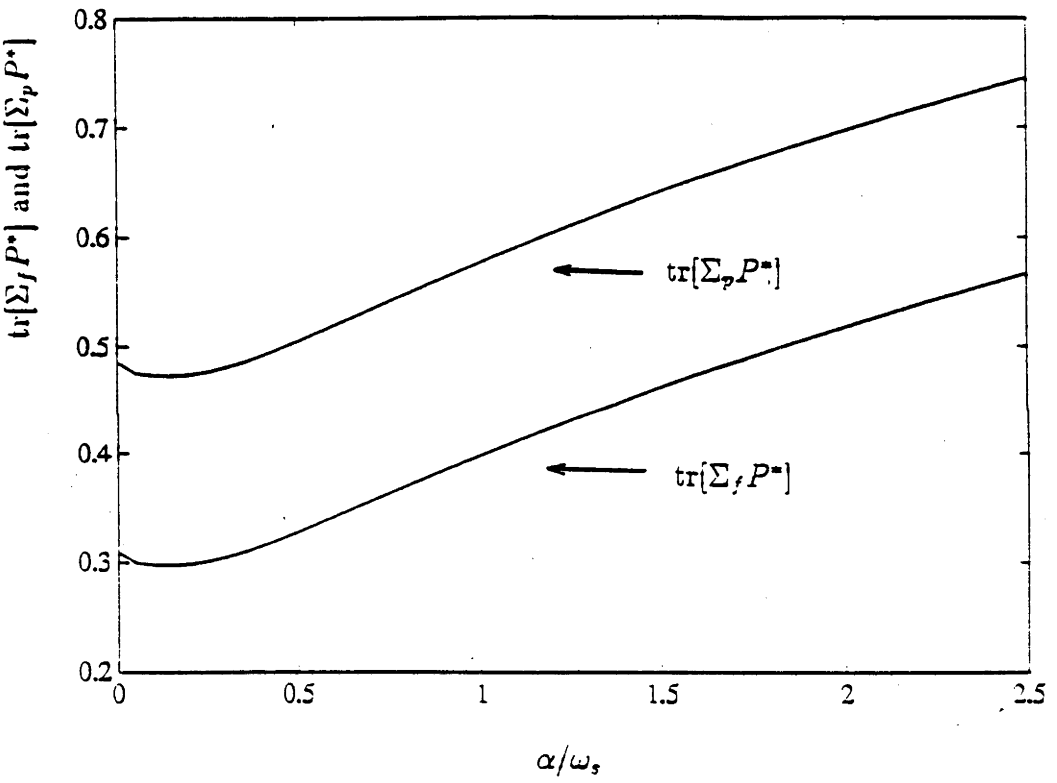

Figure 4.4.1: $\mathrm{tr}[\Sigma_f P^*]$ and $\mathrm{tr}[\Sigma_p P^*]$ vs α/ω_s

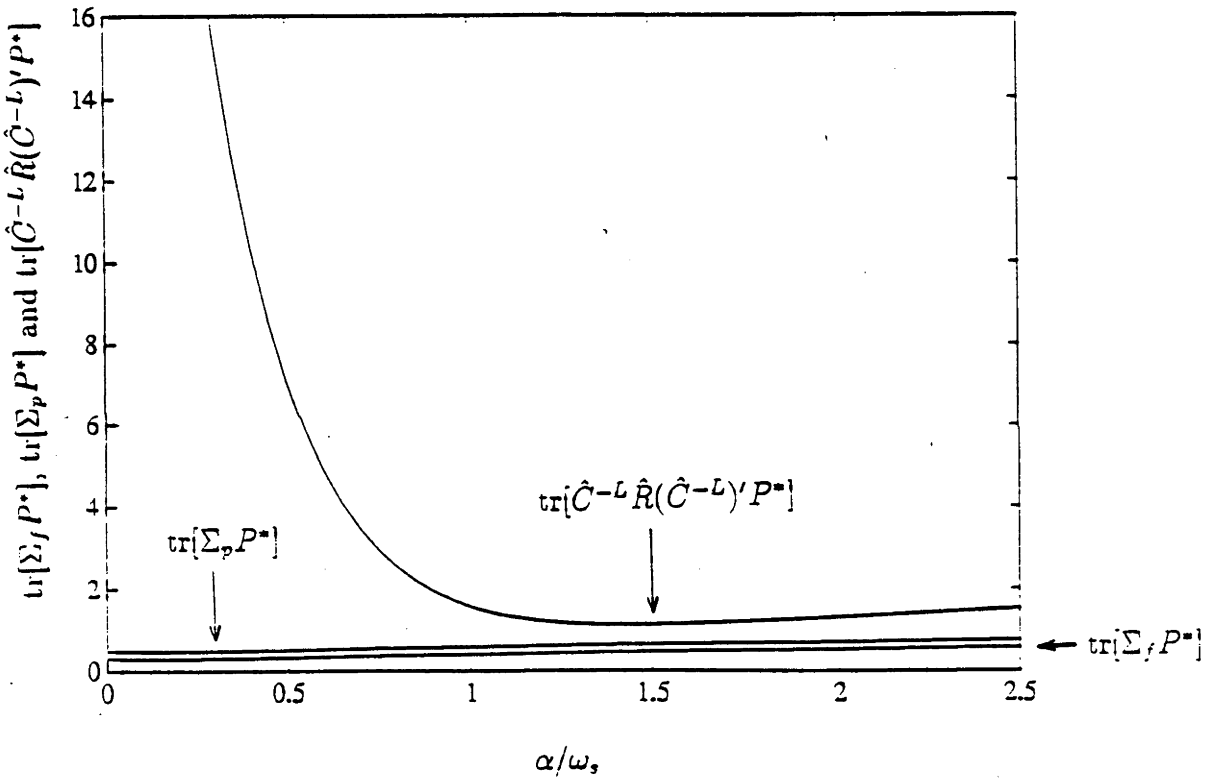

Figure 4.4.2: $\mathrm{tr}[\Sigma_f P^*]$, $\mathrm{tr}[\Sigma_p P^*]$ and $\mathrm{tr}[\hat{C}^{-L}\hat{R}(\hat{C}^{-L})'P^*]$ vs α/ω_s

increase in the entries of Σ_f and Σ_p. That $\mathrm{tr}[\Sigma_f P^*]$ is smaller than $\mathrm{tr}[\Sigma_p P^*]$ is expected. In this example, the value of $\mathrm{tr}[\hat{Q}P]$ does not swamp the values of $\mathrm{tr}[\Sigma_f P^*]$, *et al.*

Figure 4.4.2 shows the variation of $\mathrm{tr}[\hat{C}^{-L}\hat{R}(\hat{C}^{-L})'P^*]$ as a function of α/ω_s when the MROC law is implemented with $N_1^O = 3$. The values of $\mathrm{tr}[\Sigma_f P^*]$ and $\mathrm{tr}[\Sigma_p P^*]$ are also shown in the graph for comparison. It is clear from the graph that the MROC law performs worse than LQG law I and LQG law II for all values of α. The reason for the minimum trace value when the MROC law is applied is the same as that for the LQG laws.

4.5 Summary and Remarks

In this chapter, we have identified another drawback of the MROC under noise disturbances. We have shown that in a typical situation, the MROC performs significantly worse than an LQG controller with performance measured by an LQG index. It is remarkable to note that despite the fact that the MROC has the advantage of sampling the output more frequently than LQG law I, the latter still outperforms the MROC law by an enormous magnitude in a typical situation. This suggests that for practical purposes, the MROC law proposed in [33] will often need to be modified in one way or another so that the performance of MROC can be significantly enhanced.

We remark that a similar kind of study has been performed in [2] and [56]. In [2], the performance of some sort of MRIC's similar to that of [7] is studied. In [56], the performance studies of some sort of MRIC's similar to that of [7] and some sort of MROC's similar to that of [33] are carried out. Again, the comparison is in relation to the LQG control law. It is instructive to point out the differences between their schemes and our scheme. First, in the study of multirate output controller conducted in [56], the performance index considered is different from what is used here. The performance index in [56] is quadratic in

u and y rather than u and x in our study. Second, no anti-aliasing filter is used in both studies. Third, the input-rate multiplicity and output-rate multiplicity used in [56] are smaller than the controllability indices and observability indices respectively. Nevertheless, the study of [2] confirms our result that multirate output controller has poorer performance. Further, both studies of [2] and [56] show that MRIC's perform *better* than the LQG controllers.

Chapter 5

Reduced-order Multirate Output Observers for Linear State Feedback Laws

5.1 Introduction

Many control system designs are based on state feedback where the input to the system is a function only of the current state. (The linear feedback gain could be either obtained by using a pole-assignment routine to position the closed-loop poles to some pre-specified locations or calculated by solving the optimal regulation problem to minimize a certain performance index). Such state feedback designs offer many advantages with respect to both system performance and analysis. The major disadvantage of state feedback is that the system state is not always available for direct measurement. In these situations, it is not possible to implement the desired control law. Hence either the control scheme must be abandoned or a reasonable substitute for the state must be found. This leads to the problem of reconstructing the state from the available outputs via an observer.

The problem of observing (or estimating) the state of a deterministic FDLTI system was considered by Luenberger [52]-[53] who found that for any n^{th}-order system with p independent outputs, an observer of order $(n-p)$ could be

designed to yield an asymptotically error free estimate of the state. The $(n-p)$ poles of this observer could be placed arbitrarily (subject to complex conjugate placing), so long as they did not coincide with any poles of the original system.

In many cases, the state is estimated in order to realize a linear control law defined by a matrix of rank m, the number of inputs. Since m is usually less than n, one expects that an observer of dimension smaller than $(n-p)$ may be capable of estimating the m required linear functionals. In [52]-[53], Luenberger showed that for a continuous-time system, a single linear functional of the state can always be estimated with an observer of dimension $(\nu-1)$ where ν is the observability index of the system. An alternative algorithm for executing the design is described in [62].

The search for reduced-order observer designs has been an ongoing process. In [24], the problem of determining a reduced-order observer for a given control law was addressed. For a single-output system, the authors derived a necessary and sufficient condition for the existence of an observer of given order. They also showed that using a canonical form and by viewing a multiple-output system as a coupled set of single-output subsystems, a minimal-order observer can be determined for each subsystem. Further, they found that if these individual observers have common poles, a further reduction in the dimension of the composite observer is often possible.

In [76], the authors generalized and unified the concepts developed by Kalman and Luenberger pertaining to the design of discrete linear systems which estimate the state of a linear plant on the basis of both noise-free and noisy measurements of the output variables. Classes of minimal-order optimum "observer-estimators" are obtained which yield the conditional mean of the state of the dynamical system.

In [34], the authors studied controllers employing multirate sampling of the plant output and showed that arbitrary pole assignment is possible by general-

ized multirate-output controllers of reduced-order. Their approach essentially follows the discrete-time version of designing dynamic compensators developed in [69]. An augmented system is formed by connecting L delay elements, as opposed to L differentiators, to each input of the discrete-time system. A multiframe control law is then devised by employing the concept of multirate output sampling and it is shown to be equivalent to realizing the dynamic control law for the augmented system in the absence of measurement of the plant's state. One of the main results is that for a single-input system, the order of the controller, L, the output-rate multiplicity, N_i^O and the observability index, n_i^o are related by $LN_i^O \geq n_i^o$. This implies that in order to achieve arbitrary pole assignment for an n^{th}-order single-input single-output (SISO) system, the smallest order of the controller is n with single-rate sampling while with multirate output sampling, the smallest order becomes $[\frac{n}{N^O}]$, with N^O, of course, the ratio of the output sampling rate to the input sampling rate.

In this chapter, we exploit the observer theory developed by Luenberger and show that in the case of estimating a single (but pre-specified) linear functional of a system's state, a multirate output observer (an observer employing multirate sampling of the plant output) of this linear functional and of dimension much smaller than that of a single-rate output observer (an observer employing single-rate sampling of the plant output) can be designed by exploring the multirate output sampling mechanism developed in [33]. In [33], it is shown that for a m-input p-output system, if $N_i^O \geq n_i^o$ $(i = 1, 2, \cdots, p)$, then a realisation of the state feedback law is possible with no dynamics. In our approach, N_i^O satisfies $1 \leq N_i^O < n_i^o$. Furthermore, the multirate output sampling scheme employed here has uniform output-rate multiplicity. As a consequence, we are able to obtain a controller of order L satisfying $LN_i^O \geq n_i^o$, just as in [34]. The controller of this chapter can be regarded as a combined estimator and state feedback law, which is not really the same as the controller in [34]. Here, we can

choose the dynamics of the estimator separately from those of the closed-loop system with true state feedback.

The structure of the chapter is as follows: The problem formulation and some preliminary results appear in Section 5.2. The next section considers continuous-time SISO LTI systems and derives the structures and the design procedures for the single-rate output linear functional observer and multirate output linear functional observer. In Section 5.4, the results from the previous section are extended to the SIMO case. The structures and design procedures for the two types of observers for this case are also presented here. An example of a SISO system appears in Section 5.5 to illustrate the ideas and methods described. Section 5.6 contains concluding remarks.

5.2 Problem Formulation and Preliminary Results

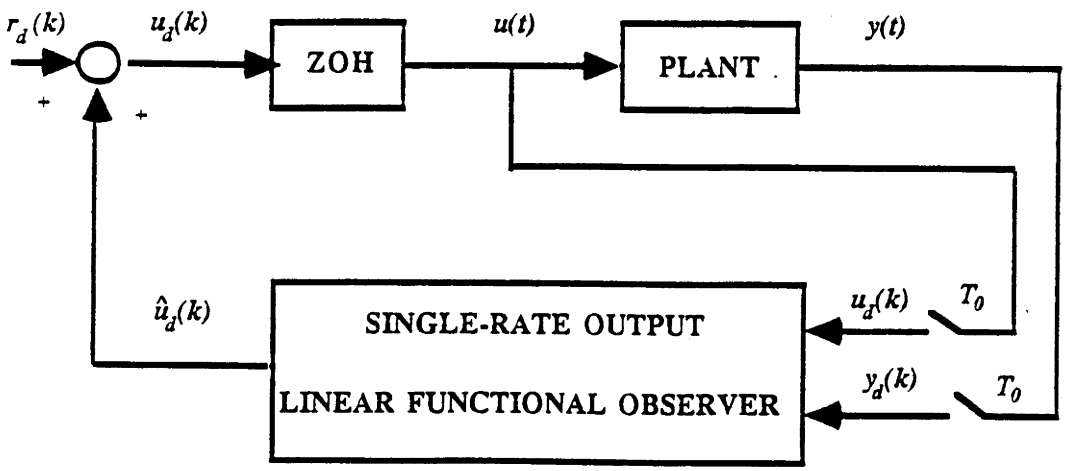

Figure 5.2.1: Connection of Plant and Observer

Consider a continuous-time FDLTI minimal (i.e. completely controllable and observable) plant of the form

$$\dot{x}(t) = Ax(t) + bu(t) \quad x(0) = x_0 \tag{5.2.1}$$

$$y(t) = Cx(t) \tag{5.2.2}$$

where $x \in \mathbb{R}^n$, $u \in \mathbb{R}^1$ and $y \in \mathbb{R}^p$. Suppose that the state is not available for measurement and the available outputs of (5.2.1)-(5.2.2) are sampled and used to drive another system which serves as an observer of the first system in that its state will tend to track a linear transformation of the state of the first system. The connection of the plant and a discrete-time observer with single-rate sampling of the plant output is shown in Figure 5.2.1.

Theorem 5.2.1 *Let the discretized version of (5.2.1)-(5.2.2) with single-rate sampling of the plant output be*

$$x_d(k+1) = A_s x_d(k) + b_s u_d(k) \tag{5.2.3}$$

$$y_d(k) = Cx_d(k) \tag{5.2.4}$$

where $x_d(k) \triangleq x(kT_0)$, $y_d(k) \triangleq y(kT_0)$ *and*

$$A_s = \exp(AT_0) \tag{5.2.5}$$

$$b_s = \int_0^{T_0} \exp(At)bdt \tag{5.2.6}$$

and $T_0 > 0$ *is the sampling period.*

Suppose that this drives the observer which is governed by

$$z_d(k+1) = Fz_d(k) + Gy_d(k) + du_d(k) \tag{5.2.7}$$

and there is a linear transformation T *satisfying*

$$TA_s - FT = GC \tag{5.2.8}$$

and

$$d = Tb_s. \tag{5.2.9}$$

Then, for some appropriate $x_d(0)$, $z_d(k) = Tx_d(k)$ *for all* $k \geq 0$.

Proof: It is easy to see that

$$\begin{aligned} z_d(k+1) - Tx_d(k+1) &= [(FT - TA_s) + GC]x_d(k) \\ &\quad + F[z_d(k) - Tx_d(k)] \end{aligned} \tag{5.2.10}$$

Using $TA_s - FT = GC$, it is immediate that $z_d(k) = Tx_d(k)$ for all $k \geq 0$ for some appropriate $x_d(0)$ such that $z_d(0) = Tx_d(0)$. □

Remark 5.2.1 If A_s, F, G and C are given, there is a unique solution T to the equation $TA_s - FT = GC$ if A_s and F have no common eigenvalues. See [29] for details.

Remark 5.2.2 $|\lambda_i(F)| < 1$ is needed in practice to ensure that nonzero initial errors $z_d(0) - Tx_d(0)$ result in $z_d(k) - Tx_d(k)$ approaching zero as $k \to \infty$.

Remark 5.2.3 The observer and the observed system need not have the same dimension.

Remark 5.2.4 The observed state $z_d(k)$ may be used to generate a feedback control $\hat{u}_d(k)$, through an equation of the form

$$\hat{u}_d(k) = py_d(k) + qz_d(k) \tag{5.2.11}$$

$$\text{or} \quad \hat{u}_d(k+1) = py_d(k) + qz_d(k) + ru_d(k) \tag{5.2.12}$$

The first equation would yield a compensator that is not strictly proper, while the second would yield a strictly proper compensator. Of course, particular matrix gains may be zero, e.g. r in (5.2.12). In general, we expect that there will be some k' such that $\hat{u}_d(k) - k'x_d(k) \to 0$ as $k \to \infty$ i.e. $\hat{u}_d(k)$ estimates $k'x_d(k)$, which is the desired feedback law.

Remark 5.2.5 Notice that $u_d(k)$, which appears in the plant equation (5.2.3) -(5.2.4) and the estimator equation (5.2.11)-(5.2.12), in general, is composed of

a sum of the feedback component $\hat{u}_d(k)$ and external input $r_d(k)$. For simplicity, we consider the case where $r_d(k) = 0$ and hence $u_d(k) = \hat{u}_d(k)$.

Before we deal with theorems concerning reduction in the dimension of the observer, we define formally the order of the observer.

Definition 5.2.1 *The order of the observer given by (5.2.7) and (5.2.11) or (5.2.12) is the dimension of the vector* $z_d(k)$ *or* $[z_d'(k) \quad \hat{u}_d'(k)]'$ *respectively.*

We note a minor point concerning the order counting of the observer. Since $\hat{u}_d(k)$ increases the dimension of both a single-rate output observer as well as a multirate output observer (as will be seen in the later sections) by at most 1 (depending on whether (5.2.11) or (5.2.12) is used), it suffices to consider the dimension of $z_d(k)$ and show that there is a reduction in this quantity using a multirate output observer.

For continuous-time systems, a major result states that any given linear function of the state, $k'x(t)$ say, can be estimated with an observer having $(\nu - 1)$ arbitrary eigenvalues, where ν is the observability index, see [52]-[53] and [62] for details. Here, we state the theorem for the discrete-time case for a SIMO system. This theorem serves as the basis of determining the orders of the multirate observers presented later.

Theorem 5.2.2 *Suppose that the single-input multiple-output discrete-time system given by (5.2.3)-(5.2.4) is observable with observability index* $\nu \geq [n/q]$ *where* $[n/q]$ *is the least integer larger than or equal to* n/q *with* n *and* q *the dimensions of the state and the row rank of the output matrix* C *respectively; then any single linear functional of the state,* $a'A_s^{-1}x_d(k)$ *can be estimated with a reduced-order discrete-time observer whose dimension of* $z_d(k)$ *is* $(\nu - 1)$.

Proof: The proof is the same as that for a SIMO continuous-time system. See [17] for more details. □

Remark 5.2.6 Note that by virtue of (5.2.5), A_s^{-1} always exists; the subsequent equations acquire a tidier form when the linear functional is written using $a'A_s^{-1}$. Of course, the observer generates $\hat{u}_d(k)$ with the property that $\hat{u}_d(k) - a'A_s^{-1}x_d(k) \to 0$ as $k \to \infty$.

Remark 5.2.7 For an n^{th}−order SISO system, the dimension of the observer required is $(n-1)$ (with single-rate sampling of the plant output).

Let us now consider multirate output observers. Suppose that output samples of (5.2.1)-(5.2.2) are collected not just at times $0, T_0, 2T_0, \cdots$, but at N^O uniformly spaced times in each interval $[iT_0, \overline{i+1}T_0)$, $i = 0, 1, 2, \cdots$. The system input, on the other hand, is maintained constant over the interval $[iT_0, \overline{i+1}T_0)$. (The integer N^O is termed the output-rate multiplicity.) If the output measurements, denoted by

$$\bar{y}_d(k) = \begin{bmatrix} y(kT_0) \\ y(kT_0 + \frac{T_0}{N^O}) \\ \vdots \\ y(kT_0 + \frac{(N^O-1)T_0}{N^O}) \end{bmatrix} \tag{5.2.13}$$

are used in lieu of $y_d(k)$ in (5.2.12), we obtain multirate output linear functional observers. To facilitate the following discussion, we also give a formal definition of the multirate output linear functional observer here.

Definition 5.2.2 *A multirate output linear functional observer for a single input system is an observer which uses the plant input and the output measurements in (5.2.13) to estimate a single linear functional, $a'A_s^{-1}x_d(k)$ of the plant's state and is given by*

$$z_d(k+1) = Fz_d(k) + G\bar{y}_d(k) + eu_d(k) \tag{5.2.14}$$

$$\hat{u}_d(k+1) = p\bar{y}_d(k) + qz_d(k) + ru_d(k) \tag{5.2.15}$$

It has the property that $\hat{u}_d(k) - a'A_s^{-1}x_d(k) \to 0$ as $k \to \infty$. The conditions on F, G et al to ensure this property are presented subsequently.

Let us observe that

$$\bar{y}_d(k) = \bar{C}x_d(k) + \bar{d}u_d(k) \tag{5.2.16}$$

where

$$\bar{C} = \begin{bmatrix} C \\ C\exp(AT_0/N^O) \\ \vdots \\ C\exp[A(N^O-1)T_0/N^O] \end{bmatrix} \tag{5.2.17}$$

$$\bar{d} = \begin{bmatrix} 0 \\ C\int_0^{T_0/N^O}\exp(At)b\,dt \\ \vdots \\ C\int_0^{(N^O-1)T_0/N^O}\exp(At)b\,dt \end{bmatrix} \tag{5.2.18}$$

Accordingly, multirate observers have information like that which would be available to a single-rate observer connected to a multiple output plant, except that the various components of $\bar{y}_d(k)$ are not all available at time kT_0, but arrive in $[kT_0, kT_0 + \frac{(N^O-1)}{N^O}T_0]$.

Concerning the order of the multirate output observer of a linear functional, we have:

Corollary 5.2.1 *For a multirate output linear functional observer, the dimension of the state, $z_d(k)$ of the observer is at least $[\frac{n}{N^O q}] - 1$ where n, q and N^O are the dimensions of the plant state, the row rank of the plant output matrix C and the output-rate multiplicity respectively.*

Proof: It is well-known that for almost all choices of T_0, the pair $(C, \exp(AT_0/N^O))$ will be observable. As a consequence, we shall have

$$\operatorname{rank}\begin{bmatrix} C \\ C\exp(AT_0/N^O) \end{bmatrix} = \operatorname{rank}\begin{bmatrix} C \\ CA \end{bmatrix} \tag{5.2.19}$$

$$\operatorname{rank}\begin{bmatrix} C \\ C\exp(AT_0/N^O) \\ C\exp(2AT_0/N^O) \end{bmatrix} = \operatorname{rank}\begin{bmatrix} C \\ CA \\ CA^2 \end{bmatrix} \tag{5.2.20}$$

et al and the ranks of these successive matrices depend on the different observability indices of the pair (C, A). In any case, the rank can never exceed the number of rows or exceed n. Hence, row rank $\bar{C} \leq N^O q$ and the result of the corollary follows. □

Remark 5.2.8 When (5.2.1)-(5.2.2) is a SISO system and $N^O \leq n$, it is evident that rank $\bar{C} = N^O$ and $\nu = [\frac{n}{N^O}]$. The dimension of $z_d(k)$ in the multirate observer can be $([\frac{n}{N^O}] - 1)$. Notice that if $N^O = n$, the result of [34] is effectively recovered.

Remark 5.2.9 In (5.2.11)-(5.2.12), we recorded the two different ways, causal or strictly causal, which could be used to generate a feedback control. Let us note that when $y_d(k)$ is replaced by $\bar{y}_d(k)$, we can no longer use (5.2.11). This is because $\bar{y}_d(k)$ actually contains quantities which are not available until time $(k + \frac{N^O-1}{N^O})T_0$. The first instant subsequent to this time at which a new value of control is required is $(k+1)T_0$. Hence, (5.2.12) is naturally replaced by

$$\hat{u}_d(k+1) = p\bar{y}_d(k) + qz_d(k) + ru_d(k) \tag{5.2.21}$$

Remark 5.2.10 If one reckons that the time required to compute the control for the measurements is effectively zero, one can obtain a causal, but not strictly causal, compensator with the following structure:

$$z_d(k+1) = Fz_d(k) + G\tilde{y}_d(k+1) + eu_d(k) \tag{5.2.22}$$

$$\hat{u}_d(k+1) = p\tilde{y}_d(k+1) + qz_d(k) \tag{5.2.23}$$

where

$$\tilde{y}_d(k+1) = \begin{bmatrix} y_d(k + \frac{1}{N^O}) \\ y_d(k + \frac{2}{N^O}) \\ \vdots \\ y_d(k+1) \end{bmatrix} \tag{5.2.24}$$

$$\tilde{C} = \begin{bmatrix} c\exp(AT_0/N^O) \\ c\exp(2AT_0/N^O) \\ \vdots \\ c\exp(AT_0) \end{bmatrix} \tag{5.2.25}$$

$$\tilde{d} = \begin{bmatrix} c\int_0^{T_0/N^O}\exp(At)bdt \\ c\int_0^{2T_0/N^O}\exp(At)bdt \\ \vdots \\ c\int_0^{T_0}\exp(At)bdt \end{bmatrix} \tag{5.2.26}$$

The output is still sampled N^O times as frequently as the input, but the output samples are grouped differently. The conditions for existence of the observer are the solvability for a stable F of the equation

$$TA_s - FT = G\tilde{C} \tag{5.2.27}$$

together with satisfaction of the following equations:

$$e = Tb_s - G\tilde{d} \tag{5.2.28}$$

$$a' = p\tilde{C} + qT \tag{5.2.29}$$

$$a'A_s^{-1}b_s = p\tilde{d} \tag{5.2.30}$$

See Appendix B for proof.

Nevertheless, this alternative is not generally practical because of the heavy computation involved in updating the control law which employs the output measurements given by (5.2.24). Hence, the strictly causal compensator is preferred in practice.

5.3 Single-input Single-ouptut Case

5.3.1 Single-rate Output Linear Functional Observer

In this section, we review the general structure of the single-rate output observer and a design procedure for its construction for a SISO system. It also serves as the basis of deriving the multirate output linear functional observer and comparing the reduction in the dimension of the observer in the later sections.

Structure of Observer

Without loss of generality, we assume that (5.2.3)-(5.2.4) inherits the controllability and observability properties of (5.2.1)-(5.2.2). Since not all the states of (5.2.3) are directly measurable, we propose a compensator (comprising an observer and a rule for computing the control) of the form

$$z_d(k+1) = Fz_d(k) + gy_d(k) + d\hat{u}_d(k) \tag{5.3.1}$$

$$\hat{u}_d(k+1) = py_d(k) + qz_d(k) + r\hat{u}_d(k) \tag{5.3.2}$$

where $z_d(k) \in \mathbb{R}^{(n-1)}$ and $\hat{u}_d(k)$ is a scalar which approximates the linear feedback $a'A_s^{-1}x_d(k)$. (Note that $\hat{u}_d(k)$ is used in lieu of $u_d(k)$ because we consider only the case where the external input $r_d(k) = 0$ here.) The first equation (5.3.1) follows directly from the preliminary results on the observation of a system. The second equation (5.3.2) is used in lieu of the discrete-time equivalence of the observer proposed in [52]-[53] which would be given by

$$\hat{u}_d(k) = py_d(k) + qz_d(k) \tag{5.3.3}$$

The problem with the latter observer's structure is that, as already discussed, it becomes non-causal if one were to extend it to the multirate output observer by replacing $y_d(k)$ by $\bar{y}_d(k)$.

Lemma 5.3.1 *The state $z_d(k)$ of (5.2.7) is an estimate of $Tx_d(k)$ with $x_d(k)$ defined by (5.2.3) if and only if the following conditions hold.*

Condition a: F *is stable*

Condition b: $TA_s - FT = gc$

Condition c: $d = Tb_s$

Proof: A sufficiency proof is given in the proof of Theorem 5.2.1. For the necessity proof, first observe that the error vector $e_d(k) = z_d(k) - Tx_d(k)$ is

governed by

$$e_d(k+1) = Fe_d(k) - (TA_s - FT - gc)x_d(k) + (d - Tb_s)\hat{u}_d(k) \qquad (5.3.4)$$

where $\hat{u}_d(k)$ approximates $a'A_s^{-1}x_d(k)$. Now, suppose that $e_d(k) \to 0$ for all $\hat{u}_d(k), x_d(0)$ and $z_d(0)$; then letting $x_d(0)$ and $\hat{u}_d(k)$ vanish (which ensures that $x_d(k) = 0$ for all k) establishes condition a. Next, condition c must hold, otherwise a $\hat{u}_d(.)$ would always exist to make the last term in (5.3.4) arbitrarily large. Similarly, the controllability of the plant implies that the second term in (5.3.4) can always be made large unless condition b is satisfied. □

Lemma 5.3.2 *Suppose that the plant given by (5.2.3)-(5.2.4) is controllable. Then, $\hat{u}_d(k)$ of (5.2.12) estimates $a'A_s^{-1}x_d(k)$ if there exists T such that $z_d(k)$ estimates $Tx_d(k)$ and*

$$a' = pc + qT \qquad (5.3.5)$$

$$r = a'A_s^{-1}b_s \qquad (5.3.6)$$

Proof: Observe that

$$\hat{u}_d(k+1) - a'A_s^{-1}x_d(k+1)$$

$$\begin{aligned} &= py_d(k) + qz_d(k) + r\hat{u}_d(k) - a'x_d(k) - a'A_s^{-1}b\hat{u}_d(k) \\ &= pcx_d(k) + qTx_d(k) - a'x_d(k) + qe_d(k) \\ &= qe_d(k) \end{aligned} \qquad (5.3.7)$$

□

Remark 5.3.1 Note that here p is a scalar and q is a row vector of dimension $(n-1)$. Hence, solvability of (5.3.5) for p and q, given c, T and a is guaranteed if $\text{rank}[c' \quad T' \quad a] = \text{rank}[c' \quad T'] = n$, which is the dimension of the system's state. This condition is generally fulfilled.

Remark 5.3.2 The observer is open-loop stable if and only if $|r| < 1$. Notice that stability is guaranteed for sufficiently small sampling time, T_0. This can be argued by observing that as $T_0 \to 0$, a' remains bounded, $A_s^{-1} \to I$ and $b_s \to 0$. Theoretically speaking, it does not matter whether the observer is open-loop stable or not so long as the closed-loop system is stable. As a matter of fact, the stability of r does not affect the closed-loop eigenvalues in our set-up. (See Appendix C for proof). However, an open-loop unstable observer is difficult to start-up and, in practice, we do wish the observer to be open-loop stable.

Design Procedure for Observer

The problem at hand boils down to determining the dimension of the observer required and finding F, g, d, p, q and r such that the output of the observer $\hat{u}_d(k)$ estimates $a' A_s^{-1} x_d(k)$. It is clear that such an observer must itself be observable (otherwise its dimension can be reduced).

To facilitate the construction of the observer, we provide here a design procedure for the single-rate observer.

1. Select T_0 according to the recommendations given in [10], [28] and [57].

2. Discretize the continuous-time plant with the selected T_0. Let the discretized plant be represented by (A_s, b_s, c).

3. Using Theorem 5.2.2, the smallest dimension of $z_d(k)$ is $(n-1)$.

4. Choose a stable F (for simplicity, choose F to be diagonal with distinct eigenvalues) and $q = [1 \quad 1 \quad \cdots \quad 1] \in \mathbb{R}^{1\times(n-1)}$. Solve for $p \in \mathbb{R}^1$, $g \in \mathbb{R}^{(n-1)}$ and $T \in \mathbb{R}^{(n-1)\times n}$ from $TA_s - FT = gc$ and $a' = pc + qT$, using the algorithm of [62]. Note that there always exists a unique triple p, g and T solving these equations if A_s and F do not have common eigenvalues.

5. Compute $d = Tb_s$ and $r = a'A_s^{-1}b_s$.

5.3.2 Multirate Output Linear Functional Observer

For a single-output system, multirate output sampling effectively produces N^O independent values of the output over each time interval $[iT_0, \overline{i+1}T_0)$, $i = 0, 1, 2, \cdots$. As shown in the proof of Corollary 5.2.1, this increases the row rank of the output matrix $\bar{C}$ and thereby reduces the observability index of the discretized plant. In other words, further reduction in the order of the observer is possible with multirate output sampling. This inspires us to investigate the structure of the multirate output observer and a design procedure for its construction.

Structure of Observer

Recall that with multirate output sampling, the discretized plant becomes:

$$x_d(k+1) = A_s x_d(k) + b_s u_d(k) \tag{5.3.8}$$

$$\bar{y}_d(k) = \bar{C} x_d(k) + \bar{d} u_d(k) \tag{5.3.9}$$

where A_s and b_s are given by (5.2.5) and (5.2.6) respectively and

$$\bar{y}_d(k) = \begin{bmatrix} y_d(k) \\ y_d(k+\frac{1}{N^O}) \\ \vdots \\ y_d(k+\frac{N^O-1}{N^O}) \end{bmatrix} \tag{5.3.10}$$

$$\bar{C} = \begin{bmatrix} c \\ c\exp(AT_0/N^O) \\ \vdots \\ c\exp[A(N^O-1)T_0/N^O] \end{bmatrix} \tag{5.3.11}$$

$$\bar{d} = \begin{bmatrix} 0 \\ c\int_0^{T_0/N^O} \exp(At)bdt \\ \vdots \\ c\int_0^{(N^O-1)T_0/N^O} \exp(At)bdt \end{bmatrix} \tag{5.3.12}$$

In the same spirit as the single-rate observer, we propose the following structure for the multirate output observer:

$$z_d(k+1) = Fz_d(k) + G\bar{y}_d(k) + e\hat{u}_d(k) \tag{5.3.13}$$

$$\hat{u}_d(k+1) = p\bar{y}_d(k) + qz_d(k) + r\hat{u}_d(k) \tag{5.3.14}$$

A few important observations can be made about (5.3.14). First, notice that (5.3.14) is obtained by replacing $y_d(k)$ in (5.2.7) by $\bar{y}_d(k)$. Second, as mentioned in the previous section, the order of the observer can be regarded as the dimension of the vector $[z_d'(k) \quad \hat{u}_d(k)]'$ i.e. $\dim(F)+1$. Third, no account is being taken of the possible need to store entries of $\bar{y}_d(k)$ (which become available at different times) in defining the state dimension of the observer. Fourth, as mentioned in the previous section, there is a need to introduce a delay in $\hat{u}_d(k)$ so that the multirate output observer is causal. This can be easily seen by substituting (5.3.10) into $\hat{u}_d(k) = p\bar{y}_d(k) + qz_d(k)$ and examining the time index on both sides of the equality.

The condition for $z_d(k)$ to be an estimate of $Tx_d(k)$ is noted in the following lemma which is a trivial variant of Lemma 5.3.1.

Lemma 5.3.3 *The state $z_d(k)$ of (5.3.13) is an estimate of $Tx_d(k)$ if and only the following conditions hold.*

Condition a: F *is stable*

Condition b: $TA_s - FT = G\bar{C}$

Condition c: $e = Tb_s - G\bar{d}$

Proof: The same approach as proof of Lemma 5.3.1 □

The construction of $\hat{u}_d(k)$ proceeds virtually the same way as in Lemma 5.3.2.

Lemma 5.3.4 *Suppose that the plant given by (5.3.8)-(5.3.9) is observable. Then, $\hat{u}_d(k)$ of (5.3.14) estimates $a'A_s^{-1}x_d(k)$ if there exists T such that $z_d(k)$ estimates $Tx_d(k)$ and*

$$a' = p\bar{C} + qT \tag{5.3.15}$$

$$r = a'A_s^{-1}b_s - p\bar{d} \tag{5.3.16}$$

Remark 5.3.3 The multirate output observer is open-loop stable if and only if $|r| < 1$. This condition is in turn guaranteed for sufficiently small frame period, T_0. This can be deduced by observing that as $T_0 \to 0$, a' and p remain bounded, $A_s^{-1} \to I$, b_s and $\bar{d} \to 0$. Remark 5.3.2 on the open-loop stability of the single-rate observer also applies here. Further, as in the single-rate observer, the closed-loop stability is independent of r. The proof follows essentially the same approach as that in Appendix C.

Design Procedure for Observer

The design procedure uses the ideas of the preceding lemmas, together with the scheme of [62].

1. Select T_0 according to the recommendations given in [10], [28] and [57].

2. Choose an output-rate multiplicity N^O and discretize the continuous-time plant with T_0 obtained in (1). Let the discretized plant be represented by $(A_s, b_s, \bar{C}, \bar{d})$.

3. Using Corollary 5.2.1, the dimension of $z_d(k)$ is $([\frac{n}{N^O}] - 1)$.

4. Choose a stable F (again for simplicity, choose F to be diagonal with distinct eigenvalues) and $q = [1 \quad 1 \quad \cdots 1] \in \mathbb{R}^{1\times([\frac{n}{N^O}]-1)}$. Solve for $p \in \mathbb{R}^{1\times N^O}$, $G \in \mathbb{R}^{([\frac{n}{N^O}]-1)\times N^O}$ and $T \in \mathbb{R}^{([\frac{n}{N^O}]-1)\times n}$ from $TA_s - FT = G\bar{C}$ and $a' = p\bar{c} + qT$, using the algorithm of [62]. Again, provided A_s and F do not have common eigenvalues, there always exists a triple T,G and p.

5. Compute $e = Tb_s - G\bar{d}$ and $r = a'A_s^{-1}b_s - p\bar{d}$.

5.4 Single-input Multiple-output Case

5.4.1 Single-rate Linear Functional Observer

For SIMO systems, the general structure of the single-rate observer turns out to be a direct extension from the SISO case. For completeness, the structure of the strictly causal observer for estimating $a'A_s^{-1}x_d(k)$ and conditions for its existence are summarized here.

The structure of the single-rate observer for a SIMO system is

$$z_d(k+1) = Fz_d(k) + Gy_d(k) + d\hat{u}_d(k) \tag{5.4.1}$$

$$\hat{u}_d(k+1) = py_d(k) + qz_d(k) + r\hat{u}_d(k) \tag{5.4.2}$$

and the conditions for its existence are the solvability for a stable F of the equation

$$TA_s - FT = GC \tag{5.4.3}$$

together with satisfaction of the following equations:

$$d = Tb_s \tag{5.4.4}$$

$$a' = pC + qT \tag{5.4.5}$$

$$r = a'A_s^{-1}b_s \tag{5.4.6}$$

where T is a linear transformation such that $z_d(k)$ estimates $Tx_d(k)$.

A design procedure is available in [62], for which the smallest dimension of $z_d(k)$ of the observer is $([\frac{n}{q}] - 1)$ where q is the row rank of the matrix C.

5.4.2 Multirate Output Linear Functional Observer

As foreshadowed in the introduction, the multirate output sampling scheme employed here is one with uniform output-rate multiplicity i.e.

$N_1^O = N_2^O = \cdots = N_p^O = N^O$. The structure of the multirate output observer with uniform output-rate multiplicity and the associated design procedure also turn out to be a direct extension from the SISO case. The structure of the multirate output observer is thus given by:

$$z_d(k+1) = Fz_d(k) + G\bar{y}_d(k) + e\hat{u}_d(k) \tag{5.4.7}$$

$$\hat{u}_d(k+1) = p\bar{y}_d(k) + qz_d(k) + r\hat{u}_d(k) \tag{5.4.8}$$

with F stable and T satisfying

$$TA_s - FT = G\bar{C} \tag{5.4.9}$$

There also holds

$$e = Tb_s - G\bar{d} \tag{5.4.10}$$

$$a' = p\bar{C} + qT \tag{5.4.11}$$

$$\bar{C} = \begin{bmatrix} C \\ C\exp(AT_0/N^O) \\ \vdots \\ C\exp[A(N^O-1)T_0/N^O] \end{bmatrix} \tag{5.4.12}$$

$$\bar{d} = \begin{bmatrix} 0 \\ C\int_0^{T_0/N^O}\exp(At)b\,dt \\ \vdots \\ C\int_0^{(N^O-1)T_0/N^O}\exp(At)b\,dt \end{bmatrix} \tag{5.4.13}$$

$$r = a'A_s^{-1}b_s - p\bar{d} \tag{5.4.14}$$

The design procedure for a multirate output observer is also the same as that for a SISO system in Section 5.3. The smallest dimension of $z_d(k)$ of the observer is given by $([\frac{n}{r}] - 1)$ where rank $\bar{C} = r$. The condition for solvability of (5.4.11) is rank$[\bar{C}' \quad T' \quad a]$ = rank$[\bar{C}' \quad T']$.

5.5 An Example

To illustrate the ideas presented, we give an example involving a model of an electrical circuit consisting of resistors, capacitors and inductors used in [42] which is given by:

$$\begin{aligned} \dot{x}(t) &= Ax(t) + bu(t) \\ y(t) &= cx(t) \end{aligned}$$

where

$$A = \begin{bmatrix} -2 & 1 & 0 & 0 & 0 & 0 \\ 1 & -2 & 1 & 0 & 1 & -1 \\ 0 & 1 & -2 & 1 & 0 & 0 \\ 0 & 0 & 1 & -1 & 0 & 1 \\ 0 & -1 & 0 & 0 & 0 & 0 \\ 0 & 1 & 0 & -1 & 0 & 0 \end{bmatrix} \quad b = \begin{bmatrix} 1 \\ 0 \\ 0 \\ 0 \\ 1 \\ 0 \end{bmatrix} \quad c = [0\ 0\ 0\ 1\ 0\ 0]$$

Assume that the states are not available for measurement.

Single-rate Linear Functional Observer

Using $T_0 = 0.2$, the discretized plant is given by

$$\begin{aligned} x_d(k+1) &= A_s x_d(k) + b_s u_d(k) \\ y_d(k) &= c x_d(k) \end{aligned}$$

where

$$A_s = \begin{bmatrix} 0.6837 & 0.1339 & 0.0135 & 0.0020 & 0.0154 & -0.0153 \\ 0.1339 & 0.6666 & 0.1359 & 0.0308 & 0.1646 & -0.1624 \\ 0.0135 & 0.1359 & 0.6983 & 0.1503 & 0.0155 & 0.0010 \\ 0.0020 & 0.0308 & 0.1503 & 0.8168 & 0.0022 & 0.1790 \\ -0.0154 & -0.1646 & -0.0155 & -0.0022 & 0.9824 & 0.0175 \\ 0.0153 & 0.1624 & -0.0010 & -0.1790 & 0.0175 & 0.9639 \end{bmatrix}$$

$$b_s = \begin{bmatrix} 0.1669 \\ 0.0330 \\ 0.0021 \\ 0.0002 \\ 0.1977 \\ 0.0023 \end{bmatrix}$$

The open-loop poles of the discretized plant are 0.5083, 0.6440, $0.8509 \pm 0.2343i$ and $0.9788 \pm 0.0958i$. Suppose that the closed-loop poles were assigned to 0.2472, 0.6183, $0.8150 \pm 0.2342i$ and $0.9332 \pm 0.1142i$ via a linear feedback gain $a'A_s^{-1} = [-1.5255 \quad 0.3548 \quad -1.5366 \quad 0.2746 \quad -1.0297 \quad 0.005]$ or $a' = [-1 \quad 0 \quad -1 \quad 0 \quad -1 \quad 0]$.

Now, the problem at hand is to find a minimal-order observer to estimate the control law, $a'A_s^{-1}x_d(k)$. Using Theorem 5.2.2, the dimension of $z_d(k)$ is 5. Hence, a sixth-order observer (with $z_d(k)$ of dimension 5 and with strict causality) is sufficient to estimate the control law by Definition 5.2.1 (Note that if strict causality were not required, we would use an observer of dimension 5).

Next, the structure of the observer is given by

$$z_d(k+1) = Fz_d(k) + gy_d(k) + du_d(k)$$

where

$$\begin{aligned} TA_s - FT &= gc \\ d &= Tb_s \end{aligned}$$

Choose

$$F = \begin{bmatrix} 0.1 & 0 & 0 & 0 & 0 \\ 0 & 0.2 & 0 & 0 & 0 \\ 0 & 0 & 0.3 & 0 & 0 \\ 0 & 0 & 0 & 0.4 & 0 \\ 0 & 0 & 0 & 0 & 0.5 \end{bmatrix}$$

and

$$q = [1 \quad 1 \quad 1 \quad 1 \quad 1]$$

Since F and A_s have no common eigenvalues, there is a unique triple p, g and T to $TA_s - FT = gc$ and $pc + qT = a'$. Using the algorithm of [62], we get

$$p = -108.32$$

$$g = 10^3 \begin{bmatrix} 3.9371 \\ -6.3123 \\ 3.0116 \\ -0.4018 \\ 0.0023 \end{bmatrix}$$

$$T = 10^4 \begin{bmatrix} -0.0040 & 0.0361 & -0.1470 & 0.5518 & -0.0033 & -0.1074 \\ 0.0182 & -0.1084 & 0.3430 & -1.0379 & 0.0137 & 0.2197 \\ -0.0275 & 0.1101 & -0.2666 & 0.6066 & -0.0184 & -0.1363 \\ 0.0165 & -0.0427 & 0.0761 & -0.1128 & 0.0093 & 0.0235 \\ -0.0033 & 0.0048 & -0.0056 & 0.0032 & -0.0014 & 0.0004 \end{bmatrix}$$

Further,

$$d = Tb_s = \begin{bmatrix} -5.7416 \\ 31.5805 \\ -53.2774 \\ 33.8502 \\ -6.7547 \end{bmatrix}$$

$$r = a' A_s^{-1} b_s = -0.4497$$

Hence, the desired single-rate observer is

$$\begin{bmatrix} z_{1d}(k+1) \\ z_{2d}(k+1) \\ z_{3d}(k+1) \\ z_{4d}(k+1) \\ z_{5d}(k+1) \end{bmatrix} = \begin{bmatrix} 0.1 & 0 & 0 & 0 & 0 \\ 0 & 0.2 & 0 & 0 & 0 \\ 0 & 0 & 0.3 & 0 & 0 \\ 0 & 0 & 0 & 0.4 & 0 \\ 0 & 0 & 0 & 0 & 0.5 \end{bmatrix} \begin{bmatrix} z_{1d}(k) \\ z_{2d}(k) \\ z_{3d}(k) \\ z_{4d}(k) \\ z_{5d}(k) \end{bmatrix} + 10^3 \begin{bmatrix} 3.9371 \\ -6.3123 \\ 3.0116 \\ -0.4018 \\ 0.0023 \end{bmatrix} y_d(k)$$

$$+ \begin{bmatrix} -5.7416 \\ 31.5805 \\ -53.2774 \\ 33.8502 \\ -6.7547 \end{bmatrix} \hat{u}_d(k)$$

$$\hat{u}_d(k+1) = -108.32 y_d(k) + \begin{bmatrix} 1 & 1 & 1 & 1 & 1 \end{bmatrix} \begin{bmatrix} z_{1d}(k) \\ z_{2d}(k) \\ z_{3d}(k) \\ z_{4d}(k) \\ z_{5d}(k) \end{bmatrix}$$

$$- 0.4497 \hat{u}_d(k)$$

Note that the observer is open-loop stable and strictly causal.

Multirate Output Linear Functional Observer

Using a multirate output linear functional observer with the same T_0 and output-rate multiplicity $N^O = 3$, we obtain the following discretized plant:

$$\begin{aligned} x_d(k+1) &= A_s x_d(k) + b_s u_d(k) \\ \bar{y}_d(k) &= \bar{C} x_d(k) + \bar{d} u_d(k) \end{aligned}$$

where

$$\begin{aligned} \bar{y}_d(k) &= \begin{bmatrix} y_d(k) \\ y_d(k+1/3) \\ y_d(k+2/3) \end{bmatrix} \\ \bar{C} &= \begin{bmatrix} 0 & 0 & 0 & 1.0000 & 0 & 0 \\ 0.0001 & 0.0041 & 0.0604 & 0.9354 & 0.0001 & 0.0644 \\ 0.0006 & 0.0149 & 0.1099 & 0.8745 & 0.0007 & 0.1241 \end{bmatrix} \\ \bar{d} &= 10^{-4} \begin{bmatrix} 0 \\ 0.0308 \\ 0.4618 \end{bmatrix} \end{aligned}$$

From Corollary 5.2.1, the dimension of $z_d(k)$ is 1. Hence, a second-order observer is sufficient to estimate the same control law.

Choose $f = 0.1$ and $q = 1$. Solving $tA_s - ft = g\bar{C}$ and $p\bar{C} + qt = a'$ for the triple p, g and t, we obtain

$$\begin{aligned} p &= 10^3 [9.5084 \quad -2.8670 \quad -0.0573] \\ g &= 10^4 [-0.0082 \quad 0.5417 \quad -1.1263] \\ t &= 10^3 [-0.0007 \quad 0.0125 \quad 0.1785 \quad -6.7765 \quad -0.0007 \quad 0.1917] \end{aligned}$$

Also

$$\begin{aligned} e &= tb_s - g\bar{d} = -0.0104 \\ r &= a' A_s^{-1} b_s - p\bar{d} = -0.4382 \end{aligned}$$

Hence, the desired multirate output observer is given by

$$\begin{aligned} z_d(k+1) &= 0.1z_d(k) + 10^4\,[-0.0082 \quad 0.5417 \quad -1.1263] \begin{bmatrix} y_d(k) \\ y_d(k+1/3) \\ y_d(k+2/3) \end{bmatrix} \\ &\quad - 0.0104\hat{u}_d(k) \\ \hat{u}_d(k+1) &= 10^3\,[9.5084 \quad -2.8670 \quad -0.0573] \begin{bmatrix} y_d(k) \\ y_d(k+1/3) \\ y_d(k+2/3) \end{bmatrix} \\ &\quad + z_d(k) - 0.4382\hat{u}_d(k) \end{aligned}$$

which is open-loop stable and strictly causal. In both cases, the observer gains are large. This is a consequence of the choice of very fast estimator dynamics.

5.6 Summary

In this chapter, we have given a new insight into using multirate output sampling in designing reduced-order observers for estimating a single linear functional of the system's state for the purpose of implementing a feedback control law. Specifically, we have shown via theory and examples that reduction in the order of the observer is possible using a multirate output observer with uniform output-rate multiplicity for single-input systems. It turns out that the order of the observer only depends on the observability index of the discretized plant induced via sampling of the continuous-time plant. The multirate output observer is strictly causal and open-loop stable for sufficiently small frame period, T_0. The same type of ideas could of course be used to achieve dimension reduction in the multiple-input multiplie-output case. The algorithm of [63] would be relevant here. Further, in the next chapter, we shall emploit the ideas developed here to design reduced-order multirate input compensators for output injection feedback laws.

Chapter 6

Reduced-order Multirate Input Compensators for Output Injection Feedback Laws

6.1 Introduction

Output injection feedback is a special kind of pole-positioning mechanism whereby linear combinations of the output measurements are fed directly into the plant's state. Using output injection feedback, arbitrary closed-loop pole assignment can be achieved so long as the plant is completely observable. Nevertheless, this mechansim is in general impractical because inputs to the plant normally have to be applied though the input matrix rather than directly to the plant's state. In order to secure, at least approximately, the pole-positioning effect of output injection feedback while applying feedback at the correct input point, a dual-observer based compensator introduced in [53] is used. The dual-observer based compensator is essentially a linear dynamical system whose input and output are the plant's output and input respectively. Its implementation positions the closed-loop system poles at the eigenvalues of the compensator and those assigned via output injection feedback. In effect, it circumvents the problem of feeding back to an inaccessible point viz the plant state, and allows the implementation of output injection feedback. A review of the concept of a

dual-observer based compensator will be given in Section 6.2.

Since the seminal work of [52]-[53], the search for reduced-order compensator designs has been an ongoing process [23],[24], [34], [69] and [76]. Of these, the results of [34] and [23] are particularly interesting. As we have reviewed in the previous chapter, the authors of [34] studied controllers employing multirate sampling of the plant output and showed that arbitrary pole assignment is possible by generalized multirate-output controllers of reduced-order. One of the main results is that for a single-input system, the order of the controller, L, the output-rate multiplicity, N_i^O and the observability index, n_i^o are related by $LN_i^O \geq n_i^o$. This implies that in order to achieve arbitrary pole assignment for an n^{th}-order SISO system, the smallest order of the controller is n with single-rate sampling while with multirate output sampling, the smallest order becomes $[\frac{n}{N^O}]$, with N^O, of course, the ratio of the output sampling rate to the input sampling rate.

In [23], it was shown that in the case of estimating a single (but pre-specified) linear functional of a system's state, a multirate output linear functional observer (employing multirate sampling of the plant output) has advantage over a single-rate output linear functional observer (employing single-rate sampling of the plant output). To be precise, it was shown that by exploring the multirate output sampling mechanism developed in [33], one can design a multirate output linear functional observer of dimension much smaller than that of the single-rate output linear functional observer. The controller therein can be regarded as a combined estimator and state feedback law, which is not really the same as the controller in [34]. In the controller of [23], the dynamics of the estimator can be chosen separately from those of the closed-loop system with true state feedback. Nevertheless, the order of the controller is the same as that in [34].

In view of the substantial order reduction achievable by the multirate out-

put linear functional observer in implementing linear state feedback laws, it is natural to ask whether the same result could be achieved in output injection feedback laws. In this chapter, we show that this is indeed possible. First, we consider discrete-time systems and derive the equivalent dual-observer based compensator, herein termed a single-rate input compensator. Next, by exploring the mechanism of multirate input sampling developed in [7], we show that in the case of realizing the pole-positioning effect of output injection feedback, a multirate input compensator (employing multirate input sampling of the plant input) of dimension much smaller than that of a single-rate input compensator (employing single-rate sampling of the plant input) can be designed. At this juncture, it is important to point out that N_i^I in [7] satisfies $N_i^I \geq n_i^c$ $(i = 1, \cdots, m)$ where N_i^I and n_i^c are the input-rate multiplicity and controllability index respectively. In our scheme, N_i^I satisfies $1 \leq N_i^I < n_i^c$. Furthermore, the multirate input sampling employed here has uniform input-rate multiplicity i.e. $N_1^I = N_2^I = \cdots = N_m^I = N^I$.

The structure of the chapter is as follows: a review of the concept of a dual-observer based compensator appears in Section 6.2. The next section considers SISO continuous-time FDLTI systems and derives the structures and design procedures for the single-rate input compensator and multirate input compensator. Results pertaining to the orders of both compensators are also presented. In Section 6.4, the results from the previous section are extended to the multiple-input single-output (MISO) case. The structures and design procedures for the two types of compensators together with results concerning the orders of the compensators for this case are also presented here. An example of a SISO system appears in Section 6.5 to illustrate the ideas and methods described. Section 6.6 contains concluding remarks.

6.2 Review of Concept of Dual-Observer Based Compensator

In this section, we shall review the concept of a dual-observer based compensator introduced in [53]. We recall first the notion of output injection feedback. There is prescribed a continuous-time FDLTI minimal plant of the form

$$\dot{x}(t) = Ax(t) + Bu(t) \quad x(0) = x_0 \tag{6.2.1}$$

$$y(t) = Cx(t) \tag{6.2.2}$$

where $x(t) \in \mathbb{R}^n$, $u(t) \in \mathbb{R}^m$ and $y(t) \in \mathbb{R}^p$. Output injection feedback is the process of postulating a feedback from the output directly to the state derivative, so that (6.2.1) is replaced by

$$\begin{aligned} \dot{x}(t) &= Ax(t) + Bu(t) + K_e y(t) \\ &= (A + K_e C)x(t) + Bu(t) \end{aligned} \tag{6.2.3}$$

For observable (A, C) , it is always possible to select a K_e, termed output injection gain, so that the eigenvalues of $(A + K_e C)$ take prescribed values.

As foreshadowed in the introduction, output injection would be a desirable way of repositioning the poles of a system, except that in general it is impractical: inputs to the plant normally have to be applied "through" B, rather than directly, as in (6.2.3). The question therefore arises: can we secure, at least approximately, the pole-positioning effect of output injection feedback, while applying feedback at the correct input point ? As will be shown in the sequel, this is possible using a dual-observer based compensator.

To facilitate the following development, we shall use the concept of a dual system.

Definition 6.2.1 *[67] The continuous-time LTI system*

$$\dot{\xi}(t) = F'\xi(t) + H'\eta(t) \tag{6.2.4}$$

$$w(t) = G'\xi(t) + E'\eta(t) \tag{6.2.5}$$

is said to be the dual of the system (and vice versa)

$$\dot{x}(t) = Fx(t) + Gu(t) \tag{6.2.6}$$

$$y(t) = Hx(t) + Eu(t) \tag{6.2.7}$$

To understand what a dual-observer based compensator is, let us first recall the concept of an observer based compensator. There is prescribed a plant in state variable form given by (6.2.1)-(6.2.2). To this plant, we wish to apply linear state feedback

$$u(t) = Kx(t) + v(t) \tag{6.2.8}$$

to position the closed-loop poles. (Here, $v(t)$ is an external input). Because of the unavailability of the plant state, $x(t)$, as a measured signal, an estimator or observer of $x(t)$, or perhaps more efficiently, $Kx(t)$ is used. An observer of $Kx(t)$, termed a linear functional observer, is itself a linear system, driven by $u(t)$ and $y(t)$, of the form

$$\dot{z}(t) = Fz(t) + Gy(t) + Eu(t) \tag{6.2.9}$$

$$w(t) = Py(t) + Qz(t) \tag{6.2.10}$$

and a necessary and sufficient condition for $w(t)$ to estimate $Kx(t)$, in the sense that $w(t) - Kx(t) \to 0$ as $t \to \infty$ for all $v(t)$, $x(0)$ and $z(0)$, is that

$$\mathrm{Re}\lambda_i(F) < 0 \tag{6.2.11}$$

$$TA - FT = GC \tag{6.2.12}$$

$$E = TB \tag{6.2.13}$$

$$K = PC + QT \tag{6.2.14}$$

where T is a linear transformation such that $z(t)$ estimates $Tx(t)$. Procedures for selecting F, G *et al* to satisfy (6.2.11)-(6.2.14), including procedures which determine the dimension of F, can be found in [62]. We note that $(z(t) - Tx(t)) \to 0$ at a rate determined by the eigenvalues of F, and that

$\dim(z(t)) = \dim(x(t))$ (Kalman filter type observer),
$\dim(z(t)) = \dim(x(t)) - \dim(y(t))$ (Luenberger reduced-order observer, given independent outputs of (6.2.1)-(6.2.2)) and $\dim(z(t))$ =observability index (given scalar $u(t)$, and linear functional observer design).

The compensator resulting from the above design results in replacing (6.2.8) by

$$u(t) = w(t) + v(t) \tag{6.2.15}$$

and is

$$\dot{z}(t) = (F + EQ)z(t) + (G + EP)y(t) + Ev(t) \tag{6.2.16}$$

$$w(t) = Py(t) + Qz(t) \tag{6.2.17}$$

(Its inputs are $y(t)$ and $v(t)$ and output is $w(t)$).

When the compensator is implemented, the closed-loop transfer function matrix, obtainable from the combined system equations

$$\begin{bmatrix} \dot{x}(t) \\ \dot{z}(t) \end{bmatrix} = \begin{bmatrix} A + BPC & BQ \\ (G + EP)C & F + EQ \end{bmatrix} \begin{bmatrix} x(t) \\ z(t) \end{bmatrix} + \begin{bmatrix} B \\ E \end{bmatrix} v(t) \tag{6.2.18}$$

$$y(t) = [C \quad 0] \begin{bmatrix} x(t) \\ z(t) \end{bmatrix} \tag{6.2.19}$$

is precisely $C(sI - A - BK)^{-1}B$, as would result from use of (6.2.8). The combined system (6.2.18)-(6.2.19) has uncontrollable modes with eigenvalues $\lambda_i(F)$.

We now outline how a dual-observer based compensator for (6.2.1) -(6.2.2) is obtained. (Details will be given subsequently). First, the dual system of (6.2.1)-(6.2.2), with transfer function matrix $B'(sI - A')^{-1}C'$ is found. Next, we design an observer-based compensator for this dual plant. Then we take the dual of the compensator and use it on the original plant. It turns out that the associated closed-loop system transfer function matrix is of the form $C(sI - A - K_dC)^{-1}B$, which has the form that would result if output injection feedback were applied to (6.2.1)-(6.2.2).

To understand the details, consider the dual plant

$$\dot{\xi}(t) = A'\xi(t) + C'\eta(t) \tag{6.2.20}$$

$$w(t) = B'\xi(t) \tag{6.2.21}$$

and suppose we wish to apply a linear feedback

$$\eta(t) = K_d'\xi(t) + \zeta(t) \tag{6.2.22}$$

to reposition the closed-loop poles. Here, $\zeta(t)$ is an external input. With $\xi(t)$ unavailable for measurement, we construct an observer for $K_d'\xi(t)$, of the form

$$\dot{\lambda}(t) = F_d\lambda(t) + G_d w(t) + E_d\eta(t) \tag{6.2.23}$$

$$\mu(t) = P_d w(t) + Q_d\lambda(t) \tag{6.2.24}$$

with

$$\mathrm{Re}\lambda_i(F_d) < 0 \tag{6.2.25}$$

$$T_d A' - F_d T_d = G_d B' \tag{6.2.26}$$

$$E_d = T_d C' \tag{6.2.27}$$

$$K_d' = P_d B' + Q_d T_d \tag{6.2.28}$$

where T_d is a linear transformation such that $\lambda(t)$ estimates $T_d\xi(t)$. The associated compensator, obtained like (6.2.16)- (6.2.17) by combining the state feedback law (6.2.22) with the estimator (6.2.23)-(6.2.24), is

$$\dot{\lambda}(t) = (F_d + E_d Q_d)\lambda(t) + (G_d + E_d P_d)w(t) + E_d\zeta(t) \tag{6.2.29}$$

$$\mu(t) = P_d w(t) + Q_d\lambda(t) \tag{6.2.30}$$

It follows also that the closed-loop transfer function matrix of the combined equations

$$\begin{bmatrix}\dot{\xi}(t)\\ \dot{\lambda}(t)\end{bmatrix} = \begin{bmatrix} A' + C'P_dB' & C'Q_d \\ (G_d + E_dP_d)B' & F_d + E_dQ_d\end{bmatrix}\begin{bmatrix}\xi(t)\\ \lambda(t)\end{bmatrix} + \begin{bmatrix}C'\\ E_d\end{bmatrix}\zeta(t) \tag{6.2.31}$$

$$w(t) = \begin{bmatrix}B' & 0\end{bmatrix}\begin{bmatrix}\xi(t)\\ \lambda(t)\end{bmatrix} \tag{6.2.32}$$

is $B'(sI - A' - C'K_d')^{-1}C'$. By taking the dual of (6.2.31)- (6.2.32), we see that the equation set

$$\begin{bmatrix}\dot{x}(t)\\ \dot{z}(t)\end{bmatrix} = \begin{bmatrix}A + BP_d'C & B(G_d' + P_d'E_d')\\ Q_d'C & F_d' + Q_d'E_d'\end{bmatrix}\begin{bmatrix}x(t)\\ z(t)\end{bmatrix} + \begin{bmatrix}B\\ 0\end{bmatrix}v(t) \quad (6.2.33)$$

$$\bar{y}(t) = [C \quad E_d']\begin{bmatrix}x(t)\\ z(t)\end{bmatrix} \quad (6.2.34)$$

has transfer function matrix $C(sI - A - K_dC)^{-1}B$. Observe now that the set (6.2.33)-(6.2.34) can be regarded as the interconnection of the original system (6.2.1)-(6.2.2) together with a second system, defined by

$$\dot{z}(t) = (F_d' + Q_d'E_d')z(t) + Q_d'y(t) \quad (6.2.35)$$

$$u(t) = (G_d' + P_d'E_d')z(t) + P_d'y(t) + v(t) \quad (6.2.36)$$

At the same time, a new output, $\bar{y}(t)$ is defined by

$$\bar{y}(t) = y(t) + E_d'z(t) \quad (6.2.37)$$

The second system, with input $y(t)$ and output $u(t)$ (with $v(t)$ temporarily equal to zero), is the *dual-observer based compensator.* Its implementation positions the closed-loop system poles at the eigenvalues of F_d and of $A + K_dC$. Note that from $v(t)$ to $\bar{y}(t)$ rather than from $v(t)$ to $y(t)$ is $C(sI - A - K_dC)^{-1}B$; the closed-loop modes attributable to F_d are unobservable from $\bar{y}(t)$, but in general are observable from $y(t)$.

It is instructive to consider the direct dual of (6.2.29)-(6.2.30). (Notice that (6.2.35)- (6.2.36) was obtained by splitting up the dual of an interconnection of (6.2.29)-(6.2.30) with (6.2.20)-(6.2.21). The direct dual of (6.2.29)-(6.2.30), which has two inputs ($w(t)$ and $\zeta(t)$) and one output, necessarily has one input and two outputs and is

$$\dot{z}(t) = (F_d' + Q_d'E_d')z(t) + Q_d'y(t) \quad (6.2.38)$$

$$\bar{u}(t) = (G_d' + P_d'E_d')z(t) + P_d'y(t) \quad (6.2.39)$$

$$\tilde{u}(t) = E_d'z(t) \quad (6.2.40)$$

Of course, $\bar{u}(t)$ is used as the feedback part of $u(t)$, while $\tilde{u}(t)$ is combinable with $y(t)$ to yield $\bar{y}(t)$. Further understanding of $\bar{y}(t)$ can be achieved by noting that in a (conventional) observer-based compensator, the term $Ev(t)$ in (6.2.16) or $E_d\zeta(t)$ in (6.2.29) is normally inserted. This is a second input to the observer-based compensator. In the dual-observer based compensator, the dual of this new input becomes a second output, viz $E_d'z(t)$. By deleting the input $Ev(t)$ from (6.2.16), we can obtain another compensator such that the open-loop system has unchanged eigenvalues while the modes associated with $\lambda_i(F_d)$ are now observable from the output. This is akin to the fact that with the dual-observer based compensator, the modes associated with $\lambda_i(F_d)$ show up in the transfer function from $u(t)$ to $y(t)$, but not $u(t)$ to $y(t) + E_d'z(t)$.

Apart from the appearance of the distinction between $y(t)$ and $\bar{y}(t)$, we see that the dual-observer based compensator in effect allows implementation of output injection feedback (corresponding to replacement of $C(sI - A)^{-1}B$ by $C(sI - A - K_dC)^{-1}B$ for some choice of K_d). The dynamics of the dual observer in effect circumvent the problem of feeding back to an inaccessible point, the plant state, (which is apparently needed for output injection feedback), just like the dynamics of a normal observer circumvent the problem of feeding back from an inaccessible point (again the plant's state).

In some circumstances, one type of observer may be much more attractive than the other when it comes to pole positioning. Thus, for a multiple-input single-output (MISO) system, a much lower dimension dual-observer based compensator is likely to be possible. It is this idea which will be exploited in the later material, since multirate input sampling in some ways is like having extra inputs available.

6.3 Single-input Single-output Case

6.3.1 Single-rate Input Compensator

In this section, we begin by presenting the general structure of and the design procedure for the single-rate input compensator which is the discrete-time equivalent of the dual-observer based compensator. It also serves as the basis of deriving the multirate input compensator and comparing the reduction in the dimension of the compensator presented in the later sections. The treatment is restricted here to single-input system, and extended to multiple-input systems in Section 6.4.

Structure of Compensator

Without loss of generality, we assume that the SISO discretized plant

$$x_d(k+1) = A_s x_d(k) + b_s u_d(k) \qquad x_d(0) = x_0 \tag{6.3.1}$$

$$y_d(k) = c x_d(k) \tag{6.3.2}$$

inherits the controllability and observability properties of its continuous-time counterpart. Here,

$$A_s = \exp(AT_0) \qquad b_s = \int_0^{T_0} \exp(At) b dt \tag{6.3.3}$$

where the triple (A, b, c) represents the continuous-time plant.

In the previous section, we saw that to find a dual-observer based compensator to realize the pole-positioning effect of output injection feedback is equivalent to finding a linear functional observer to estimate the single linear functional, $k_d'\xi(t)$ for the dual system and implementing the feedback. It follows that to find a single-rate input compensator to realize the pole positioning effect of output injection feedback for (6.3.1)-(6.3.2) is equivalent to finding a discrete-time linear functional observer to estimate the single linear functional, $k_e'\xi_d(k)$ where k_e and $\xi_d(k)$ are the output injection gain and the state of the dual of

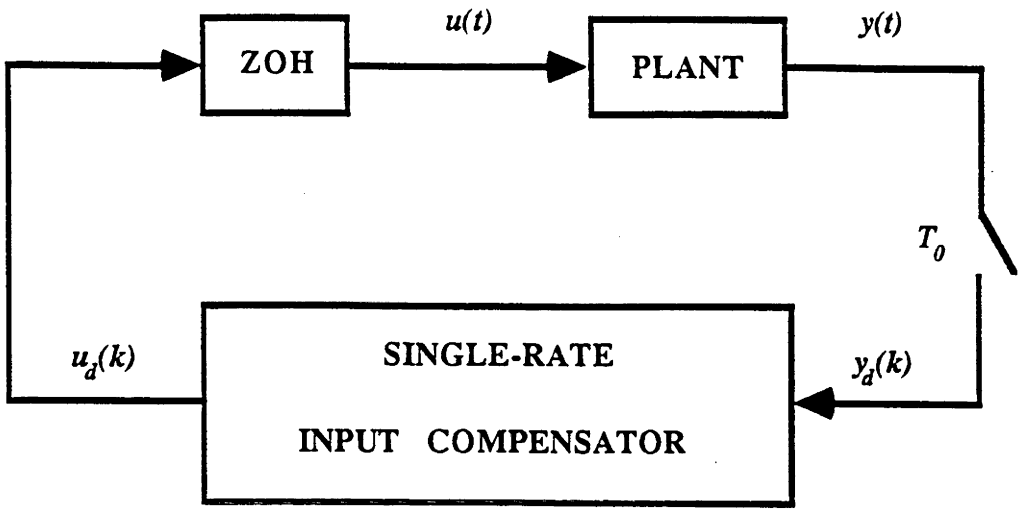

Figure 6.3.1: Connection of Plant and Single-rate Input Compensator

(6.3.1)-(6.3.2) respectively. In view of this, we obtain the following structure for the single-rate input compensator:

$$z_d(k+1) = (F' + q'e')z_d(k) + q'y_d(k) \tag{6.3.4}$$

$$u_d(k) = (g' + p'e')z_d(k) + p'y_d(k) \tag{6.3.5}$$

where the relations of F, g, e, p and q to the triple (A_s, b_s, c) are given in Lemma 6.3.1. The connection of the plant and the single-rate input compensator is shown in Figure 6.3.1.

The necessary and sufficient conditions for the existence of the single-rate input compensator are precisely those for the existence of the discrete-time linear functional observer for the dual system. These conditions are contained in the following Lemma.

Lemma 6.3.1 *The single-rate input compensator given by (6.3.4)-(6.3.5) exists if and only if the following conditions hold:*

Condition a: $|\lambda_i(F)| < 1$

Condition b: $k_e' = pb_s' + qS$

Condition c: $SA_s' - FS = gb_s'$

Condition d: $e = Sc'$

where S is linear transformation such that $\lambda_d(k)$ estimates $S\xi_d(k)$ with $\lambda_d(K)$ and $\xi_d(k)$ being the states of the duals of (6.3.1)-(6.3.2) and (6.3.4)-(6.3.5) respectively.

Proof: The proof is virtually identical with that for the continuous-time result. □

Remark 6.3.1 Note that here p is a scalar and q is a row vector. Hence, solvability of the equation in condition b for p and q, given b_s, S and k_e is guaranteed if $\text{rank}[b_s \quad S' \quad k_e] = \text{rank}[b_s \quad S'] = n$, which is the dimension of the system's state.

Order of Compensator

From the preceding material, we see that the single-rate input compensator is obtained by taking the dual of the discrete-time linear functional observer (plus feedback law). Further, the latter is designed for the dual of (6.3.1)-(6.3.2) and has dimension $(\nu - 1)$ where ν is the observability index of the dual of (6.3.1)-(6.3.2). Now, it is well-known that the discrete-time plant (6.3.1)-(6.3.2) is controllable with controllability index, $\mu = n$ and its dual is observable with observability index, $\nu = \mu = n$. Hence, the order of the compensator is $(n - 1)$ for SISO case. A more general result for the MISO case will be given in the later section.

Design Procedure for Compensator

The problem at hand boils down to finding F, g, e, p and q such that the conditions for the existence of the compensator are fulfilled. To facilitate the construction of the compensator, we outline here a design procedure for the single-rate input compensator.

1. Select T_0 according to the recommendations given in [10], [28] and [57].
2. Discretize the continuous-time plant with the selected T_0. Let the discretized plant be represented by (A_s, b_s, c).
3. Take the dual of the plant and let it be denoted by (A_s', c', b_s').
4. Choose a stable F (for simplicity, choose F to be diagonal with distinct eigenvalues) and $q = [1 \;\; 1 \;\; \cdots 1] \in \mathbb{R}^{1\times(n-1)}$. Solve for $p \in \mathbb{R}^1$, $g \in \mathbb{R}^{(n-1)}$ and $S \in \mathbb{R}^{(n-1)\times n}$ from $SA_s' - FS = gb_s'$ and $k_e' = pb_s' + qS$, using the algorithm of [62]. Note that there always exists a unique triple p, g and S solving these equations if A_s and F do not have common eigenvalues.
5. Compute $e = Sc'$.
6. Construct the required single-rate input compensator via (6.3.4)-(6.3.5).

6.3.2 Multirate Input Compensator

For a single-input system, multirate input sampling allows N^I successive and independent values of the input during each time interval $[iT_0, \overline{i+1}T_0)$, $i = 0, 1, 2, \cdots$ i.e. a new value every T_0/N^I seconds. Intuitively, this is like mantaining the original T_0 but increasing the input dimension and the column rank of the input matrix, thereby reducing the controllability index of the discretized plant. This indicates that further reduction in the order of the compensator should be possible with multirate input sampling and motivates us to study

the structure of the multirate input compensator and a design procedure for its construction.

Multirate Input Sampling

Before we deal with the structure and design procedure for a multirate input compensator, let us briefly review the concept of multirate input sampling. For single-input systems, multirate input sampling means that the plant input is changed N^I times over the time interval $[kT_0, \overline{k+1}T_0)$, $k = 0, 1, 2, \cdots$ where the integer N^I is termed the input-rate multiplicity i.e.

$$\begin{aligned} u(t) &= u(kT_0 + jT) \triangleq u_d(k + \frac{j}{N^I}) \\ & kT_0 + jT \leq t < kT_0 + (j+1)T^I \\ & (j = 0, 1, \cdots, N^I - 1; k = 0, 1, 2, \cdots) \end{aligned} \tag{6.3.6}$$

with T^I defined by

$$T^I \triangleq \frac{T_0}{N^I} \tag{6.3.7}$$

As a result of multirate input sampling, the discretized plant becomes

$$x_d(k+1) = A_s x_d(k) + \bar{B}\bar{u}_d(k) \tag{6.3.8}$$

$$y_d(k) = c x_d(k) \tag{6.3.9}$$

where A_s is given by (6.3.3),

$$\bar{B} = [\, b_m \quad A_m b_m \quad \cdots A_m^{(N^I-1)} b_m \,] \tag{6.3.10}$$

$$A_m = \exp(AT^I) \tag{6.3.11}$$

$$b_m = \int_0^{T^I} \exp(At) b dt \tag{6.3.12}$$

Also, $\bar{u}_d(k)$ is an N^I-vector, with entries given by the N^I different values assumed by $u(.)$ in the interval $[kT_0, \overline{k+1}T_0)$.

Structure of Compensator

In the same spirit as the single-rate input compensator, we propose the following structure for the multirate input compensator:

$$z_d(k+1) = (F' + q'e')z_d(k) + q'y_d(k) \tag{6.3.13}$$

$$\bar{u}_d(k) = (g' + p'e')z_d(k) + p'y_d(k) \tag{6.3.14}$$

where the relations of F, g, e, p and q to the triple $(A_s, \bar{B}, c)$ are given in Lemma 6.3.2.

The conditions for the existence of the multirate input compensator are noted in the following trivial variant on Lemma 6.3.1

Lemma 6.3.2 *The multirate input compensator given by (6.3.13)-(6.3.14) exists if and only if the following conditions hold:*

Condition a: $|\lambda_i(F)| < 1$

Condition b: $k_e' = p\bar{B}' + qS$

Condition c: $SA_s' - FS = g\bar{B}'$

Condition d: $e = Sc'$

where S is a linear transformation such that $\lambda_d(k)$ estimates $S\xi_d(k)$ with $\lambda_d(k)$ and $\xi_d(k)$ being the states of the duals of (6.3.8)-(6.3.9) and (6.3.13)-(6.3.14) respectively.

Order of Compensator

Concerning the order of the compensator, we have the following theorem.

Theorem 6.3.1 *The order of the multirate input compensator required to realize the pole-positioning effect of output injection feedback is* $\geq [n/N^I] - 1$ *where* n *and* N^I *are the dimension of the state and the input-rate multiplicity respectively.*

Proof: The dual of (6.3.8)-(6.3.9) is

$$\xi_d(k+1) = A_s'\xi_d(k) + c'\eta_d(k) \tag{6.3.15}$$

$$\bar{\omega}_d(k) = \bar{B}'\xi_d(k) \tag{6.3.16}$$

where $\xi_d(k) \in \mathbb{R}^n$, $\eta_d(k) \in \mathbb{R}^1$ and $\bar{\omega}_d(k) \in \mathbb{R}^{N^I}$ correspond to the state, input and output of the dual system. Now, it is well-known that for almost all choices of T_0,

$$\text{rank}(b_s) = \text{rank}(\int_0^{T_0} \exp(At)bdt) = \text{rank}(b) \tag{6.3.17}$$

$$\text{rank}(b_m) = \text{rank}(\int_0^{T_0/N^I} \exp(At)bdt) = \text{rank}(b) \tag{6.3.18}$$

and $(b', \exp(A'T_0/N^I))$ will be observable. As a consequence, we have

$$\begin{aligned} \text{rank}\begin{bmatrix} b_m' \\ b_m'\exp(A'T_0/N^I) \end{bmatrix} &= \text{rank}\begin{bmatrix} b' \\ b'\exp(A'T_0/N^I) \end{bmatrix} \\ &= \text{rank}\begin{bmatrix} b' \\ b'A' \end{bmatrix} \end{aligned} \tag{6.3.19}$$

$$\begin{aligned} \text{rank}\begin{bmatrix} b_m' \\ b_m'\exp(A'T_0/N^I) \\ b_m'\exp(2A'T_0/N^I) \end{bmatrix} &= \text{rank}\begin{bmatrix} b' \\ b'\exp(A'T_0/N^I) \\ b'\exp(2A'T_0/N^I) \end{bmatrix} \\ &= \text{rank}\begin{bmatrix} b' \\ b'A' \\ b'(A')^2 \end{bmatrix} \end{aligned} \tag{6.3.20}$$

et al and the rank of these successive matrices depend on the observability indices of the pair (b', A') or controllability indices of the pair (A, b). In any case, the row rank of $\bar{B}'$ can never exceed the number of rows or exceed n. Hence, column rank $\bar{B} \leq N^I$ and the result of the theorem follows. □

Remark 6.3.2 Generically, (6.3.15)-(6.3.16) will have observability index $[n/N^I]$ and thus the equality sign will hold in the theorem statement.

Design Procedure for Compensator

From the proofs of the preceding lemmas, we summarize here the design procedure for the multirate input compensator for a SISO system.

1. Select T_0 according to the recommendations given in [10], [28] and [57].

2. Choose the input-rate multiplicity N^I and discretize the continuous-time plant with T_0 obtained in (1). Let the discretized plant be represented by $(A_s, \bar{B}, c)$.

3. Using Theorem 6.3.1, the smallest order of the compensator is $([\frac{n}{N^I}] - 1)$.

4. Take the dual of the plant and let it be denoted by $(A_s', c', \bar{B}')$.

5. Choose a stable F (again for simplicity, choose F to be diagonal with distinct eigenvalues) and $q = [1 \quad 1 \quad \cdots 1] \in \mathbb{R}^{1\times([\frac{n}{N^I}]-1)}$. Solve for $p \in \mathbb{R}^{1\times N^I}$, $g \in \mathbb{R}^{([\frac{n}{N^I}]-1)\times N^I}$ and $S \in \mathbb{R}^{([\frac{n}{N^I}]-1)\times n}$ from $SA_s' - FS = g\bar{B}'$ and $k_e' = p\bar{B}' + qS$, using the algorithm of [62]. Again, provided that A_s and F do not have common eigenvalues, there always exists a triple p, g and S.

6. Compute $e = Sc'$.

7. Steps (4), (5) and (6) result in a causal multirate output linear functional observer. The required multirate input compensator (6.3.13)-(6.3.14) is obtained by taking the dual of the constructed multirate output observer (plus feedback law).

6.4 Multiple-input Single-output Case

In this section, we indicate briefly the changes applying when the original system is multiple input.

6.4.1 Single-rate Input Compensator

When the original system is multiple-input, it turns out that the general structure of the single-rate input compensator is a direct extension from the SISO case. For completeness, the structure of the compensator to realize the pole-positioning effect of output injection feedback and the conditions for its existence are summarized here.

The structure of the single-rate input compensator for a MISO system is

$$z_d(k+1) = (F' + q'e')z_d(k) + q'y_d(k) \tag{6.4.1}$$

$$u_d(k) = (g' + p'e')z_d(k) + p'y_d(k) \tag{6.4.2}$$

and the conditions for its existence are the solvability for a stable F of the equation

$$SA_s' - FS = gB_s' \tag{6.4.3}$$

together with the satisfaction of the following equations:

$$e = Sc' \tag{6.4.4}$$

$$k_e' = pB_s' + qS \tag{6.4.5}$$

where S is a linear transformation such that $\lambda_d(k)$ estimates $S\xi_d(k)$ with $\lambda_d(k)$ and $\xi_d(k)$ being the states of the duals of the original discrete-time system and (6.4.1)-(6.4.2) respectively.

The design procedure is the same as that for SISO case except that the smallest dimension of the compensator is $(\mu - 1)$ where μ is the controllability index of the discretized plant.

6.4.2 Multirate Input Compensator

As mentioned earlier in the introduction, the multirate input sampling scheme employed here has uniform input-rate multiplicity i.e.
$N_1^I = N_2^I = \cdots = N_m^I = N^I$. The structure of the multirate input compensator with uniform input-rate multiplicity and the associated design procedure also turn out to be a direct extension from the SISO case. The structure of the multirate input compensator is thus given by

$$z_d(k+1) = (F' + q'e')z_d(k) + q'y_d(k) \tag{6.4.6}$$

$$\bar{u}_d(k) = (g' + p'e')z_d(k) + p'y_d(k) \tag{6.4.7}$$

with F stable and S satisfying

$$SA_s' - FS = g\bar{B}' \tag{6.4.8}$$

There also holds

$$e = Sc' \tag{6.4.9}$$

$$k_e' = p\bar{B}' + qS \tag{6.4.10}$$

$$\bar{B} = [B_m \quad A_m B_m \quad \cdots \quad A_m^{(N^I-1)} B_m] \tag{6.4.11}$$

$$A_m = \exp(AT_0/N^I) \tag{6.4.12}$$

$$B_m = \int_0^{T_0/N^I} \exp(At)Bdt \tag{6.4.13}$$

The design procedure for a multirate input compensator turns out to be the same as that for a SISO system. The smallest dimension of the compensator is contained in the following corollary.

Corollary 6.4.1 *The order of the multirate input compensator required to realize the pole-positioning effect of output injection feedback for a multiple-input single-output system* (A, B, c) *is* $\geq [n/N^I r] - 1$ *where* n, r *and* N^I *are the dimensions of the state, the column rank of the input matrix* B *and the uniform input-rate multiplicity respectively.*

Proof: The proof follows the same approach as that of Theorem 6.3.1. □

6.5 Illustrative Example

To illustrate the ideas presented, we give an example involving a linear model for the equations of motion of a double mass-spring system used in [28]. This system is used to study the flexible structure of some mechanical systems, for example, a communications satellite with a three-axis attitude-control. The state-space description for a particular set-up is given by:

$$\begin{aligned} \dot{x}(t) &= Ax(t) + bu(t) \\ y(t) &= cx(t) \end{aligned}$$

where

$$A = \begin{bmatrix} 0 & 1 & 0 & 0 \\ -0.91 & -0.036 & 0.91 & 0.036 \\ 0 & 0 & 0 & 1 \\ 0.091 & 0.0036 & -0.091 & -0.0036 \end{bmatrix} \quad b = \begin{bmatrix} 0 \\ 0 \\ 0 \\ 1 \end{bmatrix} \quad c = [1 \ 0 \ 0 \ 0]$$

Single-rate Input Compensator

A sampling period of $T_0 = 0.4$ is used in [28] so that the sampling frequency is 15 times faster than the closed-loop bandwidth of 1 rad/sec. With single-rate sampling of the plant input, the discretized plant becomes

$$\begin{aligned} x_d(k+1) &= A_s x_d(k) + b_s u_d(k) \\ y_d(k) &= c x_d(k) \end{aligned}$$

where

$$A_s = \begin{bmatrix} 0.9285 & 0.3876 & 0.0715 & 0.0124 \\ -0.3516 & 0.9146 & 0.3516 & 0.0854 \\ 0.0071 & 0.0012 & 0.9929 & 0.3988 \\ 0.0352 & 0.0085 & -0.0352 & 0.9915 \end{bmatrix}$$

$$b_s = \begin{bmatrix} 0.0013 \\ 0.0124 \\ 0.0799 \\ 0.3988 \end{bmatrix}$$

The open-loop poles of the discretized plant are $0.9137 \pm 0.3865i$ and 1 with multiplicity 2. In [28], the desired closed-loop poles are $0.8000 \pm 0.4000i$ and $0.9000 \pm 0.0500i$ and the pole-positioning is achieved via a state feedback law. Suppose that our desire is to implement output injection feedback rather than state feedback to position the closed-loop poles. It turns out that this is achievable via output injection feedback gain, $k_e' = [-0.4275 \ -0.1911 \ -0.2537 \ -0.0247]$. Nevertheless, we know that output injection is not feasible because inputs to the plant should be applied through b_s. Hence, we shall attempt to design a minimal order compensator to realize the the pole-positioning effect of output injection feedback. As will be shown in the sequel, this is accomplished using a single-rate input compensator of order 3. However, using a multirate input compensator, the order becomes 1.

The structure of the single-rate input compensator is given by

$$z_d(k+1) = (F' + q'e')z_d(k) + q'y_d(k)$$

where

$$\begin{aligned} SA_s' - FS &= gb_s' \\ e &= Sc' \end{aligned}$$

Choose

$$F = \begin{bmatrix} 0.1 & 0 & 0 \\ 0 & 0.2 & 0 \\ 0 & 0 & 0.3 \end{bmatrix}$$

and

$$q = [1 \ \ 1 \ \ 1]$$

Since F and A_s have no common eigenvalues, there is a unique solution p, g and S to $SA_s' - FS = gb_s'$ and $k_e' = pb_s' + qS$. Using the algorithm of [62], we get

$$p = -12.08$$

$$g = \begin{bmatrix} 415.27 \\ -587.68 \\ 199.61 \end{bmatrix}$$

$$S = \begin{bmatrix} -1.0263 & 6.0365 & -45.01 & 183.96 \\ 4.0588 & -16.48 & 87.75 & -292.20 \\ -3.4437 & 10.40 & -42.02 & 113.02 \end{bmatrix}$$

Further,

$$e = Sc' = \begin{bmatrix} -1.0265 \\ 4.0588 \\ -3.4437 \end{bmatrix}$$

Hence, the desired single-rate input compensator is

$$\begin{bmatrix} z_{1d}(k+1) \\ z_{2d}(k+1) \\ z_{3d}(k+1) \end{bmatrix} = \begin{bmatrix} -0.9263 & 4.0588 & -3.4437 \\ -1.0263 & 4.2588 & -3.4437 \\ -1.0263 & 4.0588 & -3.1437 \end{bmatrix} \begin{bmatrix} z_{1d}(k) \\ z_{2d}(k) \\ z_{3d}(k) \end{bmatrix} + \begin{bmatrix} 1 \\ 1 \\ 1 \end{bmatrix} y_d(k)$$

$$u_d(k) = \begin{bmatrix} 427.67 & -636.71 & 241.21 \end{bmatrix} \begin{bmatrix} z_{1d}(k) \\ z_{2d}(k) \\ z_{3d}(k) \end{bmatrix} - 12.08 y_d(k)$$

Note that the compensator is open-loop stable.

Multirate Input Compensator

Using a multirate input compensator with the same T_0 and input-rate multiplicity $N^I = 2$, we obtain the following discretized plant:

$$\begin{aligned} x_d(k+1) &= A_s x_d(k) + \bar{B}\bar{u}_d(k) \\ y_d(k) &= c x_d(k) \end{aligned}$$

where

$$\begin{aligned} \bar{u}_d(k) &= \begin{bmatrix} u_d(k) \\ u_d(k+1/2) \end{bmatrix} \\ \bar{B} &= \begin{bmatrix} 0.0001 & 0.0012 \\ 0.0019 & 0.0105 \\ 0.0200 & 0.0599 \\ 0.1998 & 0.1990 \end{bmatrix} \end{aligned}$$

From Theorem 6.3.1, the order of the compensator is 1. Choose $f = 0.1$ and $q = 1$. Solving $sA_s' - fs = g\bar{B}'$ and $k_e' = p\bar{B}' + qs$ for the triple p, g and s, we obtain

$$\begin{aligned} p &= [\ 806.78\ \ -279.88\ ] \\ g &= [\ 334.52\ \ -808.93\ ] \\ s &= \begin{bmatrix} -0.1696 & 1.1935 & 0.3774 & -105.54 \end{bmatrix} \end{aligned}$$

Also,

$$e = sc' = -0.1696$$

Hence, the desired multirate input compensator is given by

$$z_d(k+1) = -0.0696 z_d(k) + y_d(k)$$

$$\bar{u}_d(k) = \begin{bmatrix} 197.67 \\ -761.46 \end{bmatrix} z_d(k) + \begin{bmatrix} 806.78 \\ -279.88 \end{bmatrix} y_d(k)$$

which is again open-loop stable.

6.6 Summary

In this chapter, we have given a new insight into using multirate input sampling in designing reduced-order compensators for realizing the pole-positioning effect of output injection feedback. Specifically, we have shown via theory and examples that reduction in the order of the compensator is possible using a multirate input compensator with uniform input-rate multiplicity for single-output systems. It turns out that the order of the compensator only depends on the controllability index of the discretized plant induced via sampling of the continuous-time plant. The same type of ideas could be extended to achieve order reduction in the multiple-input multiple-output case. The algorithm of [63] would be relevant in this context.

Chapter 7

Discrete-time Loop Transfer Recovery via GSHF Based Compensator

7.1 Introduction

It is well-known that the plant input robustness properties of a state feedback design, such as measured by phase margins, for example, can evaporate with a state estimate feedback design [3], [20], [21], [48] and [72]. An important class of state feedback design is linear quadratic (LQ) design, with the associated state estimate feedback design being the linear quadratic gaussian (LQG) design.

Continuous-time LQG with loop transfer recovery (LQG/LTR) techniques, which were developed by Doyle and Stein [21]-[22] and discussed further by Stein and Athans [74], have become popular because they allow the desirable feedback properties (e.g. [72]) of state feedback schemes to be asymptotically recovered (as a design parameter tends to a limit) by output feedback schemes. One restriction of the existing LQG/LTR methods is that they can obtain arbitrarily good recovery only for continuous-time minimum-phase plants. If the plant is nonminimum-phase, the LTR techniques cannot recover the state feedback loop arbitrarily well.

The problem of applying the existing LQG/LTR method to continuous-time

nonminimum-phase systems is highlighted by [80]. In [80], the authors show that if the plant is nonminimum-phase, then the quality of the LTR will depend on the location of the nonminimum-phase zeros as well as the properties of the state feedback loop. Their approach considers a minimum-phase, all-pass factored form model for the plant and shows that when the standard LTR procedure is applied at the input, the resulting sensitivity function has a certain asymptotic property. It is further shown that if the plant is nonminimum-phase, the difference between the sensitivity function of the state feedback loop and that of the system resulting from an attempt at recovering using the LTR procedure depends on the size of the error function which reflects the difference between the actual sensitivity function and the desired sensitivity function. In summary, their result shows that exact loop recovery does not take place in general for nonminimum-phase systems and one can only hope for "almost loop recovery" at those frequencies when the norm of the error function is small enough.

A number of researchers have attempted to provide a systematic approach to deal with this problem [11],[26],[55],[61],[60],[59], [74]. Stein and Athans [74] have suggested several devices to help circumvent this problem. In [11], it is stated without proof that LQG/LTR can be applied successfully to a nonminimum-phase system if the nonminimum-phase zeros are outside the bandwidth of the state feedback loop.

In [60], the loop recovery technique is generalised for nonminimum-phase plants in the sense that the open-loop properties of certain partial state feedback designs are recovered in a state estimate feedback controller design involving the addition of fictitious plant noise. Similarly to [80], the authors employ a minimum-phase, all-pass factored form model. The partial state is the state of a minimum-phase factor in the model. Their contribution is to extend the notion of loop recovery to certain classes of state estimate feedback design for

nonminimum-phase plants. The state estimate feedback controller design is based on applying known LQG and H^∞ techniques [26] and [59]. The mechanism is the following : an initial state feedback design constrains the feedback to feedback of only the minimum-phase factor states. Next, the addition of the fictitious noise at the input to the minimum-phase factor ensures that when state estimators are employed, there is loop recovery.

The drawback of their approach is that certain nonminimum-phase plants can never be "robustly" controlled using state feedback of only the minimum-phase factor states. In the latter case, when LTR is applied, it is not expected that the resulting design will be "robust". As a consequence, the generalisation restricts the class of state feedback controllers to those which feedback only the state (or estimator) associated with the minimum-phase states in the all-pass/minimum-phase factored model. In other words, for some nonminimum-phase plants, such controllers are not expected to achieve robust designs comparable to those for minimum-phase plants.

In [61], the idea of [60] was extended to LQG designs based on H^∞/H^2 optimisation methods. The key contributions of the paper are to formulate the loop recovery objective as a standard H^∞/H^2 optimisation exercise, to avoid high estimator or control loop gains, to cope systematically with nonminimum-phase plants, and to maintain availability of the optimal state estimates when required. Unfortunately, this work inherits the shortcomings of [60] in that it only achieves partial loop recovery for nonminimum-phase plants with feedback of only the minimum-phase factor states, assuming the plant is factored into a product of a stable all-pass factor and a minimum-phase factor.

Recently, extension of the LTR design techniques to discrete-time systems has been studied by a number of researchers [36], [55], [65] and [81]. The motivation for such an interest is due to the following two reasons: firstly, guaranteed feedback properties for the discrete-time LQ optimal regulator or

Kalman filter do exist [5], [71] and [73], although they are not as attractive as in the continuous-time case. Naturally, it is desirable to have a method of recovering these properties. Secondly, as seen for continuous-time systems, the LTR procedure significantly simplifies the use of the LQG methodology. Knowing that it will be recovered in the LTR procedure, the designer can mainly concentrate on the design of the state feedback loop.

In [55], the problem of recovering properties at the plant output in discrete-time is studied. Two types of Kalman filters, namely current-estimation type and one-step-ahead prediction type, are considered for the compensator design, which is synthesized as the series connection of the Kalman filter and the optimal state estimate feedback law. One of the major and interesting results is that if the plant is minimum-phase with all its infinite zeros of order one and if the cheap regulator is applied to the current-estimation type Kalman filter, then the state feedback loop of the observer can be perfectly recovered. It is also observed that, although it is generally impossible to have perfect recovery when the plant is nonminimum-phase or when the prediction-type Kalman filter has to be used, a useful degree of recovery is often obtained. An interpretation of this phenomenon in terms of asymptotic eigenvalue locations is also provided in [55]. The LQG/LTR procedure developed in [55] will be further reviewed in Section 7.2.

In [65], the mechanism of loop recovery in [55] is studied. In order to achieve perfect loop recovery and avoid obtaining an unstable controller simultaneously, the poles of the compensator are selected so that only the minimum-phase zeros of the plant are cancelled. As a consequence, the output feedback loop transfer function is still nonminimum-phase. This in turn limits the achievable performance, and 'good' loop shapes for the target loop function are difficult to achieve.

The LTR procedure using prediction estimators for square discrete-time

minimum-phase systems is considered in [36]. It is shown that although perfect recovery is impossible, the feedback properties obtained by the recovery techniques are those that can be recovered best in the presence of the delay in the controller.

The problem of applying existing LQG/LTR method to discrete-time nonminimum-phase plants is highlighted by [81] which generalises the results of [80] to discrete-time. Adopting an approach similar to [80], the authors consider an all-pass/minimum-phase factored model for the discrete-time plants and employ the LTR procedure proposed by [55]. The results that they obtain are not surprising considering that the approach is similar to [80]; similar conclusions to those appearing in the continuous-time case are derived.

In this chapter, we consider discrete-time LTR. We explore the zero placement capability of generalised sampled-data hold functions (GSHF) developed in [38] and show that any continuous-time plant can be discretized to a minimum-phase one with a simple zero at infinity, irrespective of whether the underlying continuous-time plant is minimum-phase or not. As a consequence, employing the discrete-time LQG/LTR procedure for minimum-phase systems of [55] in conjunction with the proposed GSHF based compensator, we are able to achieve perfect loop recovery irrespective of whether the underlying continuous-time plant is minimum-phase or not.

This chapter is organised as follows. In Section 7.2, preliminaries pertaining to the discrete-time LQG/LTR design procedure in [55] are reviewed. Specifically, the problem of applying the existing method to a nonminimum-phase plant is highlighted. In Section 7.3, we present the proposed method of using GSHF to position the finite zeros of the continuous-time plant and show that the discretized plant can always be made minimum-phase with zero at infinity of order one regardless of whether the original continuous-time plant is minimum-phase or not. Results for perfect loop recovery are then developed. An example

illustrating the idea is given in Section 7.4. Conclusions are drawn in Section 7.5.

7.2 Review of Discrete-time LQG/LTR Procedure

In [55], the plant to be controlled is assumed to be modelled as

$$x_d(k+1) = A_d x_d(k) + B_d v_d(k) \tag{7.2.1}$$

$$y_d(k) = C_d x_d(k) \tag{7.2.2}$$

where $x_d(k) \in \mathbb{R}^n$ is the state, $v_d(k) \in \mathbb{R}^m$ is the input and $y_d(k) \in \mathbb{R}^m$ is the output and A_d, B_d and C_d are constant matrices. This model is induced via standard sampling, with a zeroth-order hold (ZOH), of a continuous-time, strictly proper, FDLTI system. To be specific, if the continuous-time system is given by the triple (A, B, C), then

$$A_d = \exp(AT_0) \quad B_d = \int_0^{T_0} \exp(At)Bdt \quad C_d = C \tag{7.2.3}$$

where T_0 is the sampling time. Further, we assume that the model is minimal and B_d and C_d are each full rank. The open-loop transfer function of the plant is defined as

$$P_{zoh}(z) \triangleq C_d(zI - A_d)^{-1}B_d \tag{7.2.4}$$

The design procedure is summarized as follows. First, fictitious process and measurement noise covariance matrices, $W \geq 0$ and $V > 0$, are used to obtain a steady-state Kalman filter which takes the following form:

$$\hat{x}_d(\overline{k+1}/k) = A_d\hat{x}_d(k/\overline{k-1}) + B_d v_d(k) + A_d K_f^f[y_d(k) - C_d\hat{x}_d(k/\overline{k-1})] \tag{7.2.5}$$

$$\hat{x}_d(k/k) = \hat{x}_d(k/\overline{k-1}) + K_f^f[y_d(k) - C_d\hat{x}_d(k/\overline{k-1})] \tag{7.2.6}$$

where

$$K_f^f = PC_d'(C_dPC_d' + V)^{-1} \tag{7.2.7}$$

and P is the unique positive semidefinite solution of the Riccati equation

$$P = A_d P A_d' - A_d P C_d' (C_d P C_d' + V)^{-1} C_d P A_d' + W \tag{7.2.8}$$

Note that the Kalman filter used here is the current-estimation type. (Sometimes, it is called a filtering observer).

As set out in [55], the dynamics of the plant are augmented if necessary, and the W and V matrices are adjusted until the frequency response characteristics of the Kalman filter are those which the designer would like to obtain at the output of the compensated plant. By frequency response characteristics, we mean the behaviour of indicators such as the characteristic loci or the singular values of the filter's open-loop return ratio (or sometimes called observer loop transfer function)

$$H_{ob}(z) = C_d(zI - A_d)^{-1} A_d K_f^f \tag{7.2.9}$$

and/or its closed-loop transfer function

$$\Phi(z) = H_{ob}(z)[I + H_{ob}(z)]^{-1} \tag{7.2.10}$$

Notice that the filter's open-loop return ratio is independent of the input matrix B_d of the plant.

As a next step of the design procedure, an optimal state estimate feedback controller is synthesized using the performance index

$$J = \sum_{k=0}^{\infty} (v_d'(k) R v_d(k) + x_d'(k) Q x_d(k)) \tag{7.2.11}$$

where $Q = C_d' C_d \geq 0$ and $R = I/q^2$ with q being a real number. For loop recovery purposes (and as indicated below in Theorem 7.2.1), q will be taken as very large. (The choice of $q = \infty$ will generally be acceptable in the sense that the calculations can be carried through). The optimal state estimate feedback control law is given by

$$v_d(k) = -F \hat{x}_d(k/k) \tag{7.2.12}$$

where the state feedback matrix, F is given by

$$F = (B_d'MB_d + R)^{-1}B_d'MA_d \tag{7.2.13}$$

and M is the unique positive semidefinite solution of the Riccati equation:

$$M = A_d'MA_d - A_d'MB_d(B_d'MB_d + R)^{-1}B_d'MA_d + Q \tag{7.2.14}$$

Finally, a feedback compensator is synthesized as the series connection of the current-estimation type Kalman filter (7.2.5)-(7.2.8) and the optimal state estimate feedback controller (7.2.12) in the usual way. It follows that the resulting Kalman filter based compensator can be written in the following state-space model:

$$\begin{aligned} \zeta_d(k+1) &= (A_d - B_dF)(I - K_f^fC_d)\zeta_d(k) + (A_d - B_dF)K_f^fy_d(k) \quad (7.2.15) \\ v_d(k) &= -F(I - K_f^fC_d)\zeta_d(k) - FK_f^fy_d(k) \quad (7.2.16) \end{aligned}$$

where $\zeta_d(k) = \hat{x}_d(k/\overline{k-1})$. Further, from (7.2.15)- (7.2.16), simple manipulations show that the transfer function of the compensator is given by

$$C_{kf}^{ZOH}(z) = zF[zI - (I - K_f^fC_d)(A_d - B_dF)]^{-1}K_f^f \tag{7.2.17}$$

Notice that the compensator has to operate with zero delay, i.e. a new compensator output (plant input) must be available at virtually the time a new compensator input (plant output) is introduced with the compensator output value depending on the new compensator input value.

To facilitate the following development, we define formally concepts of output feedback loop transfer function, transmission zeros, minimum-phase and nonminimum-phase systems here.

Definition 7.2.1 *When the above discrete-time LTR procedure is used, the output feedback loop transfer function, $H_{kf}^{ZOH}(z)$ is defined as*

$$H_{kf}^{ZOH}(z) \triangleq P_{zoh}(z)C_{kf}^{ZOH}(z) \tag{7.2.18}$$

where $P_{zoh}(z)$ and $C_{kf}^{ZOH}(z)$ are defined by (7.2.4) and (7.2.17) respectively.

Definition 7.2.2 *The transmission zeros of the discrete-time system (7.2.1)-(7.2.2) are defined to be the set of complex numbers a which satisfy the following inequality*

$$rank\begin{bmatrix} aI - A_d & B_d \\ C_d & 0 \end{bmatrix} < n + m$$

The multiplicity of a is equal to its algebraic multiplicity as defined in [54].

Definition 7.2.3 *The discrete-time system (7.2.1)-(7.2.2) is termed minimum-phase if all transmission zeros lie (strictly) inside the unit circle in the complex plane.*

A key result concerning discrete-time perfect loop recovery for a minimum-phase system is the following theorem.

Theorem 7.2.1 *[55] If $P_{zoh}(z)$ given by (7.2.4) is minimum-phase, $det(C_dB_d) \neq 0$ and the above discrete-time LTR procedure is used to obtain the Kalman filter based compensator given by (7.2.17), then, as $q \rightarrow \infty$, perfect loop recovery can be achieved asymptotically at the plant output i.e. as $q \rightarrow \infty$,*

$$H_{kf}^{ZOH}(z) \rightarrow H_{ob}(z)$$

Remark 7.2.1 If $\det(C_dB_d) = 0$, then $P_{zoh}(z)$ has fewer than $(n - m)$ finite zeros. In this case, even if $P_{zoh}(z)$ is minimum-phase, there are now not enough finite zeros to cancel all the poles introduced by $C_{kf}^{ZOH}(z)$ and perfect recovery is again impossible. As remarked in [55], the requirement $\det(C_dB_d) \neq 0$ can be satisfied by most sampled-data systems. However, we point out that there is an example in [32] where $\det(C_dB_d) = 0$ for all nonzero sampling time.

Remark 7.2.2 The mechanism by which recovery is achieved is thus essentially the same as in the continuous-time case: the compensator cancels the plant zeros and possibly some of the stable poles and inserts the compensator's

zeros. Clearly, this will fail if the plant is nonminimum-phase, the reason being that there would have to be open-loop unstable pole-zero cancellations leading to instability. This is potentially an even more serious limitation for discrete-time than for continuous-time since the standard sampling process with ZOH applied to a strictly proper continuous-time plant is known to introduce zeros, some of which always lie outside the unit circle at least for small sampling time [9].

Remark 7.2.3 In the continuous-time case, loop recovery is also achievable by designing a state feedback law to give an acceptable (input) loop gain, and then designing an estimator with a process noise covariance matrix which is specially chosen. (Of course, the plant must also be minimum-phase). When the approach is attempted in the discrete-time case, the estimator becomes a one-step ahead prediction type rather than current-estimation type, and consequently, exact recovery is no longer possible, just as when the processing delays require for the method described earlier the replacement of (7.2.12) via $v_d(k) = -F\hat{x}_d(k/\overline{k-1})$.

Remark 7.2.4 Even with perfect recovery, recall that the robustness properties will not be as attractive in general as those obtainable in the continuous-time case.

7.3 Perfect Loop Transfer Recovery via GSHF Based Compensator

In this section, we exploit the power of GSHF and show that the finite zeros of the discrete-time system formed by cascade of GSHF, plant and sampler can be arbitrarily placed so that the resulting discretized plant is minimum-phase. A block diagram illustrating the interconnection of the continuous-time plant and

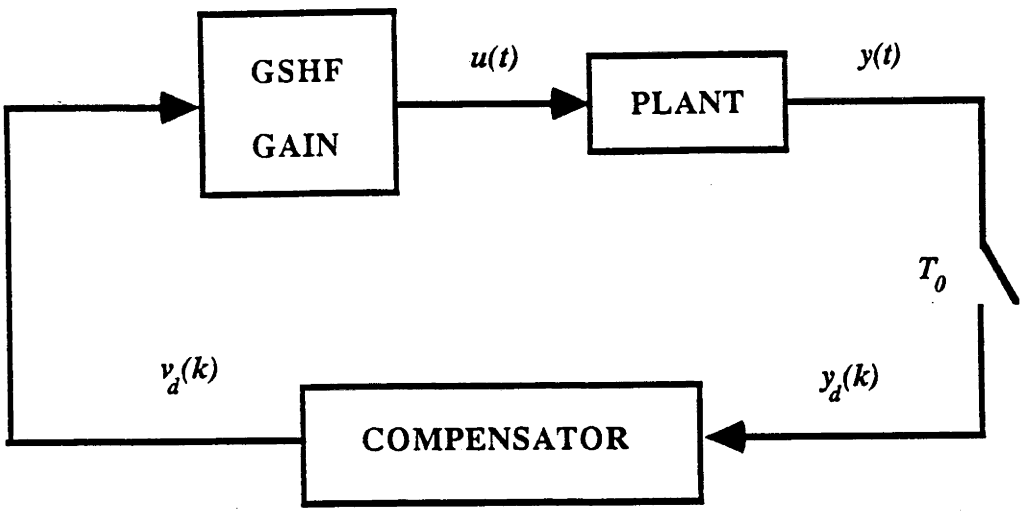

Figure 7.3.1: Connection of Plant and GSHF Based Compensator

the GSHF based compensator is shown in Figure 7.3.1; the subsystem GSHF is defined further below.

To fix idea, we begin with a continuous-time, strictly proper, FDLTI, square plant with a minimal state-space model:

$$\dot{x}(t) = Ax(t) + Bu(t) \tag{7.3.1}$$

$$y(t) = Cx(t) \tag{7.3.2}$$

where $u \in \mathbb{R}^m$ and $y \in \mathbb{R}^m$ are the input and output respectively, $x \in \mathbb{R}^n$ is the state vector, and A, B, C are constant matrices.

Using GSHF, the input to the plant, $u(t)$ becomes

$$u(t) = F(t)v_d(k) \quad \text{for} \quad t \in [kT_0, \overline{k+1}T_0) \tag{7.3.3}$$
$$k = 0, 1, 2, \cdots$$

where $T_0 > 0$ is the sampling period, $F(t)$ is a T_0-periodic integrable and bounded hold function matrix of appropriate dimension (selectable by the de-

signer), and $v_d(k)$, whose dimension is the same as that of $u(t)$, is the output of the Kalman filter based compensator.

The following equation

$$\int_0^{T_0} \exp[A(T_0 - t)]BF(t)dt = G_d \tag{7.3.4}$$

for the unknown $F(t)$ with G_d a given constant matrix, plays an important role in the design of the GSHF based compensator. The properties with respect to (7.3.4) are summarized in the following Lemma.

Lemma 7.3.1 *[79] Let (A, B) be controllable, G_d be given and*

$$W(A, B, T_0) = \int_0^{T_0} \exp[A(T_0 - t)]BB' \exp[A'(T_0 - t)]dt \tag{7.3.5}$$

Then

1. *$F_0(t) = B' \exp[A'(T_0 - t)]W^{-1}(A, B, T_0)G_d$ is the unique optimal solution of (7.3.4) in the sense of minimizing tr $\int_0^{T_0} F'(t)F(t)dt$;*

2. *for almost all $T_0 > 0$, there exists a piecewise constant solution of (7.3.4) taking at most n different values in the interval $[0, T_0]$;*

3. *for almost all $T_0 > 0$, there exists a sequence of piecewise constant solutions $F_k(t)$ of (7.3.4) which uniformly converges to $F_0(t)$ in the interval $[0, T_0]$ under a usual matrix norm.*

Applying (7.3.3) to the system (7.3.1)-(7.3.2) and sampling the continuous-time state and output, we obtain the following discrete-time system from $v_d(k)$ to $y_d(k)$:

$$x_d(k+1) = A_d x_d(k) + G_d v_d(k) \tag{7.3.6}$$

$$y_d(k) = C_d x_d(k) \tag{7.3.7}$$

where A_d and C_d are related to A and C as in (7.2.3) and G_d is related to the GSHF gain $F(t)$ as in (7.3.4). The associated transfer function is

$$P_{gshf}(z) \triangleq C_d(zI - A_d)^{-1}G_d \tag{7.3.8}$$

Concerning the discrete-time plant (7.3.8), we have the following important lemma.

Lemma 7.3.2 *The discrete-time plant $P_{gshf}(z)$ can always be made minimum-phase with zero at infinity of order one via choice of a suitable GSHF gain, $F(t)$ irrespective of whether the underlying continuous-time system (7.3.1)-(7.3.2) is minimum-phase or nonminimum-phase.*

Proof: Take arbitrary $T_0 > 0$ such that

$$T_0 \neq \frac{2k\pi}{\mathrm{Im}(p_i - p_j)} \quad \text{for all integers } k$$

whenever $\mathrm{Re}(p_i - p_j) = 0$ with p_i, p_j being the poles of the plant. Then (A_d, C_d) is observable and (A_d, G_d) is stabilisable, [40], moreover, we can generically choose an $n \times m$ constant matrix G_d such that

$$\begin{aligned} \det(C_dG_d) &\neq 0 \\ \mathrm{rank}\begin{bmatrix} zI - A_d & G_d \\ C_d & 0 \end{bmatrix} &= n + m \ \forall \ z \in \bar{D} \end{aligned}$$

where $\bar{D} = \{z \in \mathbb{C} : |z| \geq 1\}$ with $\mathbb{C} = \{\text{complex numbers}\}$. For such a G_d, the above inequalities evidently imply that all finite zeros are minimum-phase and $lim_{z\to 0} zP_{gshf}(z)$ is nonsingular. A systematic procedure for choosing G_d is given in Appendix D. □

Next, we adopt a similar procedure of introducing fictitious process and measurement noise covariance matrices, W and V, as in Section 7.2 to obtain a

GSHF based compensator. The Kalman filter in the GSHF based compensator takes the following form:

$$\hat{x}_d(\overline{k+1}/k) = A_d\hat{x}_d(k/\overline{k-1}) + G_dv_d(k) + A_dK_f^f[y_d(k) - C_d\hat{x}_d(k/\overline{k-1})] \quad (7.3.9)$$

$$\hat{x}_d(k/k) = \hat{x}_d(k/\overline{k-1}) + K_f^f[y_d(k) - C_d\hat{x}_d(k/\overline{k-1})] \quad (7.3.10)$$

where K_f^f and P are as defined in (7.2.7) and (7.2.8) respectively.

Next, the optimal state estimate feedback law is synthesized using the discrete-time performance index given by (7.2.11) with the same state weighting matrix, Q and control weighting matrix, R as before i.e. $Q = C_d'C_d \geq 0$ and $R = I/q^2$ with q being a real number. The optimal state estimate feedback controller is given by

$$v_d(k) = -\tilde{F}\hat{x}_d(k/k) \quad (7.3.11)$$

where the state feedback matrix, $\tilde{F}$ is given by

$$\tilde{F} = (G_d'\tilde{M}G_d + R)^{-1}G_d'\tilde{M}A_d \quad (7.3.12)$$

and $\tilde{M}$ is the unique positive semidefinite solution of the Riccati equation:

$$\tilde{M} = A_d'\tilde{M}A_d - A_d'\tilde{M}G_d(G_d'\tilde{M}G_d + R)^{-1}G_d'\tilde{M}A_d + Q \quad (7.3.13)$$

Finally, a GSHF based feedback compensator is synthesized as the series connection of the current-estimation type Kalman filter given by (7.2.7)-(7.2.8) and (7.3.9)-(7.3.10) and the optimal state estimate feedback controller (7.3.11). It is easy to see that the state-space model of the GSHF based compensator can be written as

$$\zeta_d(k+1) = (A_d - G_d\tilde{F})(I - K_f^fC_d)\zeta_d(k) + (A_d - G_d\tilde{F})K_f^fy_d(k) \quad (7.3.14)$$

$$v_d(k) = -\tilde{F}(I - K_f^fC_d)\zeta_d(k) - \tilde{F}K_f^fy_d(k) \quad (7.3.15)$$

where $\zeta_d(k) = \hat{x}_d(k/\overline{k-1})$. It follows that the transfer function of the compensator is given by

$$C_{kf}^{GSHF}(z) = z\tilde{F}[zI - (I - K_f^fC_d)(A_d - G_d\tilde{F})]^{-1}K_f^f \quad (7.3.16)$$

The following definition is needed in the subsequent development.

Definition 7.3.1 *When the discrete-time LTR procedure using the proposed GSHF based compensator is used, the output feedback loop transfer function,* $H_{kf}^{GSHF}(z)$ *is defined as*

$$H_{kf}^{GSHF}(z) \triangleq P_{gshf}(z)C_{kf}^{GSHF}(z) \tag{7.3.17}$$

where $P_{gshf}(z)$ *and* $C_{kf}^{GSHF}(z)$ *are defined by (7.3.8) and (7.3.16) respectively.*

Now, we state the main result concerning discrete-time loop recovery using GSHF based compensator.

Theorem 7.3.1 *Consider the minimum-phase discrete-time* $P_{gshf}(z)$ *with zero at infinity of order one given by (7.3.8). If the prescribed LTR procedure is applied to obtain the GSHF based compensator given by (7.3.16), then, as* $q \rightarrow \infty$, *perfect loop recovery can be achieved asymptotically at the plant output i.e. as* $q \rightarrow \infty$,

$$H_{kf}^{GSHF}(z) \rightarrow H_{ob}(z)$$

Proof: The result follows from Theorem 7.2.1 and Lemma 7.3.2 □

7.4 Illustrative Example

To illustrate the ideas presented, we give an example involving a nonminimum phase system used in [80] which is given by:

$$\begin{aligned} \dot{x}(t) &= Ax(t) + bu(t) \\ y(t) &= cx(t) \end{aligned}$$

where

$$A = \begin{bmatrix} 0 & -3 \\ 1 & -4 \end{bmatrix} \qquad b = \begin{bmatrix} -5 \\ 1 \end{bmatrix} \qquad c = [0 \;\; 1]$$

Note that the system has stable poles at -3, -1 and an unstable zero at 5.

Suppose that the goals of our design are to adjust the fictitious process and measurement noise covariance matrices V and W so that the step-response of the closed-loop system (7.2.10) meet the following specifications.

(a) Rise time, $t_r \simeq 0.1$ *sec*

(b) Settling time, $t_s \leq 0.5$ *sec*

(c) Maximum overshoot, $M_p \leq 15$ %

It is well-known that for a second-order discrete-time system without any finite zeros , t_r, t_s, M_p and the phase margin, PM are related to the damping coefficient, ζ and the closed-loop bandwidth, ω_{cl} as follows [28]:

(i) $t_r = \frac{1.8}{\omega_{cl}}$

(ii) $t_s = \frac{4.6}{\zeta\omega_{cl}}$

(iii) $\zeta \geq 0.6(1 - \frac{M_p}{100})$

(iv) PM $\geq 100\zeta$

Even though we are interested in sampled data control of a continuous-time system, the discretisation of which has a finite zero, we will use these guidelines as an initial basis for a design. Using guideline (iii), specification (c) implies that the damping coefficient ζ must be ≥ 0.51. (Incidentally, this is in line with the recommendation of $0.4 \leq \zeta \leq 0.8$ for good design given in [28]). Here, we choose $\zeta = 0.6$. It follows from specification (b) and guideline (ii) that $\omega_{cl} \geq 15.3$ *rad/sec*. This in turn implies that $t_r \leq 0.12$ *sec* according to guideline (i). Also, with $\zeta = 0.6$, it follows from guideline (iv) that $PM \geq 60^o$.

Next, following the recommendations given in [28], the sampling period T_0 is chosen to be 0.04 *sec*. With this value of T_0 and a ZOH interconnecting the continuous-time plant and the Kalman filter based compensator, the discretized plant becomes

$$\begin{aligned} x_d(k+1) &= A_d x_d(k) + b_d v_d(k) \\ y_d(k) &= c x_d(k) \end{aligned}$$

where

$$A_d = \exp(AT_0) = \begin{bmatrix} 0.9977 & -0.1108 \\ 0.0369 & 0.8500 \end{bmatrix}$$
$$b_d = \int_0^{T_0} \exp(At)bdt = \begin{bmatrix} -0.2021 \\ 0.0331 \end{bmatrix}$$

and obviously, the input to the plant, $u(t)$ is related to the output of the compensator, $v_d(k)$ as follows:

$$u(t) = v_d(k) \quad kT_0 \leq t \leq (k+1)T_0$$

It is not difficult to see that the only finite unstable zero is 1.223. Thus, the discretized plant is still nonminimum-phase and with the Kalman filter based compensator given by (7.2.17), perfect loop recovery (in fact, even near perfect recovery) cannot be achieved. We shall now present some simulation results to further illustrate this.

It turns out that with $v = 0.04$ and $W = \begin{bmatrix} 1 & 0 \\ 0 & 0 \end{bmatrix}$, the aforementioned specifications for the step response are met for (7.2.10) i.e. with no loop recovery introduced and for a discrete-time rather than sampled-data system. The step-response of the closed-loop system is shown in Figure 7.4.1. Notice that this is for the discrete-time system, even though the curve is drawn continuously. From Figure 7.4.1, t_r, t_s and M_p are found to be 0.12 *sec*, 0.44 *sec* and 14.9 % respectively. The steady-state position error of $< 5\%$ is due to the fact the closed-loop system is of type 0.

Corresponding to the aforementioned values of v and W, the Kalman filter gain is $k_f^f = [\,3.8173 \quad 0.3874\,]'$ and the filter's open-loop return ratio, $h_{ob}(z)$ is

$$h_{ob}(z) = \frac{0.4702(z - 0.702)}{(z - 0.9608)(z - 0.8869)}$$

A Nyquist plot of $h_{ob}(z)$ is presented in Figure 7.4.2. From the graph, the gain margin and the phase margin are found to be 59^o and 13.3 dB respectively.

Using the LQ optimisation technique with the performance index given by (7.2.11) with $Q = \begin{bmatrix} 0 & 0 \\ 0 & 1 \end{bmatrix}$ and $r = 1/q^2$, the optimal state estimate feedback

gain f is calculated as q varies. For each q, the Nyquist diagram of $h_{kf}^{ZOH}(z)$ is then evaluated using (7.2.18). In Figure 7.4.3, the solid curve is the desired response shown in Figure 7.4.2. The other curves indicate the Nyquist plots of $h_{kf}^{ZOH}(z)$ as q varies from 3 to 1000. As q increases beyond 1000, there are no noticeable changes in the curves. From Figure 7.4.3, it can be seen that the GM's for different q are always smaller than 13.3 dB for all q. The PM's cannot be determined from the plots as $h_{kf}^{ZOH}(z)$ never intersects the unit circle for the frequency range of interest. We further show the corresponding step responses when loop recovery is attempted with the Kalman filter based compensator as q varies over the range as before. The simulation results are displayed in Figure 7.4.4. In Figure 7.4.4, the solid curve is the desired response of Figure 7.4.1. The other curves show the step responses for increasing q. The control input for $q = 3$ is displayed in Figure 7.4.5. The simulation results clearly demonstrate that perfect loop recovery cannot be achieved using the existing method of discrete-time LTR.

Next, using the procedure of selecting g_d outlined in Appendix D the discretized plant is made minimum-phase by $g_d = [27 \quad 2]'$. Sampling the continuous-time plant with the same T_0 and a GSHF (whose gains are defined later) interconnecting the continuous-time plant and the Kalman filter based compensator yields

$$\begin{aligned} x_d(k+1) &= A_d x_d(k) + g v_d(k) \\ y_d(k) &= c x_d(k) \end{aligned}$$

It can be readily shown that the finite zero is now at 0.5. The discretized plant from $v_d(k)$ to $y_d(k)$ is evidently minimum phase. Moreover, the product $cg_d = 2 \neq 0$. Hence, perfect loop recovery is asymptotically achievable according to Theorem 7.3.1. The input to the plant, $u(t)$ is related to the output of the compensator, $v_d(k)$ as follows:

$$u(t) = f(t)v_d(k) \qquad kT_0 \leq t \leq (k+1)T_0$$

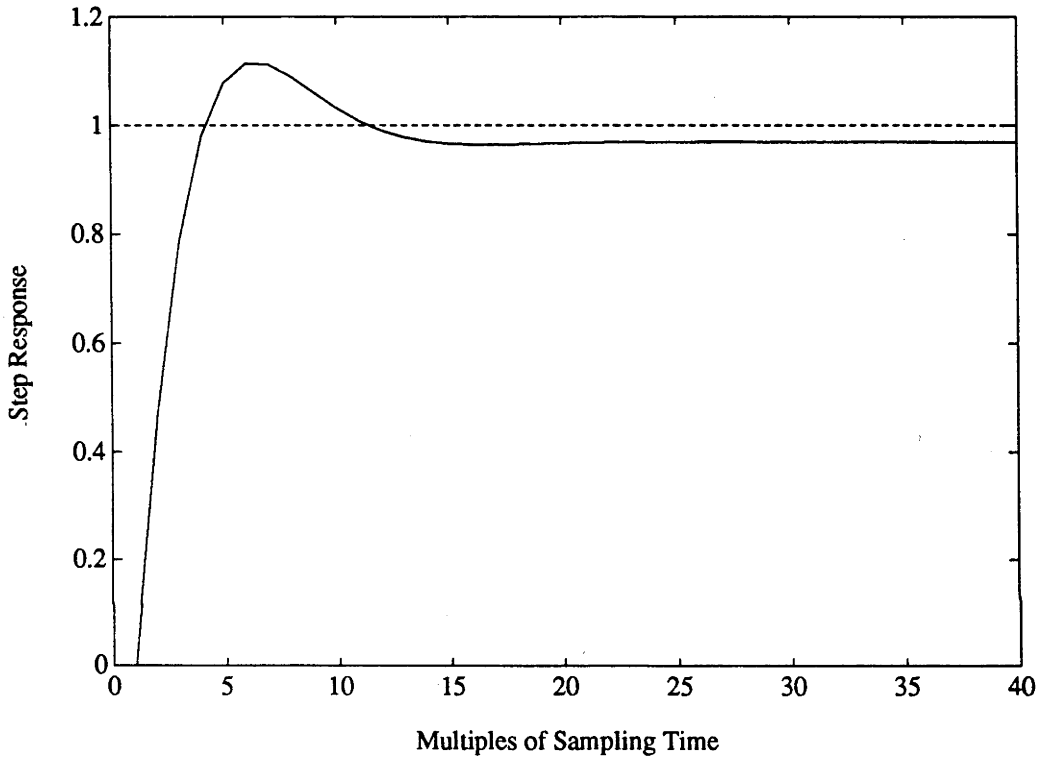

Figure 7.4.1: Step Response of Closed-loop System

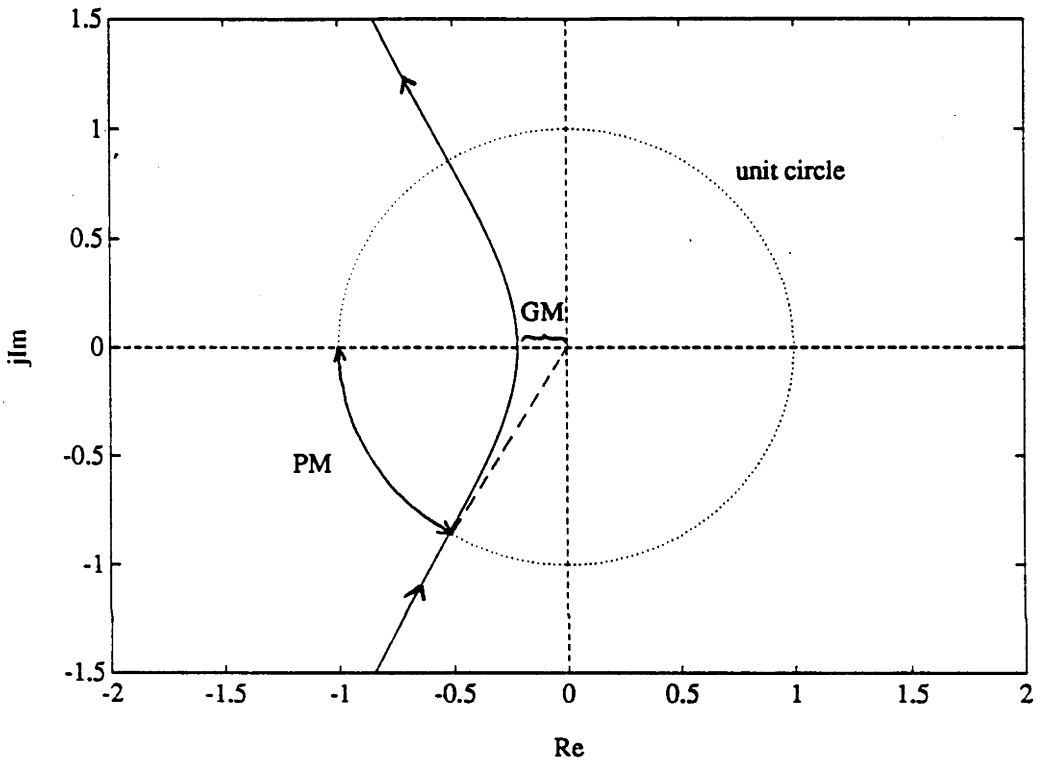

Figure 7.4.2: Nyquist Plot of $h_{ob}(z)$

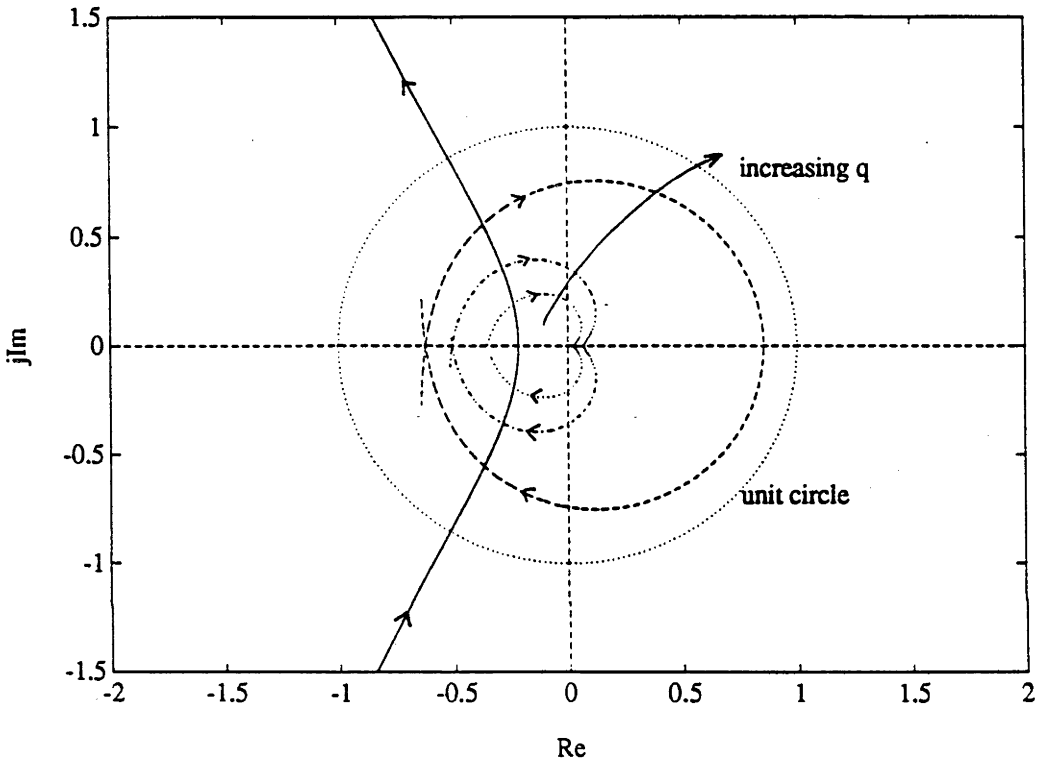

Figure 7.4.3: Nyquist Plots of $h_{ob}(z)$ and $h_{kf}^{ZOH}(z)$

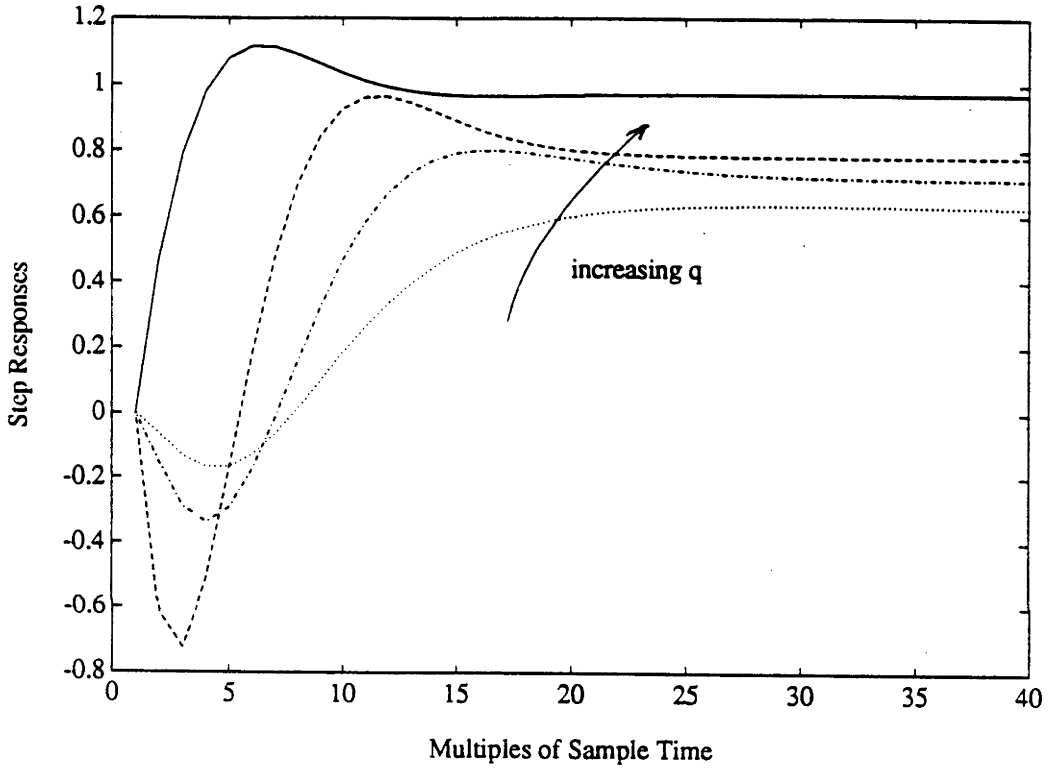

Figure 7.4.4: Step Responses for Loop Transfer Recovery with $C_{kf}^{ZOH}(z)$

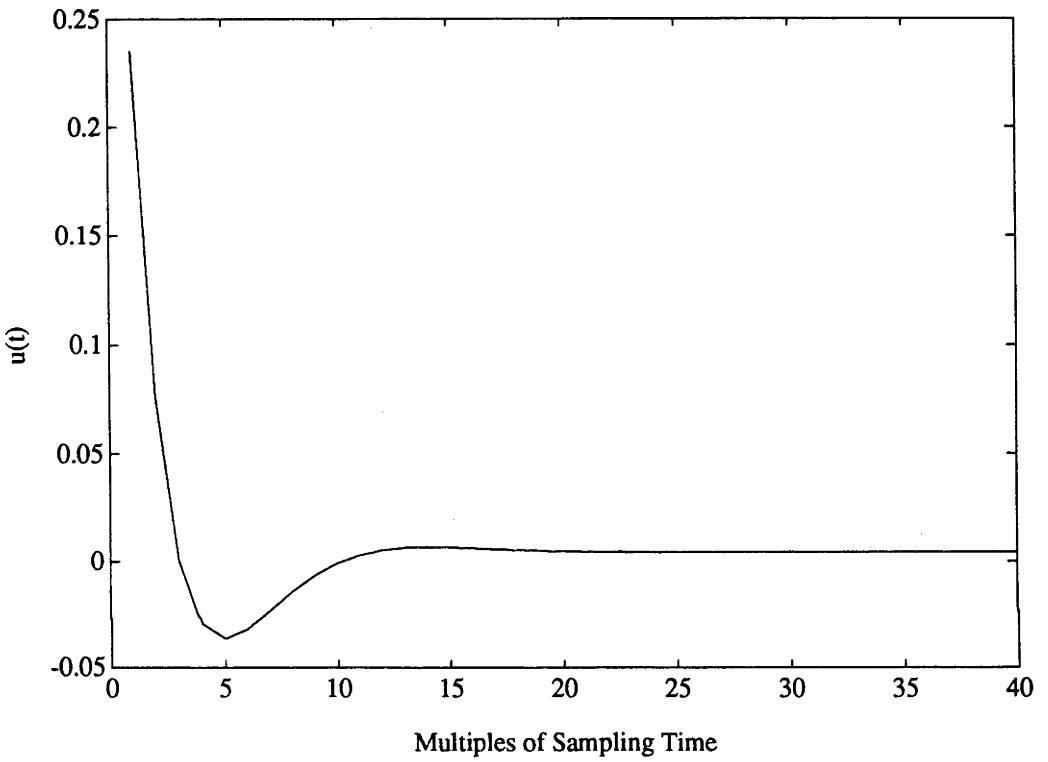

Figure 7.4.5: Plant Input, $u(t)$ for Loop Transfer Recovery with $C_{kf}^{ZOH}(z)$

with the GSHF gains associated with g_d given by:

$$f(t) = \begin{cases} -1957 & 0 \leq t < 0.02 \\ 1707 & 0.02 \leq t \leq 0.04 \end{cases}$$

To further demonstrate that perfect recovery is asymptotically achieved using the proposed method, we show some Nyquist plots for the loop transfer function, $h_{kf}^{GSHF}(z)$ when q varies over the same range as before. Following the same procedure of LQ optimisation outlined in Section 7.3, the Nyquist plot of $h_{kf}^{GSHF}(z)$ is displayed in Figure 7.4.6. Again, in Figure 7.4.6, the solid curve is the desired response shown in Figure 7.4.2. The dotted curve shows the Nyquist plot of $h_{kf}^{GSHF}(z)$ for $q = 3$. As q increases beyond 9, the Nyquist plots of $h_{kf}^{GSHF}(z)$ overlap with the desired one. We further present the simulation results for the step responses when loop recovery using the GSHF based compensator is attempted. The step responses for different values of q are recorded in Figure 7.4.7. In Figure 7.4.7, the solid curve is the desired response of Figure 7.4.1 and is of course a continuous-time step response. It turns out that the step response for $q = 3$, which is the dotted curve, coincides with the desired one. The corresponding control input is displayed in Figure 7.4.8. Here, the disadvantage of the scheme becomes evident: large values of the control variable are encountered. By choosing a smaller value of q, the control excursion will become smaller, with some deterioration in the step response. Nevertheless, it is clear from the simulation results that perfect loop recovery is asymptotically achievable using the proposed method.

7.5 Summary

A new approach to discrete-time LQG/LTR is proposed. The idea revolves around the capability of arbitrary zero placement using GSHF. By exploiting this power of GSHF, an arbitrary strictly proper, continuous-time, FDLTI plant can always be discretized to a minimum-phase one. As a consequence, perfect loop recovery is asymptotically achievable using the proposed GSHF based

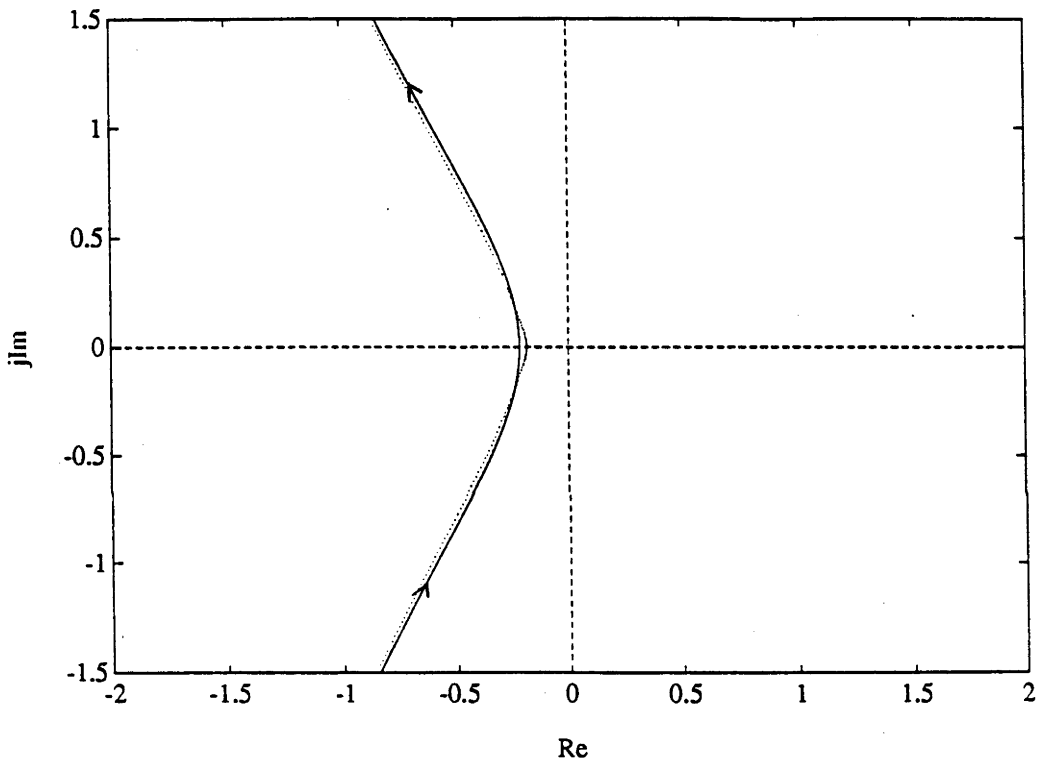

Figure 7.4.6: Nyquist Plots of $h_{ob}(z)$ and $h_{kf}^{GSHF}(z)$

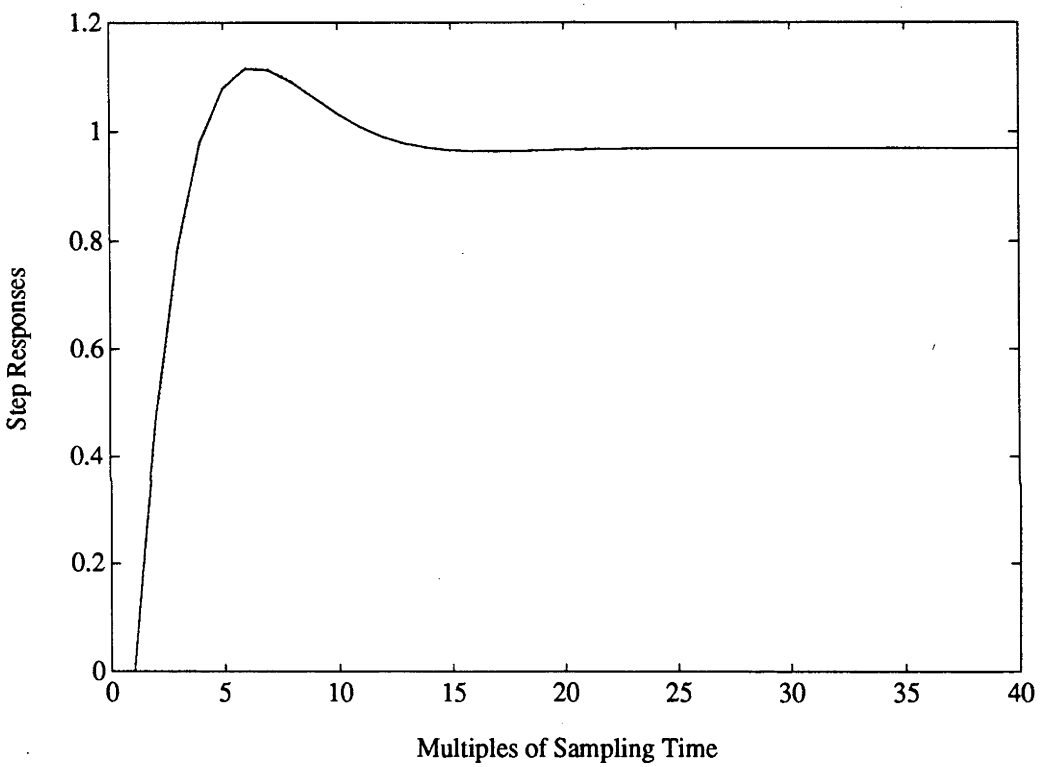

Figure 7.4.7: Step Response for Loop Transfer Recovery with $C_{kf}^{GSHF}(z)$

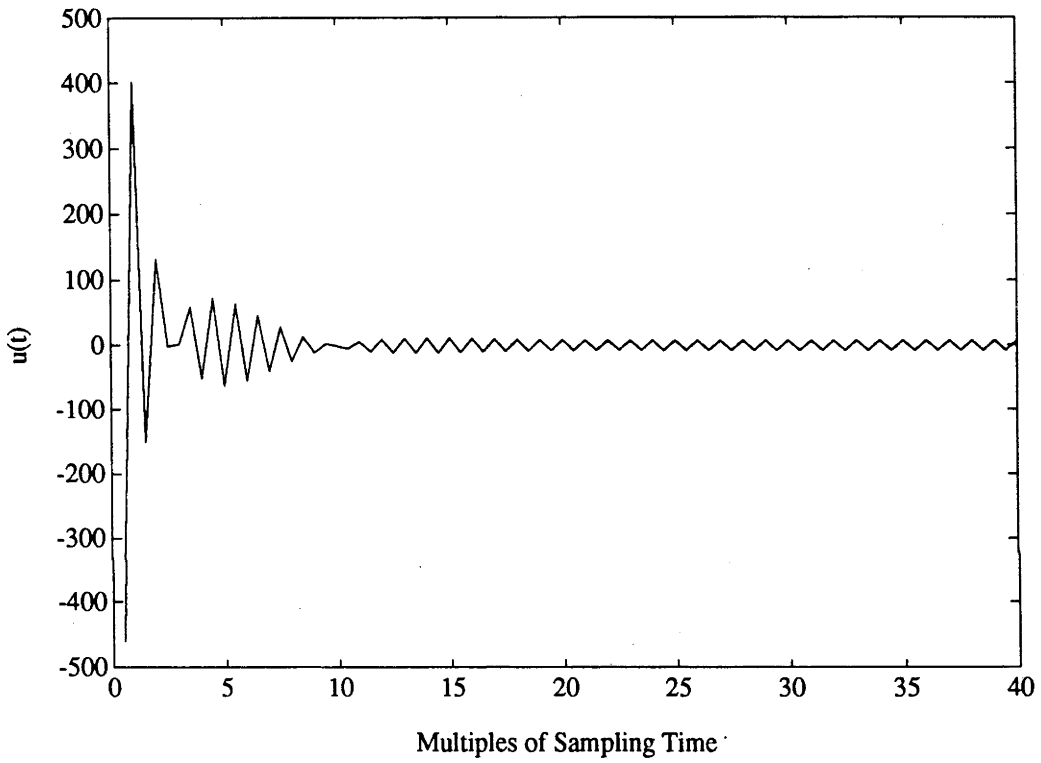

Figure 7.4.8: Plant Input, $u(t)$ for Loop Transfer Recovery with $C_{kf}^{GSHF}(z)$

compensator irrespective of whether the underlying continuous-time plant is minimum-phase or not. This idea is both substantiated by theories and illustrated by an example.

Chapter 8

Gain Margin Improvement Using GSHF Based Multirate Output Compensator

8.1 Introduction

As foreshadowed in Chapter 1, periodic controllers used in conjunction with FDLTI plants can offer a new dimension of flexibility in the design process. To recap, they have been used to achieve equivalent state feedback without observers, pole assignment, zero assignment, gain margin improvement, strong and simultaneous stabilisation and the removal of decentralised fixed modes in decentralised control. One of these results which is both theoretically interesting and practically significant corresponds to the problem of gain margin improvement. The advantage of periodic controllers over LTI controllers in improving the gain margin for a nonminimum-phase FDLTI plant seems to have been first indicated in [44]. Nevertheless, the result of [44] is only relevant to SISO discrete-time FDLTI bicausal plants with periodic discrete-time dynamic compensators. Some years later, a similar gain margin result for SISO continuous-time FDLTI plants with periodic continuous-time dynamic compensators of a particular form was reported in [49]. At this juncture, it is important to mention that these two results do not involve the implementation of a digital

controller with a continuous-time plant (through A/D elements, etc). Recently, it was shown in [25] that for a discrete-time FDLTI plant, LTI dynamic precompensation with decimation of the plant output (which is equivalent to the use of a particular form of linear periodic dynamic compensator) can arbitrarily position the finite zeros of the resulting closed-loop system. Using this idea, the gain margin result in [44] was generalized to the multivariable case. To be precise, it was shown that the gain margin can be arbitrarily assigned likewise for a multivariable continuous-time FDLTI plant by way of discretizing the plant with a sufficiently small sampling time and suitable choice of a digital periodic controller. The design procedure together with its drawback for this kind of controller, termed a conventional periodic controller, have been briefly reviewed in Chapter 2.

As we have also seen in Chapter 2, another kind of digital periodic controller which possesses the capability of gain margin improvement is a GSHF based dynamic compensator proposed in [79]. In [79], further improvement of gain margin using a GSHF dynamic compensator over a conventional periodic controller was revealed. The approach therein is different from that of [25]. The key idea revolves around positioning the finite zeros of the discretized plant via the use of a GSHF developed in [38]. One of the interesting results is that for a SISO, strictly proper, continuous-time, FDLTI plant, significant gain margin improvement using a GSHF based dynamic compensator over a conventional periodic digital controller is achieved. Unfortunately, the compensator so designed is not necessarily strictly causal. The disadvantages of a nonstrictly causal compensator are two-fold: first, it is well-known that it is practically difficult or sometimes impossible to implement a nonstrictly causal compensator due to the implied assumption of zero computation time. Second, as has been shown in [77], stabilisation by a nonstrictly proper controller is never robust against singular perturbations whereas stabilisation by a strictly proper

controller is always robust against singular perturbations. In this chapter, we explore the concept of multirate sampling of the plant output developed in [33] and propose a new type of GSHF based compensator which employs multirate sampling of the plant output with output-rate multiplicity, $N^O = 2$. Using the proposed compensator, not only the maximal level of gain margin obtained in [79] can be achieved, but also, more importantly, the new compensator is strictly causal. As a consequence, it is more easily realisable and guaranteed to be robust against singular perturbations.

The chapter is organised as follows: a review of the GSHF dynamic compensator developed in [79] appears in Section 8.2. In particular, the formula for the maximal level of achievable gain margin derived in [79] is simplified. In the next section, the GSHF based multirate output compensator is proposed. An explicit formula for the maximal achievable gain margin achievable by the new compensator for the SISO plant considered in Section 8.2 is derived. A design procedure for the construction of the proposed compensator is also outlined. It is further shown that the maximal level of gain margin obtained in [79] can be achieved by the new compensator. An example appears in Section 8.4 to illustrate the ideas and methods presented. Section 8.5 contains concluding remarks.

8.2 Review of GSHF Based Dynamic Compensator

Consider a SISO, strictly proper, continuous-time, FDLTI plant $P(s)$ with a minimal state-space model given by

$$\dot{x}(t) = Ax(t) + bu(t) \quad x(0) = x_0 \tag{8.2.1}$$

$$y(t) = cx(t) \tag{8.2.2}$$

For simplicity, the following assumption is made.

Assumption 8.2.1: All the unstable poles of $P(s)$ are assumed to be simple and in H.

The GSHF dynamic compensator proposed in [79] has the form

$$\begin{aligned} z_d(k+1) &= A_c z_d(k) + b_c y_d(k) && (8.2.3)\\ v_d(k) &= c_c z_d(k) + d_c y_d(k) && (8.2.4)\\ u(t) &= f(t) v_d(k) && (8.2.5)\\ & t \in [kT_0, (k+1)T_0) \\ & k = 0, 1, 2, \cdots \end{aligned}$$

where $z_d(k) \in \mathbb{R}^{n_c}$, $y_d(k) \in \mathbb{R}^1$, $v_d(k) \in \mathbb{R}^1$, $T_0 > 0$ is the frame period (which is also the sampling period for single-rate sampling), A_c, b_c, c_c and d_c are constant matrices of appropriate dimensions and $f(t)$ is a T_0-periodic integrable and bounded matrix function of an appropriate dimension. Note that the frame period T_0 is chosen according to the recommendations given in [10], [28] and [57] and such that $T_0 \neq 2k\pi/\mathrm{Im}(p_i - p_j)$ whenever $\mathrm{Re}(p_i - p_j) = 0$, $k = 0, 1, 2, \cdots$. The latter condition ensures that the discrete-time poles are also simple. Note also that in general $d_c \neq 0$ so that the compensator is not strictly causal.

The following equation

$$\int_0^{T_0} \exp[A(T_0 - t)] b f(t) dt = g_d \qquad (8.2.6)$$

for the unknown $f(t)$ with g_d a given constant vector, plays an important role in the design of the GSHF based compensator. The properties with respect to (8.2.6) are summarized in Lemma 7.3.1 of the previous chapter.

Applying the GSHF control law of (8.2.3)-(8.2.5) to the continuous-time plant (8.2.1)-(8.2.2) and sampling the continuous-time state and output with single-rate T_0, we obtain the following discrete-time system from $v_d(k)$ to $y_d(k)$.

$$\begin{aligned} x_d(k+1) &= A_d x_d(k) + g_d v_d(k) && (8.2.7)\\ y_d(k) &= c x_d(k) && (8.2.8) \end{aligned}$$

where

$$A_d = \exp(AT_0) \tag{8.2.9}$$

and g_d is related to the GSHF gain $f(t)$ as in (8.2.6).

The associated transfer function is

$$P(z) = c(zI - A_d)^{-1}g_d \tag{8.2.10}$$

Note that the discretized plant is strictly causal.

The following definition is needed in the subsequent development.

Definition 8.2.1 *Let $P(s)$ denote the transfer function of the SISO continuous-time FDLTI plant given by (8.2.1)-(8.2.2). For a given $T_0 > 0$, define the maximal achievable gain margin K_{T_1} of $P(s)$ with respect to GSHF compensation as*

$$K_{T_1} \triangleq \sup\{k_2/k_1 : 0 < k_1 < 1 < k_2 \text{ and there exists a controller (8.2.3)-(8.2.5) stabilising } kP(s) \text{ for all } k \in [k_1, k_2]\}$$

Concerning the maximal achievable gain margin for (8.2.1)-(8.2.2), we have the following theorem.

Theorem 8.2.1 *[79] Adopt Assumption* 8.2.1. *Let K_{T_1} be as defined in Definition 8.2.1; then, for almost all sampling periods $T_0 > 0$,*

$$K_{T_1} = \left(\frac{1+\alpha_T}{1-\alpha_T}\right)^2 \tag{8.2.11}$$

where

$$\alpha_T = \sqrt{1 - eL_T^{-1}e'} \tag{8.2.12}$$

and

$$e \triangleq [1 \;\; 1 \;\; \cdots \;\; 1] \in \mathbb{R}^{1\times N_2} \tag{8.2.13}$$

$$L_T \triangleq \left[\frac{1}{1-\exp[-(p_i+\bar{p}_j)T_0]}\right]_{i,j=1,2,\cdots,N_2} \in \mathbb{R}^{N_2\times N_2} \tag{8.2.14}$$

where $p_i \quad i = 1, 2, \cdots, N_2$ *are the unstable poles of the continuous-time plant* $P(s)$.

In the sequel, we shall show that the above expression can be simplified to a form which does not involve matrix inversion.

Theorem 8.2.2 *Adopt Assumption* 8.2.1. *The maximal level of achievable gain margin,* K_{T_1}, *in Theorem 8.2.1 can be written as*

$$K_{T_1} = \left(\frac{1 + \exp[(-\sum_{i=1}^{N_2} p_i)T_0]}{1 - \exp[(-\sum_{i=1}^{N_2} p_i)T_0]} \right)^2 \tag{8.2.15}$$

where the $p_i, \quad i = 1, 2, \cdots, N_2$ *denote the unstable poles of the continuous-time system* $P(s)$.

Proof: Define $\lambda_i \triangleq \exp(-p_i T_0)$. Observe that

$$L_T = [1/(1 - \lambda_i \bar{\lambda}_j)]_{i,j=1,2,\cdots,N_2} \tag{8.2.16}$$

Further,

$$\det \begin{bmatrix} L_T & e' \\ e & 1 \end{bmatrix} = (1 - eL_T^{-1}e')\det(L_T) = \det(L_T - e'e) \tag{8.2.17}$$

Since $|\lambda_i| < 1$, it follows that

$$\begin{aligned} L_T &= [\textstyle\sum_{k=0}^{\infty}(\lambda_i \bar{\lambda}_j)^k]_{i,j=1,2,\cdots,N_2} \\ &= \sum_{k=0}^{\infty} \left(\begin{bmatrix} (\lambda_1)^k \\ (\lambda_2)^k \\ \vdots \\ (\lambda_{N_2})^k \end{bmatrix} \begin{bmatrix} (\bar{\lambda}_1)^k & (\bar{\lambda}_2)^k & \cdots & (\bar{\lambda}_{N_2})^k \end{bmatrix} \right) \\ &= \sum_{k=1}^{\infty} \left(\begin{bmatrix} (\lambda_1)^k \\ (\lambda_2)^k \\ \vdots \\ (\lambda_{N_2})^k \end{bmatrix} \begin{bmatrix} (\bar{\lambda}_1)^k & (\bar{\lambda}_2)^k & \cdots & (\bar{\lambda}_{N_2})^k \end{bmatrix} \right) + e'e \end{aligned} \tag{8.2.18}$$

So,

$$L_T - e'e = \sum_{k=1}^{\infty} \left(\begin{bmatrix} (\lambda_1)^k \\ (\lambda_2)^k \\ \vdots \\ (\lambda_{N_2})^k \end{bmatrix} [(\bar{\lambda}_1)^k \quad (\bar{\lambda}_2)^k \quad \cdots \quad (\bar{\lambda}_{N_2})^k] \right)$$

$$= \text{diag}\{\lambda_i\} L_T \text{diag}\{\bar{\lambda}_i\} \quad (i = 1, 2, \cdots, N_2) \tag{8.2.19}$$

It follows from (8.2.17) and (8.2.19) that

$$(1 - eL_T^{-1}e')\det(L_T) = \det(\text{diag}\{\lambda_i\})\det(L_T)\det(\text{diag}\{\bar{\lambda}_i\}) \tag{8.2.20}$$
$$(i = 1, 2, \cdots, N_2)$$

i.e.

$$1 - eL_T^{-1}e' = \prod_{i=1}^{N_2} |\lambda_i|^2$$

or

$$\alpha_T = \prod_{i=1}^{N_2} |\lambda_i|$$

Since complex conjugates always occur in pairs and $|\lambda_i| = \lambda_i$ for each real λ_i, we have

$$\alpha_T = \prod_{i=1}^{N_2} \lambda_i = \exp[(-\sum_{i=1}^{N_2} p_i)]T_0$$

Hence, the result of the theorem is established. □

8.3 GSHF Based Multirate Output Compensator

The proposed GSHF based dynamic compensator employing multirate sampling of the plant output with output-rate multiplicity, $N^O = 2$ consists of an LTI compensator and a GSHF control law as follows:

$$z_d(k+1) = \bar{A}_c z_d(k) + \bar{B}_c \bar{y}_d(k) \tag{8.3.1}$$

$$v_d(k) = \bar{C}_c z_d(k) \tag{8.3.2}$$

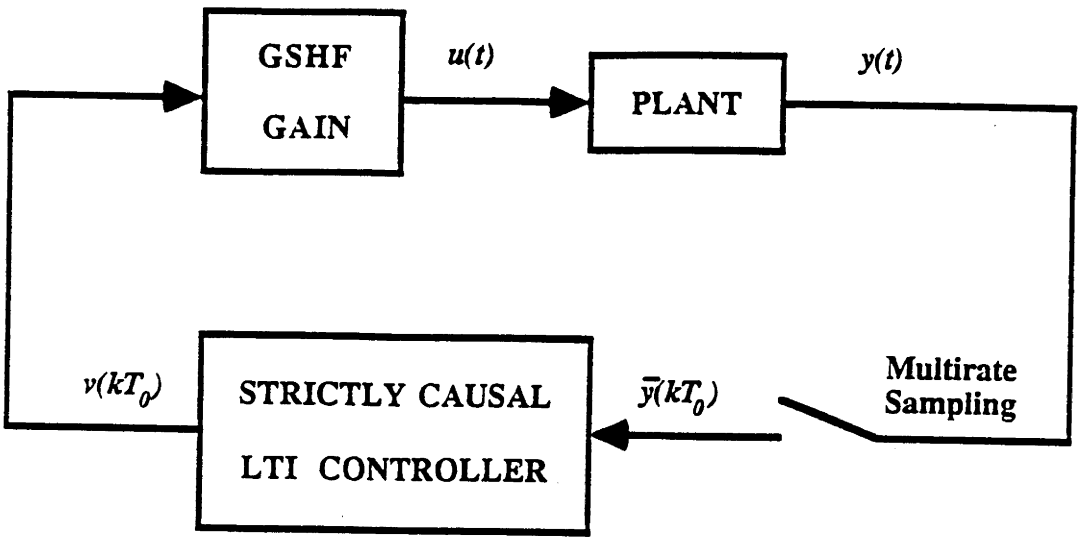

Figure 8.3.1: Closed-loop Configuration with the Proposed Compensator

$$\begin{aligned} u(t) &= f(t)v_d(k) \qquad (8.3.3)\\ & t \in [kT_0, (k+1)T_0)\\ & k = 0, 1, 2, \cdots \end{aligned}$$

where $z_d(k) \in \mathbb{R}^{n_c}$, $v_d(k) \in \mathbb{R}^1$ and the collection of the output measurements in the time interval $[kT_0, \overline{k+1}T_0)$, $k = 0, 1, 2, \cdots$ are given by

$$\bar{y}_d(k) = \begin{bmatrix} y(kT_0) \\ y(kT_0 + T^O) \end{bmatrix} \in \mathbb{R}^2 \qquad (8.3.4)$$

Here, $T_0 > 0$ is the frame period, $T^O = T_0/N^O$ is the sampling time, $N^O = 2$ is the output-rate multiplicity, $\bar{A}_c$, $\bar{B}_c$ and $\bar{C}_c$ are constant matrices of appropriate dimensions and $f(t)$ is a T_0-periodic integrable and bounded hold function matrix of appropriate dimension.

Applying the proposed compensator (8.3.1)-(8.3.3) and sampling the continuous-time state by single-rate T_0, and the output with multirate, T^O, the following discrete-time system from $v_d(k)$ to $\bar{y}_d(k)$ is obtained:

$$x_d(k+1) = A_d x_d(k) + g_d v_d(k) \qquad (8.3.5)$$

$$\bar{y}_d(k) = \bar{C}_d x_d(k) + \bar{d}_d v_d(k) \tag{8.3.6}$$

where A_d is as defined in (8.2.9) and

$$g_d = \int_0^{T_0} \exp[A(T_0 - t)]bf(t)dt \tag{8.3.7}$$

$$\bar{C}_d = \begin{bmatrix} c \\ c\exp(AT_0/2) \end{bmatrix} \tag{8.3.8}$$

$$\bar{d}_d = \begin{bmatrix} 0 \\ \int_0^{T^O} \exp[A(T_0 - t)]bf(t)dt \end{bmatrix} \tag{8.3.9}$$

The associated transfer function is

$$\bar{P}(z) = \bar{d}_d + \bar{C}_d(zI - A_d)^{-1}g_d \tag{8.3.10}$$

By suitable choice of g_d, the discretized plant can merely have finite and stable zeros. A procedure for choosing g_d for this purpose is given in Appendix D. For a given constant matrix g_d, the relation of g_d to the GSHF gain, $f(t)$ is as defined in (8.2.6). Further, Lemma 7.3.1 applies here. A block diagram showing the closed-loop configuration with the proposed compensator is shown in Figure 8.3.1.

Note that the discretized plant has a direct feedthrough term, $\bar{d}_d$. We remark that the notation, though perhaps standard, is a little misleading; in view of (8.3.4), the two entries of $\bar{y}_d(k)$ are not both available at time kT_0, but one is available only at time $kT_0 + T^O$. A non-strictly causal compensator using $\bar{y}_d(k)$ as input at time kT_0 could not then actually operate. In (8.3.2), $v_d(k)$ assumed to be available at time kT_0, depends on $\bar{y}_d(l)$ for $l < k$ and thus the time for complete receipt of $\bar{y}_d(k)$, which is $(k - 1/2)T_0$ until kT_0, is available for computation.

The following definitions are needed for the subsequent development.

Definition 8.3.1 *The zeros of a discrete-time system are termed stable if they lie strictly inside the unit circle in the complex plane.*

Definition 8.3.2 *Let $P(s)$ denote the transfer function of the SISO continuous-time FDLTI plant given by (8.2.1)-(8.2.2). For a given $T_0 > 0$, define the maximal achievable gain margin K_{T_2} of $P(s)$ with respect to the GSHF based multirate output compensation as*

$$K_{T_2} \triangleq sup\{k_2/k_1 : 0 < k_1 < 1 < k_2 \text{ and there exists a strictly causal controller (8.3.1)-(8.3.3) stabilising } kP(s) \text{ for all } k \in [k_1, k_2]\}$$

As foreshadowed in the introduction, the proposed compensator is strictly causal rather than just causal. Before we give a theorem concerning the existence of such a controller, we state here a result concerning the existence of a strictly causal LTI controller for achieving any prescribed gain margin.

Lemma 8.3.1 *[79] Let $P(z)$ be the discrete-time plant which has no unstable zero except an infinity zero of multiplicity 1. Assume that the unstable poles of $P(z)$ are $\exp(p_i T_0)$, $(i = 1, 2, \cdots, N_l)$ and are simple where $Rep_i, T_0 > 0$. Then the maximal gain margin of $P(z)$ with respect to proper LTI controllers tends to infinity when T_0 goes to zero.*

Now, we state and prove the theorem concerning the existence of a strictly causal GSHF based multirate output compensator.

Theorem 8.3.1 *Adopt Assumption 8.2.1. Consider the SISO, strictly proper, continuous-time, LTI minimal plant $P(s)$ given by (8.2.1)-(8.2.2). Let K_{T_1} be as defined in Definition 8.2.1. For a prescribed level of gain margin $k_2/k_1 < K_{T_1}$ with $0 < k_1 < 1 < k_2$, there always exists a strictly causal GSHF based multirate output compensator (8.3.1)-(8.3.3) stabilising $kP(s)$ for all $k \in [k_1, k_2]$.*

Proof: Let R denote the ring of proper rational functions which are stable in the discrete-time sense. Then $\bar{P}(z)$ in (8.3.10) has a Smith-McMillan form over R as follows:

$$\begin{bmatrix} n_1/d_1 \\ 0 \end{bmatrix}$$

where 0 represents the zero matrix of appropriate size, (n_1, d_1) are coprime over R and n_1/d_1 will have unstable poles $\exp(p_i T_0)$ $(i = 1, \cdots, N_2)$ but stable finite zeros (owing to suitable choice of g_d described in Appendix D). (See [39] for details on Smith McMillan form.) Applying Lemma 8.3.1 to n_1/zd_1, we can conclude that there is no problem in constructing a strictly causal compensator $c_1(z)$ stabilizing n_1/d_1 for all $k \in [k_1, k_2]$ and achieving any prescribed gain margin, $k_2/k_1 < K_{T_1}$. (An outline of a procedure for constructing the compensator is given subsequently). Hence, the result of the theorem is established. □

Remark 8.3.1 In [79], it was shown that given k_1 and k_2, a strictly causal GSHF compensator stabilising $kP(s)$ for all $k \in [k_1, k_2]$ can be constructed for a SISO continuous-time FDLTI plant. Nevertheless, the plant considered is bicausal rather than strictly proper.

Corollary 8.3.1 *Let K_{T_1} and K_{T_2} be as defined in Definition 8.2.1 and Definition 8.3.2 respectively. Then,*

$$K_{T_2} \geq K_{T_1} \tag{8.3.11}$$

Proof: The result follows from the proof of Theorem 8.3.1 and Definition 8.3.2. □

A systematic procedure towards constructing a strictly causal GSHF based multirate output compensator is now outlined:

1. Select T_0 according to the recommendations given in [10], [28] and [57] and $T_0 \neq 2k\pi/\mathrm{Im}(p_i - p_j)$ whenever $\mathrm{Re}(p_i - p_j) = 0$, $k = 0, 1, 2, \cdots$. The latter condition ensures that the discrete-time poles are also simple under Assumption 8.2.1.

2. Choose an output-rate multiplicity $N^O = 2$ and discretize the continuous-time plant with T_0 obtained in (1). Let $\bar{P}(z)$ denote the transfer function matrix of the discretized plant.

3. Choose a g_d so that the plant has no unstable zeros. A procedure for this purpose is given in Appendix D. The corresponding $f(t)$ can be computed via Lemma 7.3.1.

4. With a suitable unimodular matrix, $U(z)$, transform $\bar{P}(z)$ to the following Smith-McMillan form in R i.e.

$$U(z)\bar{P}(z) = \begin{bmatrix} p_1(z) \\ 0 \end{bmatrix}$$

where the zeros of $p_1(z)$, denoted by $z_{d,i}$, $i = 1, 2, \cdots, N_2$, are finite and stable. The reason for obtaining stable zeros is to simplify the construction of the sensitivity function in the next step.

5. Given k_1 and k_2 with $k_2/k_1 < K_{T_1}$, compute N from

$$k_2/k_1 = \left(\frac{N + \exp[-(\sum_{i=1}^{N_2} p_i)T_0]}{N - \exp[-(\sum_{i=1}^{N_2} p_i)T_0]} \right)^2 \tag{8.3.12}$$

By (8.2.15), there always exists $N > 1$. As will be shown later, this form of k_2/k_1 is related to obtaining a strictly causal compensator. Further, the value N has implication on the stability of the sensitivity function, $s_1(z)$.

6. Construct a sensitivity function $s_1(z)$ according to the procedure outlined in Appendix E. One such sensitivity function $s_1(z)$, is

$$s_1(z) = \frac{4k_1k_2N\prod_{i=1}^{N_2}[z - \exp(p_iT_0)][\exp(p_iT_0)z - 1]}{A(z)}$$

where

$$\begin{aligned} A(z) = {} & (k_2 - k_1)N^2 \prod_{i=1}^{N_2}[\exp(p_iT_0)z - 1]^2 \\ & - 2(k_2 + k_1 - 2k_1k_2)N \prod_{i=1}^{N_2}[z - \exp(p_iT_0)][\exp(p_iT_0)z - 1] \\ & + (k_2 - k_1) \prod_{i=1}^{N_2}[z - \exp(p_iT_0)]^2 \end{aligned}$$

with $N > 1$.

7. The corresponding LTI compensator is given by

$$\begin{aligned} c_1(z) &= \frac{1 - s_1(z)}{s_1(z)p_1(z)} \\ &= \frac{A(z) - 4k_1k_2N\prod_{i=1}^{N_2}[z - \exp(p_iT_0)][\exp(p_iT_0)z - 1]}{4k_1k_2\prod_{i=1}^{N_2}[\exp(p_iT_0)z - 1][z - z_{d,i}]} \\ &= \frac{[(N\prod_{i=1}^{N_2}\exp(p_iT_0) - 1)^2k_2 - (N\prod_{i=1}^{N_2}\exp(p_iT_0) + 1)^2k_1]}{4k_1k_2N\prod_{i=1}^{N_2}[\exp(p_iT_0)z - 1](z - z_{d,i})}z^{2N_2} \\ &\quad + \frac{\text{terms of degrees lower than } 2N_2}{4k_1k_2N\prod_{i=1}^{N_2}[\exp(p_iT_0)z - 1](z - z_{d,i})} \end{aligned}$$

where $z_{d,i}$'s are the stable and finite zeros of $p_1(z)$.

8. Define

$$\begin{aligned} C(z) &\triangleq [c_1(z) \quad 0]U(z) \\ &= [c_{1,1}(z) \quad c_{1,2}(z)] \end{aligned}$$

where each $c_{1,j}(z)$, $j = 1, 2$ is of the form

$$c_{1,j}(z) = d_j + \frac{b_{j,1}z^{n-1} + b_{j,2}z^{n-2} + \cdots + b_{j,n}}{z^n + a_1z^{n-1} + a_2z^{n-2} + \cdots + a_n}$$

and

$$d_j = [(N\prod_{i=1}^{N_2}\exp(p_iT_0) - 1)^2k_2 - (N\prod_{i=1}^{N_2}\exp(p_iT_0) + 1)^2k_1]/A_j$$

where A_j's, a_i's and $b_{j,i}$'s are constants. Note that with the choice of k_2/k_1 in step (5), $d_j = 0$ $j = 1, 2$.

9. The proposed GSHF based multirate output compensator can then be constructed as

$$z_{j,d}(k+1) = \begin{bmatrix} -a_1 & -a_2 & -a_3 & \cdots & -a_{n-1} & -a_n \\ 1 & 0 & 0 & \cdots & 0 & 0 \\ \vdots & \vdots & \vdots & & \vdots & \vdots \\ 0 & 0 & 0 & \cdots & 1 & 0 \\ 0 & 0 & 0 & \cdots & 0 & 1 \end{bmatrix} z_{j,d}(k) + \begin{bmatrix} 1 \\ 0 \\ 0 \\ \vdots \\ 0 \end{bmatrix} \overline{y(k+\frac{1}{j}T_0)} \quad (j=1,2)$$

$$v_d(k) = [\, b_{1,1} \;\; b_{1,2} \;\; \cdots \;\; b_{1,n} \;\; b_{2,1} \;\; b_{2,2} \;\; \cdots \;\; b_{2,n} \,] \begin{bmatrix} z_{1,d}(k) \\ z_{2,d}(k) \end{bmatrix}$$

We remark that from step (6) of the design procedure, it can be seen that the ratio of the constant term of $A(z)$ and the coefficient of z^{2N_2} is given by

$$R = \frac{(k_2-k_1)(N^2\exp[(\sum_{i=1}^{N_2} 2p_i)T_0]+1) - 2(k_2+k_1-2k_1k_2)N\exp[(\sum_{i=1}^{N_2} p_i)T_0]}{(k_2-k_1)(N^2+\exp[(\sum_{i=1}^{N_2} 2p_i)T_0]) - 2(k_2+k_1-2k_1k_2)N\exp[(\sum_{i=1}^{N_2} p_i)T_0]}$$

It is easy to see that $R \to 1$ as $N \to 1$. As a consequence, the product of the poles of $s_1(z) \to 1$. This implies that the sensitivity function tends to instability.

8.4 An Example

For the following example

$$P(s) = \frac{s-1}{(s+1)(s-2)}$$

it has been calculated in [79] that the maximal gain margin of the plant using a *causal* GSHF compensator is given by

$$K_{T_1} = \left(\frac{1+\exp(-2T_0)}{1-\exp(-2T_0)}\right)^2$$

In particular,

$$K_{T_1} = \begin{cases} 100.63 & T_0 = 0.1 \\ 25.67 & T_0 = 0.2 \\ 4.68 & T_0 = 0.5 \\ 3.99 & T_0 = 0.55 \end{cases}$$

From this data, it is observed that K_{T_1} decreases rapidly as T_0 increases.

Now, we shall construct a GSHF based multirate output compensator and show that the same level of gain margin is obtained.

Consider the following state-space model of the plant

$$A = \begin{bmatrix} -1 & 0 \\ 0 & 2 \end{bmatrix} \quad b = \begin{bmatrix} 1/3 \\ 1/3 \end{bmatrix} \quad c = [2 \quad 1]$$

Choose $T_0 = 0.1$, $N^O = 2$ and $g_d = \begin{bmatrix} 0 \\ 1 \end{bmatrix}$ so that the plant has finite and stable zeros . One of the GSHF gains associated with g_d can be found as follows:

$$f(t) = \begin{cases} 370.6 & 0 \le t \le 0.05 \\ -352.5 & 0.05 \le t \le 0.1 \end{cases}$$

Then,

$$\begin{aligned} \bar{P}(z) &= \bar{d}_d + \bar{C}_d[zI - \exp(AT_0)]^{-1} g_d \\ &= \frac{1}{z - 1.2214} \begin{bmatrix} 1 \\ 18.6409(z - 1.1621) \end{bmatrix} \end{aligned}$$

where

$$\begin{aligned} \bar{C}_d &= \begin{bmatrix} c \\ c\exp(AT_0/2) \end{bmatrix} = \begin{bmatrix} 2 & 1 \\ 1.9025 & 1.1052 \end{bmatrix} \\ \bar{d}_d &= \begin{bmatrix} 0 \\ c\int_0^{T_0/2} \exp[A(T_0 - t)] b f(t) dt \end{bmatrix} = \begin{bmatrix} 0 \\ 18.6409 \end{bmatrix} \end{aligned}$$

With the following unimodular matrix

$$U(z) = \begin{bmatrix} \frac{z+1.6005}{z+0.5} & \frac{0.05365z+0.0623}{z+0.5} \\ -\frac{18.6409(z-1.2214)}{z+0.5} & \frac{1}{z+0.5} \end{bmatrix}$$

$\bar{P}(z)$ has the following Smith-McMillan form in R

$$U(z)\bar{P}(z) = \begin{bmatrix} \frac{z+0.5}{z-1.2214} \\ 0 \end{bmatrix} = \begin{bmatrix} p_1(z) \\ 0 \end{bmatrix}$$

Using the procedure of constructing a sensitivity function, $s_1(z)$ outlined in Appendix E, the required sensitivity function is

$$s_1(z) = \frac{4k_1k_2N(z-1.2214)(1.2214z-1)}{A(z)}$$

where

$$\begin{aligned} A(z) &= [4.8856Nk_1k_2 + (1.2214N-1)^2k_2 - (1.2214N+1)^2k_1]z^2 \\ &\quad - [9.9673Nk_1k_2 - 2(2.4918N - 1.2214(N^2+1))k_2 \\ &\quad - 2(2.4918N + 1.2214(N^2+1))k_1]z \\ &\quad + [4.8856Nk_1k_2 + (N-1.2214)^2k_2 - (N+1.2214)^2k_1] \end{aligned}$$

For $N = 1.01$,

$$\begin{aligned} A(z) &= (4.9345k_1k_2 + 0.0546k_2 - 4.989k_1)z^2 \\ &\quad - [10.067k_1k_2 - 0.0988k_2 - 9.9682k_1]z \\ &\quad + [4.9345k_1k_2 + 0.0477k_2 - 4.9792k_1] \end{aligned}$$

Then, the corresponding LTI compensator is

$$\begin{aligned} c_1(z) &= \frac{1-s_1(z)}{s_1(z)p_1(z)} \\ &= \frac{(0.0546k_2 - 4.989k_1)z^2 + (0.0988k_2 + 9.9682k_1)z + (0.0477k_2 - 4.9792k_1)}{4.04k_1k_2(1.2214z-1)(z+0.5)} \end{aligned}$$

Define

$$\begin{aligned} C(z) &\triangleq [c_1(z) \quad 0]U(z) \\ &= [c_{1,1}(z) \quad c_{1,2}(z)] \end{aligned}$$

where

$$\begin{aligned} c_{1,1}(z) &= (\frac{0.0111}{k_1} - \frac{1.0111}{k_2}) \\ &\quad + \frac{(\frac{0.0377}{k_1} + \frac{1.9833}{k_2})z^2 + (\frac{0.0417}{k_1} + \frac{2.2242}{k_2})z + (\frac{0.0155}{k_1} - \frac{1.615}{k_2})}{z^3 + 0.1813z^2 - 0.5687z - 0.2046} \end{aligned}$$

$$c_{1,2}(z) = \left(\frac{0.0006}{k_1} - \frac{0.0542}{k_2}\right) + \frac{\left(\frac{0.0018}{k_1} + \frac{0.2249}{k_2}\right)z^2 + \left(\frac{0.00018}{k_1} + \frac{0.0717}{k_2}\right)z + \left(\frac{0.0006}{k_1} - \frac{0.0629}{k_2}\right)}{z^3 + 0.1813z^2 - 0.5687z - 0.2046}$$

It follows that the compensator is strictly causal if and only if $k_2/k_1 = 91.37$. This is the gain margin achieved by the proposed compensator for $T_0 = 0.1$. For comparison, it has been calculated in [25] that the maximal gain margins achieved by conventional LTI compensator and conventional periodic controllers with the same T_0 are 4 and 25.67 respectively. Further, as shown earlier, with respect to causal GSHF compensator with the same T_0, the maximal gain margin is 100.63. Note that our compensator is strictly causal, rather than just causal. As a consequence, it is more easily realisable and guaranteed to be robust against singular perturbations whereas the compensator in [79] may not be.

Observe also that with $k_2/k_1 = 91.37$, the ratio of the constant term and the coefficient of z^2 of the sensitivity function $s_1(z)$ is < 1 for $k_2 > 1 > k_1 > 0$. Hence, the sensitivity function is stable. It can be shown that by taking N even closer to 1, the gain margin achieved by the proposed compensator tends to 100.63. Nevertheless, as mentioned earlier, the sensitivity function tends to instability.

The proposed GSHF compensator with multirate output sampling can be constructed as

$$z_{1,d}(k+1) = \begin{bmatrix} -0.1813 & 0.5687 & 0.2046 \\ 1 & 0 & 0 \\ 0 & 1 & 0 \end{bmatrix} z_{1,d}(k) + \begin{bmatrix} 1 \\ 0 \\ 0 \end{bmatrix} y_d(k)$$

$$z_{2,d}(k+1) = \begin{bmatrix} -0.1813 & 0.5687 & 0.2046 \\ 1 & 0 & 0 \\ 0 & 1 & 0 \end{bmatrix} z_{2,d}(k) + \begin{bmatrix} 1 \\ 0 \\ 0 \end{bmatrix} y_d(\overline{k+1/2})$$

$$v_d(k) = \begin{bmatrix} \frac{0.0377}{k_1} + \frac{1.9833}{k_2} & \frac{0.0417}{k_1} + \frac{2.2242}{k_2} & \frac{0.0155}{k_1} - \frac{1.615}{k_2} & \frac{0.0018}{k_1} + \frac{0.2249}{k_2} \\ \frac{0.0018}{k_1} + \frac{0.0717}{k_2} & \frac{0.0006}{k_2} - \frac{0.0629}{k_1} \end{bmatrix} \begin{bmatrix} z_{1,d}(k) \\ z_{2,d}(k) \end{bmatrix}$$

$$u(t) = f(t)v_d(k) \quad t \in [kT_0, \overline{k+1}T_0), \quad k = 0, 1, 2, \cdots$$

8.5 Summary

In this chapter, we have shown that for a SISO, strictly proper, nonminimum phase, continuous-time, FDLTI plant, the closed-loop gain margin obtained via GSHF based dynamic compensator employing multirate sampling of the plant output is significantly improved over that achieved via a conventional periodic controller used in [25]. It turns out that the maximal level of gain margin improvement obtained in [79] can be achieved by the proposed compensator. More significantly, our compensator is strictly causal rather than just causal. As a consequence, our compensator could be implemented in practice and is guaranteed to be robust against singular perturbations whereas the compensator proposed in [79] may not be.

Chapter 9

Conclusions and Directions for Future Research

9.1 Conclusions

This thesis has further identified some advantages and disadvantages of peridoic controllers for FDLTI systems. On the one hand, we have mainly been concerned with identifying possible drawbacks of MROC's so that they can be possibly accepted by engineers and managers in the industry. On the other hand, our research has been mainly directed towards identifying possible advantages of periodic controllers in solving other control problems. In retrospect, the major contributions can be summarized as follows.

We have identified two possible drawbacks of MROC's in their practical applications. The first one involves identifying two situations where the gain matrix of the controller will acquire extremely large entries as a result of inappropriate choice of the frame period, T_0. This results in amplification of noise or nonlinearity in a practical situation even though the ideal plant will remain well-behaved. To help circumvent the problem, we provide some rules of thumb for the choice of the frame period, T_0 that will ensure that excessive gain values are avoided for both cases when using the MROC's. The second one concerns the operation of the MROC's under process and/or measurement disturbances. By prescribing a certain linear quadratic performance index and deriving the

equivalent discrete-time models for the two types of control laws, namely the MROC law and the LQG laws, we show that for a typical plant, the MROC law performs worse than two LQG laws, termed LQG law I and LQG law II, in the presence of noise disturbances. To recap, the LQG law I uses a one-step ahead prediction estimate of the state and LQG law II uses a true filtered estimate of the state. These two possible drawbacks associated with the MROC's were reported in Chapters 3 and 4 respectively. Having seen two possible drawbacks of the MROC's, it is natural to ask whether there are other potential problems associated with the MROC's. At this stage, it remains not clear whether this will be the case.

In contrast with identifying possible disadvantages of MROC's, we have identified further advantages of periodic controllers for FDLTI plants. The advantages fall into two aspects, namely order reduction and robustness improvement. In the case of order reduction, we have given some new insights into using multirate sampling in designing reduced-order compensators. We have shown that in the case of designing a discrete-time linear functional observer, multirate output sampling has an advantage over single-rate output sampling. To be precise, a multirate output linear functional observer employing multirate sampling of the plant output of dimension much *smaller* than that of a single-rate output linear functional observer can be designed. A sort of dual result is obtained using multirate input sampling. This is shown in the case of implementing output injection feedback law rather than state feedback law. Here, we show that in the case of designing a discrete-time dual observer-based compensator for achieving the pole positioning effect of output injection feedback, multirate input sampling has advantage. To be specific, a multirate input compensator employing multirate sampling of the plant input of dimension much *smaller* than that of the single-rate input compensator can be designed. These two new results are reported in Chapters 5 and 6 respectively. Further, as briefly mentioned in the

text, the same type of ideas could be used to achieve dimension reduction for multiple-input multiple-output systems using the alorgithm of [63].

Chapters 7 and 8 are concerned with further advantages of periodic controllers in improving robustness. In Chapter 7, a new approach to discrete-time loop transfer recovery was presented. The key idea revolves around the zero placement capability of GSHF. Using this power of GSHF, we show that any strictly proper, continuous-time, FDLTI system can be discretized to a minimum-phase one with zero at infinity of order one. As a consequence, discrete-time perfect loop recovery can always be asymptotically achieved irrespective of whether the underlying continuous-time plant is minimum-phase or not. In Chapter 8, a GSHF based dynamic multirate output compensator was proposed. It is shown to possess the capability of improving the closed-loop gain margin over a conventional periodic controller for a SISO, strictly proper, nonminimum-phase, continuous-time, FDLTI plant. The level of improvement is found to be at least the same as that achieved by the GSHF based dynamic compensator with single-rate sampling of the plant output. More importantly, the new compensator, being strictly causal, is more easily realisable and is robust against singular perturbations. Having seen the advantages of GSHF based dynamic compensator, it is natural to ask whether there are any disadvantages associated with this type of controllers. To our knowledge, one disadvantage of the GSHF based compensator is that the GSHF gain tends to acquire large positive and negative values when the frame period becomes small. The implication of this is that the plant inputs will take large positive and negative values during the transient response to, for example, a step.

9.2 Future Directions of Research

Though opportunities for future research abound, we only propose some most promising and significant directions and open questions.

1. Clearly, there are probably more disadvantages to be discovered in other types of periodic controllers such as the recently developed block multirate input-output controllers reported in [1]. We foresee that the work in this direction will be welcomed by the academic as well as the industry community. The reasons are three fold: first, engineers and managers in the industry will have no confidence in applying any of the existing periodic controllers unless they are aware of their possible potential drawbacks in the real-life environment; second, given the very few industrial applications of the existing periodic controllers, it will be more fruitful to continue to devise other periodic controllers to tackle some other control problems only when one can see more successful applications in the real-world; third, the need of practical control topics, which are critical to the successful operation of real-life control system and yet left out in most textbooks, has been advocated by some authors, [10], [19], [50] and [75]. The work in this direction will certainly help to bridge the well-known 'gap' between control theory and practice.

2. As we have seen in Chapter 4, the performance of the MROC's is significantly degraded in the presence of noise disturbances. This is mainly due to the fact that noise is perturbing the true state and the MROC's use the output measurements nonoptimally. To circumvent the disadvantage of MROC's under noise disturbances, it is proposed that some form of filtering be incorporated in the MROC's. Intuitively, if optimal filtering is applied, the quality of the estimate will be improved. It is then conjectured that the performance of the controller will be enhanced. Nevertheless, note that the introduction of the optimal filter will lead to an increase in the order of the resulting compensator consisting of the MROC and the optimal filter.

3. As we have seen in Chapter 8, the proposed GSHF based dynamic multirate output compensator manifests its superiority over LTI control in improving gain margin and reducing the conflict between gain margin and sensitivity. It is our view that periodic control may overcome or reduce more conflicts peculiar to LTI control. A particularly interesting question is whether the proposed controller or other form of periodic controller can achieve an arbitrary phase margin, as opposed to gain margin, and at the same time maintain the minimal sensitivity.

4. In a more recent paper on multirate systems, [68], the design capabilities of a class of periodic systems, namely multirate systems with multirate input sampling and single-rate output sampling were studied with application to the eigenstructure assignment robust design technique. The criteria for the selection of minimum sample rates to produce the extra design freedom and the implication of this choice on the eigenstructure procedure was outlined. Further, the use of the extra freedom to produce perfectly decoupled closed-loop model responses was examined and the improved insensitivity properties of these methods were demonstrated. It is natural to ask if a similar kind of result can be obtained for systems with single-rate input sampling and multirate output sampling. Further, which multirate systems will offer better improvement in insensitivity properties ?

5. As the real-world problems become more complicated each day, multi-objective control problems emerge. Given the now reasonably rich literature in periodic controllers, it is conjectured that a new trend in periodic control research is to develop some kind of multi-structured periodic controller which possibly encompasses the various advantages of the existing periodic controllers to solve the multi-objective control problems. As an example, a kind of multi-structured multirate digital controllers was proposed in [35]. Using the proposed controller, simultaneous pole assignment and

simultaneous stabilisation for a wider class of plants were obtained. With the advent of periodic controllers and the desire to solve multi-objective control problems, it is conceivable that periodic controllers might replace the currently well-accepted LTI controllers in the time to come.

6. H^∞ control is now well-known as a new trend in control engineering in that it provides a new prespective for robust control design. Indeed, it has been proven to be a promising area of active research. In line with this, an attempt has been made to incorporate H^∞ control in periodic control in [45]. More specifically, it was shown in [45] that in the problems of H^∞ optimal control of LTI plants, arbitrary nonlinear, time-varying controllers offer no advantage over LTI controllers in minimizing the induced operator norm of the input/output operator for the standard H^∞ control problem. However, as mentioned earlier, there is now a desire to solve multi-objective control problems. Indeed, recent attempts have been directed towards solving a kind of extended H^∞ control problem, termed mixed H^∞/H^2 problem by many researchers. Given this scenario, it is not clear at this stage whether any arbitrary nonlinear, time-varying controllers will not offer any advantage over LTI controllers in the new setting of control problems. It is conjectured that with some creativity, more design freedom of periodic control or some nonlinear, time-varying control can be explored to achieve better results in H^∞ multi-objective optimal control problems.

In conclusion, we point out that the above list by no means exhausts the possibilities for future research.

Appendix A

Proof of Lemma 4.3.1 in Chapter 4

It is known that the Riccati equation associated with the state equation (4.2.14) and performance index (4.3.7) is given by:

$$P(k) = Q + F'P(k+1)F - P^*(k+1) \tag{A.1}$$

$$P^*(k+1) = F'P(k+1)G[R + G'P(k+1)G]^{-1}G'P(k+1)F \tag{A.2}$$

$$P(N) = 0 \tag{A.3}$$

$$L(k) = [R + G'P(k+1)G]^{-1}G'P(k+1)F \tag{A.4}$$

Using (A.4) in (A.2) yields

$$P^*(k+1) = L'(k)[R + G'P(k+1)G]L(k) \tag{A.5}$$

We first compute the difference between $\tilde{x}_d'(k+1)P(k+1)\tilde{x}_d(k+1)$ and $\tilde{x}_d'(k)P(k)\tilde{x}_d(k)$. Using (4.2.14) in $\tilde{x}_d'(k+1)P(k+1)\tilde{x}_d(k+1)$, we have $\tilde{x}_d'(k+1)P(k+1)\tilde{x}_d(k+1)$

$$\begin{aligned}
&= [F\tilde{x}_d(k) + Gu_d(k) + \omega_{ud}(k)]'P(k+1)[F\tilde{x}_d(k) + Gu_d(k) + \omega_{ud}(k)] \\
&= [F\tilde{x}_d(k) + Gu_d(k)]'P(k+1)[F\tilde{x}_d(k) + Gu_d(k)] \\
&\quad +[F\tilde{x}_d(k) + Gu_d(k)]'P(k+1)\omega_{ud}(k) \\
&\quad +\omega_{ud}'(k)P(k+1)[F\tilde{x}_d(k) + Gu_d(k)] + \omega_{ud}'(k)P(k+1)\omega_{ud}(k)
\end{aligned} \tag{A.6}$$

Also, by (A.1), there holds $\tilde{x}_d'(k)P(k)\tilde{x}_d(k)$

$$= \tilde{x}_d'(k)[Q + F'P(k+1)F - P^*(k+1)]\tilde{x}_d(k) \tag{A.7}$$

Therefore, $\tilde{x}_d'(k+1)P(k+1)\tilde{x}_d(k+1) - \tilde{x}_d'(k)P(k)\tilde{x}_d(k)$

$$\begin{aligned} = \; & u_d'(k)G'P(k+1)Gu_d(k) + u_d'(k)G'P(k+1)F\tilde{x}_d(k) \\ & + \tilde{x}_d'(k)F'P(k+1)Gu_d(k) + [u_d'(k)Ru_d(k) - u_d'(k)Ru_d(k)] \\ & - \tilde{x}_d'(k)Q\tilde{x}_d(k) + \tilde{x}_d'(k)P^*(k+1)\tilde{x}_d(k) + \omega_{ud}'(k)P(k+1)\omega_{ud}(k) \\ & + [F\tilde{x}_d(k) + Gu_d(k)]'P(k+1)\omega_{ud}(k) \\ & + \omega_{ud}'(k)P(k+1)[F\tilde{x}_d(k) + Gu_d(k)] \end{aligned} \tag{A.8}$$

Straightforward rearrangement yields

$\tilde{x}_d'(k)Q\tilde{x}_d(k) + u_d'(k)Ru_d(k) + \tilde{x}_d'(k+1)P(k+1)\tilde{x}_d(k+1) - \tilde{x}_d'(k)P(k)\tilde{x}_d(k)$

$$\begin{aligned} = \; & [u_d(k) + L(k)\tilde{x}_d(k)]'[R + G'P(k+1)G][u_d(k) + L(k)\tilde{x}_d(k)] \\ & + \omega_{ud}'(k)P(k+1)\omega_{ud}(k) \\ & + [F\tilde{x}_d(k) + Gu_d(k)]'P(k+1)\omega_{ud}(k) \\ & + \omega_{ud}'(k)P(k+1)[F\tilde{x}_d(k) + Gu_d(k)] \end{aligned} \tag{A.9}$$

Next, observe that because $P(N) = 0$ by (A.3)

$$\begin{aligned} 0 \; = \; & \tilde{x}_d'(N)P(N)\tilde{x}_d(N) \\ = \; & \tilde{x}_d'(0)P(0)\tilde{x}_d(0) \\ & + \sum_{k=0}^{N-1} [\tilde{x}_d'(k+1)P(k+1)\tilde{x}_d(k+1) \\ & - \tilde{x}_d'(k)P(k)\tilde{x}_d(k)] \end{aligned} \tag{A.10}$$

Hence, J_N can be rewritten as

$$J_N \; = \; \frac{1}{N}E\{\tilde{x}_d'(0)P(0)\tilde{x}_d(0)$$

$$+\sum_{k=0}^{N-1}[\tilde{x}_d'(k)Q\tilde{x}_d(k)+u_d'(k)Ru_d(k)$$
$$+\tilde{x}_d'(k+1)P(k+1)\tilde{x}_d(k+1)-\tilde{x}_d'(k)P(k)\tilde{x}_d(k)]\} \qquad \text{(A.11)}$$

Using (A.9) in (A.11) yields

$$\begin{aligned} J_N &= \frac{1}{N}E\{\tilde{x}_d'(0)P(0)\tilde{x}_d(0) \\ &+\sum_{k=0}^{N-1}\{[u_d(k)+L(k)\tilde{x}_d(k)]'[R+G'P(k+1)G][u_d(k)+L(k)\tilde{x}_d(k)] \\ &+\omega_{ud}'(k)P(k+1)\omega_{ud}(k)\}+2[F\tilde{x}_d(k)+Gu_d(k)]'P(k+1)\omega_{ud}(k)\} \end{aligned} \qquad \text{(A.12)}$$

Because $\tilde{x}_d(0)$, $u_d(j)$ and $\omega_{ud}(j)$ are independent of $\tilde{x}_d(k)$ for all $j<k$, $\tilde{u}_d(k)$ is independent of $\omega_{ud}(k)$. Also, $u_d(k)$ is independent of $\omega_{ud}(k)$. Hence, the last summand has zero expectation. Consequently,

$$\begin{aligned} J_N &= \frac{1}{N}E\{\tilde{x}_d'(0)P(0)\tilde{x}_d(0) \\ &+\sum_{k=0}^{N-1}[u_d(k)+L(k)\tilde{x}_d(k)]'[R+G'P(k+1)G][u_d(k)+L(k)\tilde{x}_d(k)]\} \\ &+\sum_{k=0}^{N-1}\mathrm{tr}[\hat{Q}P(k+1)] \end{aligned} \qquad \text{(A.13)}$$

Appendix B

Proof of Existence of Causal Observer in Chapter 5

From (5.2.1)-(5.2.2), using the alternate way of multirate sampling of the plant output, we have

$$x_d(k+1) = A_s x_d(k) + b_s u_d(k) \tag{B.1}$$

$$\tilde{y}_d(k+1) = \tilde{C} x_d(k) + \tilde{d} u_d(k) \tag{B.2}$$

where A_s and b_s are defined by

$$A_s = \exp(AT_0) \qquad b_s = \int_0^{T_0} \exp(At) b dt \tag{B.3}$$

respectively and

$$\tilde{y}_d(k+1) = \begin{bmatrix} y_d(k+\frac{1}{N^O}) \\ y_d(k+\frac{2}{N^O}) \\ \vdots \\ y_d(k+1) \end{bmatrix} \tag{B.4}$$

$$\tilde{C} = \begin{bmatrix} c\exp(AT_0/N^O) \\ c\exp(2AT_0/N^O) \\ \vdots \\ c\exp(AT_0) \end{bmatrix} \tag{B.5}$$

$$\tilde{d} = \begin{bmatrix} c\int_0^{T_0/N^O} \exp(At) b dt \\ c\int_0^{2T_0/N^O} \exp(At) b dt \\ \vdots \\ c\int_0^{T_0} \exp(At) b dt \end{bmatrix} \tag{B.6}$$

Now, consider the following observer

$$z_d(k+1) = Fz_d(k) + G\tilde{y}_d(k+1) + eu_d(k) \quad \text{(B.7)}$$

$$\hat{u}_d(k+1) = p\tilde{y}_d(k+1) + qz_d(k) \quad \text{(B.8)}$$

where $\hat{u}_d(k)$ estimates $a'A_s^{-1}x_d(k)$. Note that (B.7)- (B.8) is causal, but not strictly causal.

From (B.1)-(B.2) and (B.7)-(B.8), we get

$$\begin{aligned} e_d(k+1) &= z_d(k+1) - Tx_d(k+1) \\ &= Fz_d(k) + G\tilde{y}_d(k+1) + eu_d(k) - TA_sx_d(k) - Tb_su_d(k) \\ &= Fe_d(k) + (FT - TA_s + G\tilde{C})x_d(k) \\ &\quad + (G\tilde{d} - Tb_s + e)u_d(k) \end{aligned} \quad \text{(B.9)}$$

Hence, $z_d(k)$ is an estimate of $Tx_d(k)$ if and only if

Condition a: F is stable

Condition b: $TA_s - FT = G\tilde{C}$

Condition c: $e = Tb_s - G\tilde{d}$

From (B.1)-(B.2) and (B.7)-(B.8), we have

$$\begin{aligned} &\hat{u}_d(k+1) - a'A_s^{-1}x_d(k+1) \\ &= p\tilde{y}_d(k+1) + qz_d(k) - a'A_s^{-1}[A_sx_d(k) + b_su_d(k)] \\ &= p[\hat{C}x_d(k) + \tilde{d}u_d(k)] + qTx_d(k) + qe_d(k) \\ &\quad -a'x_d(k) - a'A_s^{-1}b_su_d(k) \\ &= [p\tilde{C} + qT - a']x_d(k) + [p\tilde{d} - a'A_s^{-1}b_s]u_d(k) + qe_d(k) \end{aligned} \quad \text{(B.10)}$$

Thus, $\hat{u}_d(k)$ estimates $a'A_s^{-1}x_d(k)$ if there exists a transformation T such that $z_d(k)$ estimates $Tx_d(k)$ and

$$a' = p\tilde{C} + qT \quad \text{(B.11)}$$

$$p\tilde{d} = a'A_s^{-1}b_s \quad \text{(B.12)}$$

or equivalently

$$\begin{bmatrix} a \\ b_s' A_s^{-t} a \end{bmatrix} = \begin{bmatrix} \tilde{C}' & T' \\ \tilde{d}' & 0 \end{bmatrix} \begin{bmatrix} p' \\ q' \end{bmatrix} \tag{B.13}$$

where $A_s^{-t} \triangleq (A_s^{-1})'$.

Solvability of p and q given $\tilde{C}$, $\tilde{d}$, T *et al* is guaranteed if

$$\text{rank} \begin{bmatrix} \tilde{C}' & T' \\ \tilde{d}' & 0 \end{bmatrix} = \text{rank} \begin{bmatrix} \tilde{C}' & T' & a \\ \tilde{d}' & 0 & b_s' A_s^{-t} a \end{bmatrix} \tag{B.14}$$

Appendix C

Proof of Independence of Closed-loop Stability on r in Chapter 5

For the SISO case, with single-rate output sampling, the closed-loop system is described by

$$\begin{bmatrix} x_d(k+1) \\ z_d(k+1) \\ \hat{u}_d(k+1) \end{bmatrix} = \begin{bmatrix} A_s & 0 & b_s \\ gc & F & d \\ pc & q & r \end{bmatrix} \begin{bmatrix} x_d(k) \\ z_d(k) \\ \hat{u}_d(k) \end{bmatrix} \tag{C.1}$$

where

$$TA_s - FT = gc \tag{C.2}$$

$$d = Tb_s \tag{C.3}$$

$$a' = pc + qT \tag{C.4}$$

$$r = a'A_s^{-1}b_s \tag{C.5}$$

Now, using the following nonsingular basis change

$$W = \begin{bmatrix} I & 0 & 0 \\ -T & I & 0 \\ -a'A_s^{-1} & 0 & I \end{bmatrix} \tag{C.6}$$

$$\text{yields} \begin{bmatrix} x_d(k+1) \\ z_d(k+1) - Tx_d(k+1) \\ \hat{u}_d(k+1) - a'A_s^{-1}x_d(k+1) \end{bmatrix}$$

$$= \begin{bmatrix} A_s + b_s a' A_s^{-1} & 0 & b_s \\ 0 & F & 0 \\ 0 & q & 0 \end{bmatrix} \begin{bmatrix} x_d(k) \\ z_d(k) - Tx_d(k) \\ \hat{u}_d(k) - a'A_s^{-1}x_d(k) \end{bmatrix} \tag{C.7}$$

Since the basis change is nonsingular, the modes remain the same i.e.

$$\{\lambda_i(\begin{bmatrix} A_s & 0 & b_s \\ gc & F & d \\ pc & q & r \end{bmatrix})\} = \{\lambda_i(\begin{bmatrix} A_s + b_s a' A_s^{-1} & 0 & b_s \\ 0 & F & 0 \\ 0 & q & 0 \end{bmatrix})\}$$

$$= \{\lambda_i(A_s + b_s a' A_s^{-1})\} \bigcup \{\lambda_i(F)\} \bigcup \{0\} \tag{C.8}$$

Hence, the closed-loop stability is independent of r, and is determined by the observer dynamics matrix, F and the system matrix $A_s + b_s a' A_s^{-1}$ which would be obtained if exact state feedback were used.

Appendix D

Procedure for Choosing G_d in Chapter 7

1. Using the technique of coprime fractional representation devised in [64], the plant (7.3.8) can be written as

$$P_{gshf}(z) = D_L^{-1}(z)N_L(z) \tag{D.1}$$

where

$$N_L(z) = C_d(zI - A_d + KC_d)^{-1}G_d \tag{D.2}$$

$$D_L(z) = I - C_d(zI - A_d + KC_d)^{-1}K \tag{D.3}$$

It is well-known that $P_{gshf}(z)$ is minimum-phase if and only if $N_L(z)$ is. Furthermore, the transmission zeros are not affected by feedback. Hence, to choose a G_d such that $P_{gshf}(z)$ is minimum-phase is equivalent to choosing a G_d so that $N_L(z)$ is. Similarly, $P_{gshf}(z)$ has a simple zero at infinity if and only if $N_L(z)$ has this property.

2. If (A_d, C_d) is not in the observer form of (D.8) and (D.9), transform (A_d, C_d) to observer form as follows:

   (a) Let the matrix C_d be partitioned as

$$C_d = \begin{bmatrix} c_1 \\ c_2 \\ \vdots \\ c_p \end{bmatrix} \tag{D.4}$$

   and select a set of linearly independent row vectors starting from $c_1, c_2, \cdots, c_p$, and then $c_1A_d, c_2A_d, \cdots, c_pA_d$ and so forth, until n linearly independent vectors are found. The n selected independent vectors are then rearranged as

$$M \triangleq \begin{bmatrix} c_1 \\ \vdots \\ c_1A_d^{\nu_1-1} \\ c_2 \\ \vdots \\ c_2A_d^{\nu_2-1} \\ \vdots \\ c_p \\ \vdots \\ c_pA_d^{\nu_p-1} \end{bmatrix} \tag{D.5}$$

   where ν_i's are termed the observability indices of the plant and $\sum_{i=1}^{p} \nu_i = n$.

   (b) Define

$$M^{-1} \triangleq [e_{11} \quad e_{12} \quad \cdots \quad e_{1\nu_1} \quad \cdots \quad e_{p1} \quad e_{p2} \quad \cdots \quad e_{p\nu_p}] \tag{D.6}$$

   and form Q from $e_{i\nu_i}$ $(i = 1, 2, \cdots, p)$ as follows

$$Q \triangleq [e_{1\nu_1} \quad A_de_{1\nu_1} \quad \cdots \quad A_d^{\nu_1-1}e_{1\nu_1} \quad \cdots \quad e_{p\nu_p} \quad A_de_{p\nu_p} \quad \cdots \quad A_d^{\nu_p-1}e_{p\nu_p}] \tag{D.7}$$

(c) Premultiplying and postmultiplying A_d by Q^{-1} and Q respectively, we obtain A_d in the observer form i.e.

$$\bar{A}_d = Q^{-1}A_dQ$$

$$= \left[\begin{array}{ccccc|ccccc|c|ccccc}
0 & 0 & \cdots & 0 & x & 0 & 0 & \cdots & 0 & x & & 0 & 0 & \cdots & 0 & x \\
1 & 0 & \cdots & 0 & x & 0 & 0 & \cdots & 0 & x & & 0 & 0 & \cdots & 0 & x \\
\vdots & \vdots & & \vdots & \vdots & \vdots & \vdots & & \vdots & \vdots & & \vdots & \vdots & & \vdots & \vdots \\
0 & 0 & \cdots & 1 & x & 0 & 0 & \cdots & 0 & x & & 0 & 0 & \cdots & 0 & x \\
\hline
0 & 0 & \cdots & 0 & x & 0 & 0 & \cdots & 0 & 0 & & 0 & 0 & \cdots & 0 & x \\
0 & 0 & \cdots & 0 & x & 1 & 0 & \cdots & 0 & x & & 0 & 0 & \cdots & 0 & x \\
\vdots & \vdots & & \vdots & \vdots & \vdots & \vdots & & \vdots & \vdots & & \vdots & \vdots & & \vdots & \vdots \\
0 & 0 & & 0 & x & 0 & 0 & \cdots & 1 & x & & 0 & 0 & \cdots & 0 & x \\
\hline
 & & & & & & & & & & \ddots & & & & & \\
\hline
0 & 0 & \cdots & 0 & x & 0 & 0 & \cdots & 0 & x & & 0 & 0 & \cdots & 0 & x \\
0 & 0 & \cdots & 0 & x & 0 & 0 & \cdots & 0 & x & & 1 & 0 & \cdots & 0 & x \\
\vdots & \vdots & & \vdots & \vdots & \vdots & \vdots & & \vdots & \vdots & & \vdots & \vdots & & \vdots & \vdots \\
0 & 0 & \cdots & 0 & x & 0 & 0 & \cdots & 0 & x & & 0 & 0 & \cdots & 1 & x
\end{array}\right] \qquad \text{(D.8)}$$

(d) The observer form of C_d is in turn obtained by postmultiplying C_d by Q:

$$\bar{C}_d = C_dQ$$

$$= \left[\begin{array}{ccccc|ccccc|c|ccccc}
0 & 0 & \cdots & 0 & 1 & 0 & 0 & \cdots & 0 & 0 & \cdots & 0 & 0 & \cdots & 0 & 0 \\
0 & 0 & \cdots & 0 & 0 & 0 & 0 & \cdots & 0 & 1 & \cdots & 0 & 0 & \cdots & 0 & 0 \\
\vdots & \vdots & & \vdots & \vdots & \vdots & \vdots & & \vdots & \vdots & & \vdots & \vdots & & \vdots & \vdots \\
0 & 0 & \cdots & 0 & 0 & 0 & 0 & \cdots & 0 & 0 & \cdots & 0 & 0 & \cdots & 0 & 1
\end{array}\right] \qquad \text{(D.9)}$$

(e) With this transformation, $P_{gshf}(z)$ becomes

$$P_{gshf}(z) = \bar{C}_d(zI - \bar{A}_d)^{-1}\bar{G}_d \tag{D.10}$$

where

$$\begin{aligned}
\bar{G}_d &= Q^{-1}G_d \\
&= \begin{bmatrix}
b_{1,\varepsilon_1} & 0 & \cdots & 0 \\
b_{1,\varepsilon_1-1} & 0 & \cdots & 0 \\
\vdots & \vdots & & \vdots \\
b_{1,2} & 0 & \cdots & 0 \\
b_{1,1} & 0 & \cdots & 0 \\
- & - & - & - \\
0 & b_{2,\varepsilon_2} & \cdots & 0 \\
0 & b_{2,\varepsilon_2-1} & \cdots & 0 \\
\vdots & \vdots & & \vdots \\
0 & b_{2,\varepsilon_1+2} & \cdots & 0 \\
0 & b_{2,\varepsilon_1+1} & \cdots & 0 \\
- & - & - & - \\
0 & 0 & \cdots & b_{p,\varepsilon_p} \\
0 & 0 & \cdots & b_{p,\varepsilon_p-1} \\
\vdots & \vdots & & \vdots \\
0 & 0 & \cdots & b_{p,\varepsilon_{p-1}+2} \\
0 & 0 & \cdots & b_{p,\varepsilon_{p-1}+1}
\end{bmatrix}
\end{aligned} \tag{D.11}$$

3. Since the transmission zeros are not affected by feedback, (D.10) can be written as

$$\begin{aligned}
P_{gshf}(z) &= \bar{C}_d(zI - \bar{A}_d)^{-1}\bar{G}_d \\
&= \bar{D}_L^{-1}(z)\bar{N}_L(z)
\end{aligned} \tag{D.12}$$

where

$$\bar{N}_L(z) = \bar{C}_d(zI - \bar{A}_d + \bar{K}\bar{C}_d)^{-1}\bar{G}_d \tag{D.13}$$

$$\bar{D}_L(z) = I - \bar{C}_d(zI - \bar{A}_d + \bar{K}\bar{C}_d)^{-1}\bar{K} \tag{D.14}$$

Further, since $(\bar{A}_d, \bar{C}_d)$ is observable, we can select an appropriate $\bar{K}$ such that

$$\bar{A}_d + \bar{K}\bar{C}_d = \text{diag}\{\begin{bmatrix} 0 & 0 & \cdots & 0 & -a_{i,\varepsilon_{i-1}+1} \\ 1 & 0 & \cdots & 0 & -a_{i,\varepsilon_{i-1}+2} \\ \vdots & \vdots & & \vdots & \vdots \\ 0 & 0 & \cdots & 1 & -a_{i,\varepsilon_i} \end{bmatrix}\} \tag{D.15}$$

where

$$\varepsilon_0 = 0 \tag{D.16}$$

$$\varepsilon_i = \nu_1 + \nu_2 + \cdots + \nu_i \quad (i = 1, 2, \cdots, p) \tag{D.17}$$

and $a_{i,j}$'s, $i = 1, 2, \cdots, p$, $j = \varepsilon_{i-1} + 1, \varepsilon_{i-1} + 2, \cdots, \varepsilon_i$ are constants.

It follows from (D.9), (D.11), (D.13) and (D.15) that

$$\det \bar{N}_L(z) = \prod_{i=1}^{p} N_i(z) \tag{D.18}$$

where

$$N_i(z) = \frac{b_{i,\varepsilon_i} z^{\nu_i - 1} + \cdots + b_{i,\varepsilon_{i-1}+2} z + b_{i,\varepsilon_{i-1}+1}}{z^{\nu_i} + a_{i,\varepsilon_i} z^{\nu_i - 1} + \cdots + a_{i,\varepsilon_{i-1}+2} z + a_{i,\varepsilon_{i-1}+1}} \tag{D.19}$$

with $b_{i,j}$, $i = 1, 2, \cdots, p$, $j = \varepsilon_{i-1} + 1, \varepsilon_{i-1} + 2, \cdots, \varepsilon_i$ being the entries of $\bar{G}_d$. Hence, the procedure boils down to selecting $b_{i,j}$'s, so that (D.18) is a stable polynomial and with $b_{i,\varepsilon_i} \neq 0$ for each i, to guarantee that $z = \infty$ is a simple zero. The required G_d that makes $P_{gshf}(z)$ minimum-phase is then obtained by premultiplying $\bar{G}_d$ by Q i.e.

$$G_d = Q\bar{G}_d \tag{D.20}$$

where Q and $\bar{G}_d$ are given by (D.7) and (D.11) respectively.

Appendix E

Procedure for Constructing a Sensitivity Function in Chapter 8

This appendix only serves as a guide for the construction of a sensitivity function for our problem. More details on the construction of a sensitivity function can be found in [43].

Consider the following commutative diagram of mappings:

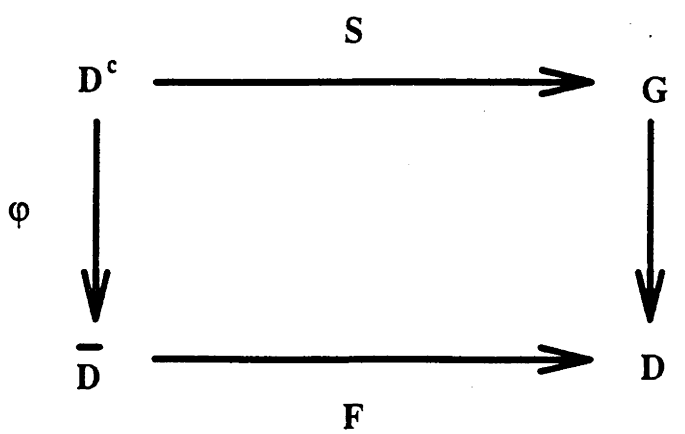

Figure E.1: Commutative Diagrams of Mapping

Here, D, $\bar{D}$ and D^c are the open unit disk, closed unit disk and complement of open unit disk respectively. The region G is defined as

$$G \triangleq \mathbb{C} \setminus \{(-\infty, -a'] \cup [b', \infty)\} \tag{E.1}$$

where $a' = k_1/(1-k_1)$ and $b' = k_2/(k_2-1)$.

Let φ be the conformal mapping from D^c to $\bar{D}$ i.e.

$$\varphi(z) = 1/z \tag{E.2}$$

Further, let $\theta(z)$ be a conformal mapping from G to D. The existence of $\theta(z)$ under standard assumptions on G is in general the consequence of the well-known Riemann Mapping Theorem [18], and there exist dictionaries, e.g. [46], where such mappings may be found. For the region of interest, G, the conformal mapping from G to D found in [43] is given by

$$\theta(z) = \frac{1-(\frac{1-z/b'}{1+z/a'})^{1/2}}{1+(\frac{1-z/b'}{1+z/a'})^{1/2}} \tag{E.3}$$

and $\theta(0) = 0$. From (E.3), it can be shown that the inverse mapping from D to G is given by

$$\theta^{-1}(z) = \frac{4k_1k_2z}{(k_2-k_1)-2(k_2+k_1-2k_1k_2)z+(k_2-k_1)z^2} \tag{E.4}$$

which is rational.

Note that in our case, the plant $p_1(z)$ has no unstable zeros and its unstable poles are $\exp(p_iT_0)$, $i = 1, 2, \cdots, N_2$. Therefore, finding a sensitivity function $S(z)$ from D^c to G with

$$S(\exp(p_iT_0)) = 0 \quad i = 1, 2, \cdots, N_2 \tag{E.5}$$

amounts to a special form of the Nevanlinna-Pick interpolation problem, namely, finding an analytic function $F(z)$ from $\bar{D}$ to D with

$$F(\frac{1}{\exp(p_iT_0)}) = 0 \quad i = 1, 2, \cdots, N_2 \tag{E.6}$$

One such mapping is

$$F(z) = \frac{\prod_{i=1}^{N_2}(z - \frac{1}{\exp(p_i T_0)})}{N\prod_{i=1}^{N_2}(\frac{z}{\exp(p_i T_0)} - 1)} \tag{E.7}$$

where $p_1, p_2, \cdots, p_{N_2}$ being the unstable poles of the continuous-time system (8.2.1)-(8.2.2) and $N > 1$. Note that other possible mappings from $\bar{D}$ to D can be constructed using a procedure described in [43].

As a consequence, the sensitivity function $S(z)$ can be constructed as follows:

$$\begin{aligned} S(z) &= \theta^{-1}(F(\varphi(z))) \\ &= \frac{4k_1k_2\phi(z)}{(k_2 - k_1) - 2(k_2 + k_1 - 2k_1k_2)\phi(z) + (k_2 - k_1)(\phi(z))^2} \end{aligned} \tag{E.8}$$

where

$$\begin{aligned} \phi(z) &\triangleq F(\varphi(z)) \\ &= \frac{\prod_{i=1}^{N_2}(z - \exp(p_i T_0))}{N\prod_{i=1}^{N_2}(\exp(p_i T_0)z - 1)} \end{aligned} \tag{E.9}$$

The features of the so constructed sensitivity function are as follows:

1. $S(z)$ is real rational and analytic from D^c to G.
2. The zeros of $S(z)$ contain $\{\exp(p_1T_0), \exp(p_2T_0), \cdots, \exp(p_{N_2}T_0)\}$ multiplicities included.

Bibliography

[1] P. ALBERTORS, "Block Multirate Input-output Model for Sampled-data Control Systems", *IEEE Trans. Automat. Contr.*, Vol. AC-35, No.9, pp.1985-1088, Sept. 1990.

[2] H.M. AL-RAHMANI AND G.F. FRANKLIN, "A Optimal Multirate Control of Linear Periodic and Time-invariant Systems", *IEEE Trans. Automat. Contr.*, Vol. AC-35, No.4, pp.406-415, 1990.

[3] B.D.O. ANDERSON AND J.B. MOORE, *Linear Optimal Control*, Englewood Cliffs, NJ, Prentice-Hall, 1971.

[4] B.D.O. ANDERSON AND J.B. MOORE, "Time-varying Feedback Laws for Decentralised Control", *IEEE Trans. Automat. Contr.*, Vol. AC-26, pp.1133-1138, 1981.

[5] B.D.O. ANDERSON AND J.B. MOORE, *Optimal Control : Linear Quadratic Methods*, Prentice Hall, 1990.

[6] M. ARAKI AND T. HAGIWARA, "Pole Assignment by Multirate Sampled-data Output Feedback", *Proc. 24th IEEE Conf. Decision Contr.*, pp.189-193, 1985.

[7] M. ARAKI AND T. HAGIWARA, "Pole Assignment by Multirate Sampled-data Output Feedback", *Int. J. Control*, Vol. 44, pp. 1661-1673, 1986.

[8] M. ARAKI AND K. YAMAMOTO, "Multivariable Multirate Sampled-data Systems: State-space Description, Transfer Characteristics and Nyquist Criterion", *IEEE Trans. Automat. Contr.*, vol. 33, pp. 145-154, 1986.

[9] K.J.ASTROM, P.HAGANDER AND J. STERNBY, "Zeros of Sampled Systems", *Automatica*, vol.20, No. 1, pp. 31-38, 1984.

[10] K.J. ASTROM AND B. WITTENMARK, *Computer-controlled Systems-Theory and Design*, 2nd ed., Prentice Hall, Inc., New Jersey, 1990.

[11] M. ATHANS, "A Tutorial on the LQG/LTR Method", *Proc. of ACC*, Vol.2, pp. 1289-1296, June 1986.

[12] M.C. BERG, N. AMIT AND J. POWELL, "Multirate Digital Control System Design", *IEEE Trans. Automat. Contr.*, vol. 33, pp. 1139-1150, 1990.

[13] W.H. BOYKIN AND B.D. FRAZIER, "Analysis of Multiloop Multirate Sampled-data Systems" *AIAA Journal*, vol. 13, pp.453-456, 1975.

[14] A.B. CHAMMAS AND C.T. LEONDES, "On the Design of Linear Time-invariant Systems by Periodic Output Feedback, Part I and II", *Int. J. Control*, Vol. 27, pp.885-903, 1978,

[15] A.B. CHAMMAS AND C.T. LEONDES, "Pole Assignment by Piecewise Constant Output Feedback", *Int. J. Control*, Vol. 29, pp.31-38, 1979.

[16] A.B. CHAMMAS AND C.T. LEONDES, "On the Finite Time Control of Linear Systems by Piecewise Constant Output Feedback", *Int. J. Control*, Vol. 30, pp. 227-234, 1979.

[17] C.T. CHEN, "Introduction to Linear System Theory", Holt, Rinehart and Winston, Inc., 1970.

[18] J.L. CURTISS, *Introduction to Functions of a Complex Variable*, New York: Marcel Dekker, 1978.

[19] E.O. DOEBELIN, *Control System Principle and Design* John Wiley & Sons, 1985.

[20] J.C. DOYLE, "Guaranteed Margins for LQG Regulators", *IEEE Trans. Automat. Contr.*, vol. AC-23, No. 4, pp. 756-757, Aug. 1978.

[21] J.C. DOYLE AND G. STEIN, "Robustness with Observers", *IEEE Trans. Automat. Contr.*, vol. AC-24, No. 4, pp. 607-611, Aug. 1979.

[22] J.C. DOYLE AND G. STEIN, "Multivariable Feedback Design : Concepts for a Classical / modern Synthesis", *IEEE Trans. Automat. Contr.*, vol. AC-26, No. 1, pp. 4-16, Feb. 1981.

[23] M.J. ER AND B.D.O ANDERSON, "Design of Reduced-order Multirate Output Observers for Linear State Feedback Laws", submitted for publication.

[24] T.E. FORTMANN AND D. WILLIAMSON, "Design of Low-order Observers for Linear Feedback Control Laws", *IEEE Trans. Automat. Contr.*, vol. 17, No. 3, pp. 301-308, June 1972.

[25] B.A. FRANCIS AND T.T. GEORGIOU, "Stability Theory for Linear Time-invariant Plants with Periodic Digital Controllers", *IEEE Trans. Automat. Contr.*, Vol. AC-33, No. 9, pp. 820-832, 1988.

[26] B.A. FRANCIS, J. HELTON AND G. ZAMES, "H^∞-optimal Feedback Controller for Linear Multivariable Systems", *IEEE Trans. Automat. Contr.*, vol. AC-29, No. 6, pp.888-900, 1984.

[27] G.F. FRANKLIN AND J.D. POWELL, *Digital Control of Dynamic Systems*, MA: Addison-Wesley, 1980.

[28] G.F. FRANKLIN, J.D. POWELL AND M.L. WORKMAN, *Digital Control of Dynamic Systems*, 2nd ed., Addison-Wesley Publishing Company, 1990.

[29] F.R. GANTMACHER, *The Theory of Matrices-Vol. I*, Chelsea Publishing Company, New York, N.Y., 1960.

[30] D. P. GLASSON, "Development and Application of Multirate Digital Control", *IEEE Contr. Syst. Mag.*, vol. 1-8, 1983.

[31] J.P. GRESCHAK AND G.C. VERGHESE, "Periodically Varying Compensation of Time-invariant Systems", *Syst. Contr. Lett.*, Vol. 2, pp. 88-93, 1982.

[32] J.W. GRIZZLE AND M.H.SHOR, "Sampling, Infinite Zeros and Decoupling of Linear Systems", *Automatica*, vol. 24, No. 3, pp.387-396, 1988.

[33] T. HAGIWARA AND M. ARAKI, "Design of a Stable State Feedback Controller Based on the Multirate Sampling of the Plant Output", *IEEE Trans. Automat. Contr.*, Vol. Ac-33, No. 9, pp. 812-819, 1988.

[34] T. HAGIWARA, T. FUJIMURA AND M. ARAKI, "Generalized Multirate-output Controllers", *Int. J. Control*, Vol. 52, No. 3, pp. 597-612, 1990.

[35] T. HAGIWARA, M. ARAKI AND H. SOMA, "Simultaneuous Pole Assignment and Stabilization by Multirate Digital Controllers", *Book of Abstracts of Int. Symp. on Mathematical Theory of Networks and Systems*, 1991.

[36] T. ISHIHARA AND H. TAKEDA, "Loop Transfer Recovery Techniques for Discrete-time Optimal Regulators Using Prediction Estimators", *IEEE Trans. Automat. Contr.*, vol. AC-31, No. 12, pp. 1149-1151, 1986.

[37] E.I. JURY, *Sampled Data Control Systems*, New York: Wiley, 1958.

[38] P.T. KABAMBA, "Control of Linear Systems Using Generalised Sampled-data Hold Functions", *IEEE Trans. Automat. Contr.*, Vol. AC-32, pp. 772-783, 1987.

[39] T. KAILATH, *Linear Systems*, Prentice-Hall, Inc., Englewood Cliffs, N.J., 1980.

[40] R.E. KALMAN, Y.C. HO AND K.S. NARENDRA, "Controllability of Linear Dynamical Systems", *Contrib. Differential Equations*, Vol. 1, pp. 189-213, 1963.

[41] R.E. KALMAN AND J.E. BERTRAM, "A Unified Approach to the Theory of Sampling Systems", *J. Franklin Instit.*, vol. 267, pp.405-436, 1959.

[42] I. KAUFMAN, "On Poles and Zeros of Linear Systems", *IEEE Trans. Circuit Theory*, CT-20, 93, 1973.

[43] P.P KHARGONEKAR AND A. TANNENBAUM, "Non-Euclidian Metrics and the Robust Stabilisation of Systems with Parameter Uncertainty", *IEEE Trans. Automat. Contr.*, Vol. AC-30, pp.1005-1013, 1985.

[44] P.P. KHARGONEKAR, K. POOLLA AND A. TANNENBAUM, "Robust Control of Linear Time-invariant Plants Using Periodic Compensation", *IEEE Trans. Automat. Contr.*, Vol. AC-30, No. 11, 1985.

[45] P.P. KHARGONEKAR AND K.R. POLLA, "Uniformly Optimal Control of Linear Time-invariant Plants: Nonlinear Time-varying Controllers", *Syst. Contr. Lett.*, no. 6. pp.303-308, January 1986.

[46] H. KOBER, *Dictionary of Conformal Representations*, New York:Dover, 1952.

[47] G.M. KRANC, "Input-output Analysis of Multirate Feedback Systems", *IRE Trans. Automat. Contr.*, vol. AC-3, pp.21-28, 1957.

[48] H. KWAKERNAAK AND R. SIVAN, *Linear Optimal Control Systems*, New York, Wiley, 1972.

[49] S. LEE, S.M. MEERKOV AND T. RUNOLFSSON, "Vibrational Feedback Control: Zeros Placement Capabilities", *IEEE Trans. Automat. Contr.*, Vol. AC-32, pp. 604-611, 1987.

[50] J.R. LEIGH, *Applied Digital Control*, Prentice-Hall, 1985.

[51] F.L. LEWIS, *Optimal Control*, John Wiley & Sons, 1986.

[52] D.G. LUENBERGER, "Observers for Multivariable Systems", *IEEE Trans. Automat. Contr.*, vol. AC-II No. 2, pp. 190-197, April 1966.

[53] D.G. LUENBERGER, "An Introduction to Observers", *IEEE Trans. Automat. Contr.*, vol. AC-16, No. 6, pp. 506-602, Dec. 1971.

[54] A.G.J. MacFarlane and N. Karcanias, "Poles and Zeros of Linear Multivariable Systems : a Survey of the Algebraic Geometric and Complex-variable Theory", *Int. J. Contr.*, vol. 24, No. 1, pp.34-74, 1976.

[55] J.M. Maciejowski, "Asymptotic Recovery for Discrete-time Systems", *IEEE Trans. Automat. Contr.*, vol. AC-30, No. 6, pp.602-605, June 1985.

[56] J.C. McEachen and D.G. Meyer, "Tradeoffs for Multirate-rate Controller Design and Exact Comparisons with Single-rate Control", *IEEE Control Systems*, pp. 30-35, October, 1991.

[57] R.H. Middleton and G.C. Goodwin, *Digital Control and Estimation - a Unified Approach*, Prentice Hall, Inc. N.J., 1990.

[58] T. Mita, B.C. Pang and K.Z. Liu, "Design of Optimal Strongly Stable Digital Control Systems and Application to Output Feedback Control of Mechanical Systems", *Int. J. Control*, Vol. 45, pp. 2071-2082, 1987.

[59] J.B. Moore, L. Xia and K. Glover, "On Improving Control Loop Robustness of Model Matching Controllers", *Syst. Contr. Lett.*, vol. 7, pp.83-87, 1986.

[60] J.B. Moore and L. Xia, "Loop Recovery and Robust State Estimate Feedback Designs", *IEEE Trans. Automat. Contr.*, vol. AC-32, No. 6, pp.512-517, June 1987.

[61] J.B. Moore and T.T. Tay, "Loop Recovery via H^∞/H^2 Sensitivity Recovery", *Int. J. Contr.*, vol. 49, No. 4, pp.1249-1271, 1989.

[62] P. Murdoch, "Observer Design for a Linear Functional of the State Vector", *IEEE Trans. Automat. Contr.*, vol. AC-18, pp. 308-310, June 1973.

[63] P. Murdoch, "Design of Degenerate Observers", *IEEE Trans. Automat. Contr.*, Vol. AC-19, No. 4, pp. 441-442, August, 1974.

[64] C.N. NETT, C.A. JACOBSON AND M.J. BALAS, "A Connection Between State-space and Doubly Coprime Fractional Representations", vol. AC-29, No. 9, pp. 831-832, 1984.

[65] H.H. NIEMANN AND P. SOGAARD-ANDERSEN, "New Results in Discrete-time Loop Transfer Recovery", Proc. of ACC, pp.2483-2489, 1988.

[66] K. OGATA, *Discrete-time Control Systems*, Englewood Cliffs, NJ:Prentice-Hall, 1987.

[67] J. O'REILLY, "Observers for Linear Systems", Academic Press, 1983.

[68] Y. PATEL AND R.J. PATTON, "Insensitivity Properties of Multirate Feedback Systems", *Proc. 30th IEEE Conf. Decision Contr.*, Brighton, England, Dec. 1991.

[69] J.B. PEARSON AND C.Y. DING, "Compensator Design for Multivariable Linear Systems", *IEEE Trans. Automat. Contr.*, Vol. AC-14, No.2, pp. 130-134, April 1969.

[70] J.R. RAGAZZINI AND G.F. FRANKLIN, *Sampled-Data Control Systems*, New York: McGraw-Hill, 1958.

[71] M.G. SAFANOV, *Stability and Robustness of Multivariable Feedback Systems*, The MIT Press, 1980.

[72] M.G. SAFANOV AND M. ATHANS, "Gain Phase Margins for Multiloop LQG Regulators", *IEEE Trans. Automat. Contr.*, vol. AC-22, No. 2, pp. 173-179, April 1977.

[73] U. SHAKED, "Guaranteed Stability Margin for the Discrete-time Linear Quadratic Optimal Regulators", *IEEE Trans. Automat. Contr.*, vol. AC-31, No. 2, pp. 162-165, 1986.

[74] G. STEIN AND M. ATHANS, "The LQG/LTR Procedure for Multivariable Feedback Control Design", *IEEE Trans. Automat. Contr.*, vol. AC-32, No. 2, pp. 105-114, Feb. 1987.

[75] G. STEPHANOPOULOS, *Chemical Process Control-An Introduction to Theory and Practice* Prentice-Hall, 1984.

[76] E. TSE AND M. ATHANS, "Optimal Minimal-order Observer-estimators for Discrete Linear Time-varying Systems", *IEEE Trans. Automat. Contr.*, vol. AC-15, No. 416-426, Aug. 1970.

[77] M. VIDYASAGAR, "Robust Stabilisation of Singular Perturbed Systems", *Systems and Control Letters*, Vol. 5, pp. 413-418, 1985.

[78] W. YAN AND B.D.O. ANDERSON, "The Simultaneous Optimisation Problem for Sensitivity and Gain Margin", *IEEE Trans. Automat. Contr.*, Vol. AC-35, No.5, pp.558-563, 1990.

[79] W. YAN, B.D.O. ANDERSON AND R.R. BITMEAD, "On the Gain Margin Improvement Using Dynamic Compensation Based on Generalised Sampled-data Hold Functions", submitted to *IEEE Trans. Automat. Contr.*.

[80] Z. ZHANG AND J.S. FREUDENBERG, "Loop Transfer Recovery with Nonminimum Phase Zeros", *Proc. of the 26th CDC*, pp. 956-957, Dec. 1987.

[81] Z. ZHANG AND J.S. FREUDENBERG, "On Discrete-time Loop Transfer Recovery", *Proc. of the ACC*, pp. 2214-2219, 1991.